~~CONFIDENTIAL~~

NLR CONTRACT REPORT

GR 93080 C

WINDSHEAR ANALYSIS USING FLIGHT DATA FROM THE DC-10 CRASH AT FARO AIRPORT

by

(Names masked by AvioConsult)

Reviewed by AvioConsult/Lt-Col ret'd Harry Horlings, Flight Test Engineer (USAF Test Pilot School, class 85A), former chief flight test RNLAF and former member of a scientific committee of the NLR, at the request of the lawyer of the victims of the accident and their next of kin.
General conditions apply, which are deposited at the Chamber of Commerce in The Hague.

DFDR and AIDS data that might be required by readers can be found in he Appendices of report: ***The last 80 seconds of Flight MP495***, downloadable in EN and NL languages from:
https://www.avioconsult.com/downloads-nl.htm

This investigation has been carried out under a contract awarded by the accidents investigation bureau of the Netherlands Department of Civil Aviation, aeronautics inspection directorate, contract number OV/634.

Division: Flight
Prepared: (Names masked by AvioConsult)
Approved:

Completed : 930219
Order number: 106.364
Typ. : AEB

CONFIDENTIAL

Is a military classification. Invalid and unnecessary.

Distribution CR 93080 C:

RLD/BVO	no(s).	1-10
(Names masked by AvioConsult)	no(s).	11
	no(s).	12
	no(s).	13
	no(s).	14
	no(s).	15
	no(s).	16
	no(s).	17
	no(s).	18
	no(s).	19
NLR-files	no(s).	20

SUMMARY

On 21 December 1992 Flight MP459, a Martinair DC-10, crashed on runway 11 at Faro airport, Portugal, while landing at 0733 GMT, resulting in total hull loss, as well as 55 casualties and more injured. Windshear conditions were suspected to have caused the accident. The flight data registered on board by the Aircraft Condition Monitoring System were processed and analyzed at NLR using available programs that had been developed earlier in the course of a windshear research project called WINDSTREAM (Ref. 1).

The wind profiles that were extracted, as well as the windshear models that were identified, showed that the aircraft passed through a relatively strong downburst during the initial part of the final approach, emerging from it at about 700 ft, and through two more smaller microbursts or "cells", immediately bordering the downburst. During the approach the wind veered from initially a 10 kts headwind to a 10 kts tailwind at just before touchdown. Although the wind changes might have caused a windshear alert, the induced aircraft response was such that the aircraft did not approach a dangerous aerodynamic flight condition. The wind turbulence can be characterized overall as being moderate to severe.

Was light according to DFDR data and ICAO definition

It is recommended to perform a flight simulator experiment using the windshear and turbulence characteristics determined at Faro to answer a number of questions concerning power lever closure times, autopilot and autothrottle failures and aircraft pitch response due to wind gradients, and to perform some additional data analysis concerning pilot-induced oscillations in relation to control wheel steering, and a functional analysis of the autothrottle system. Transcripted cockpit voice recorder data will be needed in analyzing correlations.

DFDR data do not confirm these statements at all: no downburst, no "cells", no wind change, but a non-precision approach during which the copilot interfered with inappropriate control inputs that affected autopilot and autothrottle operation (AIDS data). Confirmed by NTSB.

TABLE OF CONTENTS

TABLE OF CONTENTS (continued)

LIST OF SYMBOLS

A_Y	lateral acceleration, m/s^2
C_Y	lateral force coefficient
d	core diameter of downburst, m
dh/dt	vertical speed, m/s
F	windshear hazard factor or index
g	gravity constant, m/s^2
H	boundary layer thickness, m
h	altitude, m
m	aircraft mass, kg
q	pitch rate, rad/s
R	radius of downburst, m
r	yaw rate, rad/s
S_{tf}	tailfin area, m^2
S_Y	projected side view area, m^2
T_p	phugoid period, s
t_x	F-factor filter averaging time interval, s
V	airspeed, m/s
V_a	approach speed, m/s
Vw	windspeed, m/s
Vx,Vy	velocity components of moving windshear model, m/s
W_{at}	along-track wind component, m/s
W_{ct}	crosstrack wind component, m/s
W_x	local headwind component, m/s
W_y	local crosswind component, m/s
W_z	vertical wind component, m/s
x	north-south distance, m
Y	side force, N
Y_β	side force derivative with respect to sideslip angle, $m.(s^2.rad)^{-1}$
$Y\delta_a$	side force derivative with respect to aileron deflection, $m.(s^2.rad)^{-1}$
$Y\delta_r$	side force derivative with respect to rudder deflection, $m.(s^2.rad)^{-1}$
y	east-west distance, m
z	vertical distance, m

LIST OF SYMBOLS (continued)

α_f	fuselage angle of attack, rad
α_{vane}	alpha vane angle, rad
β	sideslip angle, rad
Γ	ring-vortex strength, m^2/s
δ_r	rudder deflection, rad
ν	turbulence signal, m/s
ρ	air density, kg/m^3
σ	turbulence rms, m/s
$\sigma_{x,y}$	turbulence rms in the x-y plane
σ_z	turbulence rms in the vertical direction
χ	wind direction, rad
ω_p	phugoid frequency, rad/s

Subscripts

L	Lower
U	Upper

ABBREVIATIONS

ACMS	Aircraft Condition Monitoring System
AP	Autopilot
AT	Autothrottle system
CAS	Calibrated Air Speed
CWS	Control Wheel Steering
EMI	Electro-Magnetic Interference
GNI	Gauss-Newton Iteration program
MAPt	Missed Approach Point
MDA	Minimum Descent Altitude
PIO	Pilot-Induced Oscillations
TAS	True Air Speed

1 INTRODUCTION

On 21 December 1992 at 0733 GMT Flight MP459, a Martinair DC-10, crashed on runway 11 at Faro airport, Portugal, while landing, resulting in total hull loss, as well as 55 casualties and more injured. Windshear conditions were suspected to have caused the accident because of the presence of thunderstorms in the vicinity of the airport.

In accident report called: AIDS

Besides the required flight data (crash) recorder the DC-10 aircraft had an on-board data-recording system called the ACMS: the Aircraft Condition Monitoring System. Because of the location of this recorder in the nose section of the aircraft, which was not damaged by fire, the ACMS-data could be extracted in a good state. The Portuguese authorities delivered the ACMS-data to the accident investigations bureau of the Department of Civil Aviation in the Netherlands for further analysis by the National Aerospace Laboratory NLR.

Since 1989 at NLR a windshear research project has been underway in collaboration with KLM, the Department of Civil Aviation RLD/LI, the Netherlands Agency for Aerospace Programs NIVR, and the Royal Netherlands Institute of Meteorology KNMI. Details of this ongoing project, called WINDSTREAM, are given in References 1 and 2. Some of the objectives of this project are to develop windshear models and models for windshear detection systems, both airborne and ground-based, and to validate the windshear models using flight data (ACMS) delivered by KLM. Only those flights are processed of B737 aircraft where a windshear alert had been reported by the on-board (reactive) windshear alert system.

The objective of this document is to report on the results of the windshear analysis of the ACMS data recorded on board the DC-10 on landing approach at Faro. In addition to the data obtained from the DC-10, also ACMS-data were processed that were registered on board a Martinair B767, which landed about 6 minutes before the DC-10. The object of this was to compare the wind profiles recorded on both flights to check for similarity between the two. In chapter 2 a discussion is provided of the data processing that was required. In section 2.1 the raw flight data are discussed and the subsequent

processing. Section 2.2 contains a description and analysis of the resulting wind profiles produced by the data processing. Section 2.3 contains a discussion on features that were added to the windshear-model identification program GNI, in order to apply it to the case at hand.

Chapter 3 reports on the results obtained, in terms of the windshear models identified, and a comparison with the wind profiles. The windshear hazard associated with these windshears is analyzed. Finally conclusions and recommendations are given in chapter 4.

2 ANALYSIS AND DISCUSSION

ACMS is not identified in the AOM (Airplane Operating Manual); the AIDS is (AOM 1.13/8). The AIDS provides the DFDR with properly conditioned signals.
If the ACMS is a (separate) maintenance system, how accurately conditioned and valid are the data for flight analysis? Is the use approved?

2.1 Raw data inspection and discussion

Sure?? Last data block not recorded because of fire, loss of power, etc. following the accident?

The flight data recorded by the ACMS were of good quality. No data drop-outs were detected, other than that the data recording, starting at an initial altitude of about 1500 ft, stopped at 44 ft above the ground. Therefore ground contact is not included in this data set. ~~This early stoppage is probably due to the landing forces which occurred, for which the system has not been certified to operate in. As a result of this the data tape skipped from the recording head, causing loss of track in the digital data stream.~~ Because of the data recording mechanism, where a batch of 4 seconds is written to the tape, this caused the loss of all data after 44 ft radio-altitude.

not a fact

No, DFDR recorded until 8 s after touchdown, including radalt data. Why not used DFDR data as well?

The parameters which were recorded were of a similar format used also by program OUTFLOW (Ref. 3) at NLR, as applied within the scope of the WINDSTREAM-project. A number of sampling rates however, did not match corresponding B737 data for which the OUTFLOW-program had been geared previously, so some modifications had to be carried out. Additionally, because of the sometimes large rudder deflections that were observed, it was felt necessary to also include rudder signals in the data processing, which had hitherto not been the case. A list of the parameters recorded and delivered to NLR is given in table 1.

Only once a large rudder deflection, to align with the runway + one smaller by pilot, and by Yaw damper due to light turbulence last 70 s of flight.

The computer program OUTFLOW, mentioned before, runs on the Cyber 692 mainframe computer installation at NLR. Also the windshear identification program, used to identify windshear-model parameters, runs on the same mainframe. Apart from that, all other data manipulations, conversions, checking, time series analysis, correlational analysis, data plotting, etc. were performed using the statistical package CSS which runs on a PC.

In the next subsections the inertial and aerodynamic raw data, as obtained from the AGMS, will be portrayed and discussed. It may sometimes be very helpful to visualize the data information in order to help form an opinion about the landing accident that took place.

and to develop an opinion on the (in)validity of the analysis.

2.1.1 Flight parameters

Concerning the flight path of the aircraft, the pitch angle, bank angle, calibrated airspeed, true airspeed, groundspeed, altitude (pressure altitude and radio-altitude), magnetic heading, track angle and drift angle are shown in figures 1 to 7. In figure 8 the engine rpm response is shown. The following observations can be made.

Sampling rate? One per second.

Track angle not in Fig.

a) pitch angle (Fig. 1). Before 07:31:40 GMT the response of the pitch angle is quite different from that after this time. Before this time the maximum pitch angle is about 5 degrees, and the lowest value is about 2 degrees; however, after this moment there is a sudden departure downwards at about 07:31:40 GMT from 4 to 0 degrees, followed by a pitch up to 6 degrees, and then followed again by another such oscillation, with a mean trend upwards. The theoretical open-loop phugoid eigenfrequency is estimated as (Ref. 5)

At this time, the airplane descended into light turbulence, 1.0 ± 0.5 g, that lasted until touchdown.

Departure? 4 deg.?
The pilot pushed the elevator control against the engaged Vert. speed mode.

$$\omega_p \doteq \sqrt{2}\,\frac{g}{V_a} = 0.193 \; rad/s$$

variation. For an oscillation, period time T is constant.

From $\omega_p = 0.193$ rad/s follows a phugoid period $T_p = 32.5$ seconds, which is exactly what is observed. The damping of this phugoid seems to be very low. The start of the oscillation in pitch at 07:31:40 GMT coincides with the pilot switching from autopilot to Control Wheel Steering (CWS)-mode. Although the aircraft is supposed to be stable in this mode (this mode is in fact an attitude-hold /rate-command type system, with the command signal being

Don't see this in Figure 1. Pilot frequently pushed and pulled the elev. control against the autopilot. From 07:31:56 manual inputs that were required during the non-precision approach. Normal. No phugoid.
Where is the elevator position data (pilot or autopilot input)?

No, CWS was at 07:31:56

was not a phugoid.

generated by the pilot's control wheel force inputs), one way to explain this type of response is that a pilot-induced oscillation (PIO) is occurring. Since control wheel forces were not contained in the ACMS data delivered to NLR, this correlation between control wheel forces and pitch variation could not be made. The triggering mechanism behind such a PIO could well be the updraft that was later found to exist at the point of switch-over in autopilot mode. Another explanation can be that the pilot is thinking the system is in CWS, but that a failure has occurred, providing the pilot with essentially open-loop control.

b) bank angle (Fig. 2). Also here a change in behaviour can be observed after 07:31:40 GMT. Before this moment there are some small bank angle changes of relatively small amplitude, thereafter the variations increase. Especially at about 07:32:40 GMT there is a "rapid" roll ~~reversal~~, from +10 degrees to -15 degrees in about ~~5 seconds~~. The -15 degrees bank angle seems to correspond with a turn to the left, made just before the end of the flight data, as can be gleaned from the heading angle. Generally, however, the maximum and minimum bank angles are well within acceptable limits.

c) calibrated airspeed (Fig. 3). Throughout the flight the CAS is above the Vref of 139 knots most of the time, except at about 07:32:22 GMT and beyond 07:32:45 GMT. The ~~bug~~speed set in the Autothrottle window was 144 kts. Also here the variations in CAS before and after 07:31:40 GMT are different. Variations are relatively small. After 07:31:40 GMT there is an immediate increase from 145 kts to nearly 155 knots, which is then followed by a dominant oscillation, with the same period as the phugoid observed before. From 07:32:40 GMT onwards the CAS steadily decreases, and drops below Vref at about 07:32:45 GMT.

d) groundspeed and true airspeed (Fig. 4). Basically the groundspeed indicates the effect of headwind relative to the aircraft. There is a minimum in groundspeed at about 07:31:00 GMT, which is due to the aircraft making a turn into the wind at this point, as can be seen from inspecting the heading angle (Fig. 6), in combination with the wind changing direction. Due to the large windspeed even small changes in wind direction cause large changes in

?? Why not? Must have been available, because these AIDS data showed up in Portuguese Accident report, Annex 9.

Sounds interesting, but is not a PIO, but pilot induced variations. The copilot pushed and pulled the (CWS) pitch control inappropriately. Not professional.

Or a pilot who could not handle CWS

Then you cannot tell whether the pitch changes are due to outside disturbance or from inside by the pilot.

Onset light turbulence

??

Was controlled by pilot.

8 seconds! Seen the rudder input? 90% to left: C_{Ldr}?

139 was set (RoA). Why would airspeed then decrease to 139?

Vthr

Gust filter in ATS increased and decreased CAS

Why? Because throttles were closed (inappropriately)

?? A variation. Why dominant? Is influence of gust filter in ATS! (5 kt increase and decrease) when turbulence above a threshold. And pitch down, increasing the CAS.

Really? Doesn't look like this.

What is the source of this ground speed? Reliable?

Turn? No, was continuing the final turn to the approach radial, then heading 125 deg. What was the wind?

Heading increased momentarily from 125° to 134° and back; the ground speed cannot have changed that much. Doubts!

Ground velocity is vector sum of velocity in the air and the wind.

How do you know? The wind was not changing. The heading was near constant during the last 80 s of flight, except during rudder input.

Large windspeed cause large changes in windspeed??? (ground speed? At 139+ kIAS? If wind is 90° from the right? Do you realize what you're saying?

Descent of non-precision approach from 2000 down to 500 ft is on the AP/ vert. speed mode. If the set Vert. speed was a little too high, or headwind was larger than anticipated, a short level flight is required to intercept the PAPI lights (5.2% gidepath). The final approach is to be flown manually using CWS. Below 200 ft, a DC-10 needs to stay above the PAPI glidepath to avoid touching down in front of the threshold, is also AOM procedure. Therefore "leveling off" shows up in the data a few times, but Is normal, is absolutely no windshear or updrafts.

windspeed. The true airspeed can be seen to show the same oscillatory pattern as the calibrated airspeed.

TAS at sea level is equal to CAS. QNH was 1013. Oscillatory? Scale is misleading - too large.

Is it? Where did the light turbulence start? Noticed pilot inputs?

e) altitude (Fig. 5). The altitude profile, i.e. barometric altitude and radio altitude versus time, is shown in figure 6. The profile is oscillatory. One way to explain this is that there seems to be what looks like a leveling off at about 07:32:10 GMT, at an altitude of 400 ft. This could correspond to leveling off at the Minimum Descent Altitude (MDA) of the VOR/DME approach which the aircraft followed. In case there are no visual cues during such an approach the pilot is required to level off, and to proceed at MDA to the missed approach point (MAPt). From the approach plate this point is 0.5 nm from the runway threshold. When the approach descent profile would be maintained, the approach path would cross over the runway at 50 ft above the threshold. Another way to explain the oscillations is that due to PIO the approach becomes more and more unstable: each time there is a "leveling off", the flight path seems to become more and more flat. The first time is at 07:31:50 GMT, the second time at 07:32:10 GMT. These ~~oscillations~~ of the altitude profile correspond with the pitch excursions discussed previously. The leveling off at MDA could therefore well be the result of the phugoid oscillation, rather than a pilot input. Data from the cockpit voice recorder can give clear clues as to what happened here exactly, i.e. whether or not the aircraft leveled off at the MDA.

No, to intercept the PAPI

1 DME

Not a large DC-10. See AOM.

No, just following procedures. An ILS approach is a constant glidepath approach, a non-precision approach is not.

Well, look at the pilot input to see pilot influence.

So?

What cues? On the CVR? The aircraft did indeed level off to intercept the PAPI before descending below MDA (400 ft). Normal procedure for a non-precision approach.

Furthermore there are some small differences between barometric and radio altitude, however, these differences are quite small and do not seem to correlate with any of the other parameters. The maximum difference is about 60 ft at the beginning of the flight data, where it is of least importance.

DFDR shows only Radalt below 230 ft. Are you sure Radalt is available above that altitude?

the 111° approach radial (is 5° offset of runway centerline (106°)).

f) magnetic heading (Fig. 6). A relatively uneventful trend is depicted. At 07:31:20 GMT the aircraft turns toward a heading of 125 magnetic, apparently to intercept the ~~runway centerline~~ (the VOR/DME radial is 111 degrees magnetic). This step towards the ~~runway heading~~ can be verified only after consulting the cockpit voice recorder. At about 07:32:20 GMT the aircraft turns left to a heading of 117 degrees magnetic, but soon afterwards turns right again to a heading of about 124 degrees. This is 18 degrees more than the runway heading of 106 degrees magnetic. It can be observed that at

No, is not on CVR.

No, yaws left, then reduces rudder again. Are not turns - inappropriate rudder inputs by copilot.

What does this large drift angle tell you?

Rudder is designed for >= 30 kt crosswind, isn't it? Why not possible to align with this large rudder deflection? Because the airplane was not on the (extended) runway centerline, but at the 117° approach radial.

Yes, change in heading, but is called a yaw, attaining a sideslip angle for alignment attempt with the runway - was unsuccessful.

DFDR data even shows an increase to 117° at touchdown. A traversing landing was made, which is not approved for the DC-10.

07:32:40 GMT there is a change in heading from 124 to 113 degrees, which was due to a large rudder input as can be seen from cross-referencing the rudder input time history (Fig. 11). At the final heading recorded of 114 degrees the aircraft still has a 8 degrees heading misalignment with the runway heading. If this heading would be maintained from the last data point up to touchdown, then a traverse landing would be made, i.e. the direction in which the wheels are going is not aligned with the direction the airplane is travelling.

You mean: are pointed

How calculated? Does NLR know what a drift angle is? Here you talk about sideslip angle!

or to the approach radial?

g) drift angle (Fig. 7). Again here also a difference can be seen to exist between the drift angle before 07:31:40 GMT, and afterwards. Before this moment there is a relatively constant change in drift angle, apparently due to the aircraft turning into the wind. After 07:31:40 GMT there are more oscillations in drift angle, with a change in drift angle from -8 to -14 degrees, i.e. a variation of 6 degrees. The same variation occurs again at 07:32:30 GMT. Evidently there is a "burst" of crosswind at these moments. At about 07:32:40 GMT the drift angle reduces to -8 degrees again, which corresponds to the aircraft flying at a crab angle of about 8 degrees towards the runway.

Drift is the angle between air and ground velocity. What is the NLR drift?

No, the pilot applied rudder, inappropriately

Rudder back to center. There was a sideslip angle due to rudder input, is not a drift angle.

the pilot applied near full rudder, increasing sideslip angle for aligning with runway, is not drift!

?? DFDR heading nearly constant. Again, what is your drift angle? You mean sideslip angle?

h) engine N1 and N2 rpm (Fig. 8). The N1 rpm of all engines were identical, and so was the case with N2, hence in figure 9 only N1 of engine No. 1, and N2 of the same engine, are shown together. It appears from comparing this figure with figure 12 later-on that the engine rpm very closely follows the power lever inputs. As is evident from this figure, the engines are operating at a fairly constant performance level around 07:31:30 GMT, but after 07:31:30 GMT more oscillations can be seen to develop. At 07:32:40 GMT the engines reach the maximum rpm of this flight segment, viz. 102 percent N1, after which moment the rpm drops rapidly to the flight idle level of 40 percent N1.

variations. Onset of light turbulence, and a copilot operating the controls against the autopilot.

Not quite during engine accels.

2.1.2 Controls

control surfaces

In this section the controls are depicted and discussed, if necessary. The controls that were delivered on ACMS to NLR are the elevator deflection (inboard and outboard), the aileron deflection (inboard and outboard), upper

and lower rudder deflection, the power lever positions and the pitch trim. The last one will not be shown because it is not of interest here.

a) elevator (Fig. 9). The average elevator control deflection was calculated and used, since it turned out that there were only very insignificant differences between inboard and outboard elevator deflections. Before 07:31:40 GMT the amplitude variations are of a different nature than after this moment, and also have a smaller amplitude. It can be seen that at the moment of the pitch departure, at 07:32:40 GMT, there is hardly any elevator input to warrant such a departure. Later-on, however, there is elevator control activity corresponding to pitch changes. Also the amplitude of the elevator variations increases more and more towards the end of the flight data, in a seemingly divergent pattern. Such a pattern can also be typical of approaching a narrow window (e.g. the landing runway) under turbulent circumstances, where, when the pilot is (too) tightly controlling the aircraft, over-control may take place.

of course, elevator changes pitch. At 07:32:40 the pilot pulled on the elevator control.

What do you mean with departure? Loss of pitch control? Cannot be confirmed with DFDR data.

CWS was engaged, which the pilot used inappropriately (NTSB).

b) aileron deflection (Fig. 10). The average aileron deflection is used, where the average deflection equals the left - right aileron deflection. This means that a positive value of the average deflection means a roll input to the left. Again noteworthy here is the difference in pattern before and after 07:31:40 GMT. Also there is an average trend of left bank input during the second part of the flight segment, and this trend increases. Also here a divergent pattern can be observed, similar to the elevator control.

Airplane descending into or entering an area with light turbulence

not divergent! Inappropriate pilot inputs.

c) rudder deflection (Fig. 11). The average rudder deflection is used, since upper and lower rudder had essentially the same response. A positive rudder deflection means a nose-right response. The time history of the rudder deflection is typical of what has been observed before. Before 07:31:40 GMT rudder inputs are relatively small, probably generated by the yaw damper. After that moment, however, the rudder inputs grow in amplitude in a divergent manner, with large rudder inputs at the end of the flight data, in an apparent attempt to decrab the aircraft. The large rudder input can be seen to change the aircraft heading, depicted in figure 6.

Looked at pilot inputs?
Rudder returned to zero just before touchdown.
Why not analyze better?

d) power levers (Fig. 12). It turned out that the power lever position signals contained several dropouts and other invalid signals. The best signal was the no. 3 power lever position. After first deleting outliers an average power lever position signal was derived from the three power lever position signals by first differencing the valid position signals, taking the average of these, and then integrating the difference signal in order to get the throttle position. Becauwe of the integration, a (small) constant bias may still be present in the calculated power lever position. The result is shown in figure 12, where both the power lever position, as well as the position rate, are given. The time history shows that power lever activity is relatively quiet during the segment from 07:31:00 GMT to 07:31:40 GMT. After this point the power lever position varies much more, mostly in correspondence with pitch changes, although not all variations do so. The overall response of the power lever position is typical of the Autothrottle system functioning and operating the power levers, since the position rate is a "continuous" signal, rather than showing portions of no activity. The CWS mode of operation of the flight control system implies that the autothrottle is switched on, which is confirmed by the type of response. Noteworthy is the power lever reduction (or closure?) at 07:32:38 GMT, immediately after having reached a maximum of 30 degrees, which is the maximum value of the flight. When cross-referencing this time history with that of altitude, it becomes apparent that the power levers were closed at an altitude of about 150 ft above the runway. This is too high an altitude for power levers to be closed by the Autothrottle system (power lever closure starts automatically at 50 ft). The power lever position rate shows that most of the time the rate is less than ± 5 deg/s, except for two events, viz. at around 07:31:50 GMT, and at 07:32:40 GMT. The power levers were pulled back from 30 degrees to 5 degrees, and then slightly forward again, and back once more. For the autothrottle system such a response is very unusual, considering the height at which this took place. Either a manual override has taken place or the system has failed in some fashion.

No, separate systems. However ATS should always be on.

Good!

2.1.3 Accelerations

The inertial accelerations were used by the OUTFLOW program, by the Kalman filter/smoother, to derive the inertial flight path, in conjunction with

How accurate is this process? Using discrete data? Sampling rate?

which?

No, the N1 variations.

other parameters. The accelerations were measured in the body frame of reference. A discussion follows below.

onset of light turbulence.

a) longitudinal and lateral acceleration (Fig. 13). As has been observed with the other data, there is a difference in character before and after 07:31:40 GMT. After this point the pitch oscillations show up more clearly in the longitudinal accelerations. The lateral acceleration shows two peak values at the end of the data set, of about 0.1g. According to section 2.2.1 this correlates directly with the aerodynamic sideslip angle.

Seen the copilot elevator control inputs against the AP, resulting in thrust variations, hence speed changes? Also the gust filter in the ATS increased and decreased the IAS with 5 kt several times, following the onset of light turbulence.

b) vertical acceleration (Fig. 14). Again the same phenomenon can be observed in character of the response. The pitch ~~oscill~~ations cause vertical accelerations to occur. Noteworthy is the vertical acceleration at the end of the data set, where the signal drops from 1.08g in a continuous downward trend to a value less than .89g. This could indicate a tendency to fall downwards and coincides with the power lever closure at 150 ft. Maximum vertical acceleration is about 1.2g maximum, and .8g minimum

= light turbulence

Pitch decreased for 2 s, then increased again. DFDR data shows this increase of g just prior to landing.

No, turbulence caused speed changes (gust filter in ATS). Copilot changed pitch inappropriately, unfamiliar with CWS.

2.2 Wind data analysis

In this section the results from the OUTFLOW-program will be discussed. This computer program (Ref. 3) computes wind time histories by subtracting the inertial from the aerodynamic flight path. Both topics are discussed in the next sections.

How does the model know the aerodynamic flight path? What are the limitations of this method?

2.2.1 Inertial flight path

The inertial flight path has been derived through a Kalman filter and smoother estimation process, using a mix of inertial platform data, such as the Euler angles (roll, pitch, yaw), ground track and drift angle, magnetic heading angle, longitude and latitude, together with the inertial accelerations measured in the body frame of reference. The pressure altitude and radio altitude are used together, and are needed to assure convergence of the Kalman filter/smoother dynamic behaviour. Various assumptions are made about the noise sources in the data. The Kalman filter and smoother process is applied in order to determine the minimum variance state trajectory of the

Influence on outcome?

Smooth flight path considered, but was it? Did you include control inputs by the piots? And the turbulence that occurred? How accurate and trustworthy is this anaylsis?

aircraft. Biases are assumed to be present in the accelerometer signals as well as in the position data from the navigation system. Various sampling rates are used for the parameters. As output the inertial flight path in terms of position (x,y,z) and velocities (u,v,w) are delivered, as well as the (constant) biases in the accelerometer signals and inertial navigational data (position). The sampling rate of these states is 4 times per second. The altitude h and vertical velocity dh/dt are of special importance because they determine the accuracy of the vertical wind extracted later-on. It is assumed that the baro-altitude signal may contain errors due to up or downdrafts, and also that the radio-altitude signal may contain errors due to non-flat terrain. A detailed description of this process is given in Reference 4.

How is this illustrated in the output data?

Differentiating discrete data samples of 4 per second? Is that allowed? No, not a good engineering practice.

2.2.2 Aerodynamic flight path

What is your aerodynamic flight path?

Sideslip angle? Or drift angle?

For determining the aerodynamic flight path, it is necessary to know the fuselage angle of attack and the sideslip angle, besides the total aerodynamic pressure. The fuselage angle of attack is measured by an angle-of-attack vane, located somewhere on the fuselage. The sideslip angle was not measured, and has to be estimated, if a good estimate of the wind components is to be made. The estimation process is further described in section 2.2.2.1.

AOA?

Is this reliable when in turbulence?

How and why? Sideslip is zero while yaw damper is active and feet on the floor.

2.2.2.1 Sideslip angle estimation

sideslip angle or drift angle?

The sideslip angle β is required in order to have a good estimate of the wind vector. In the case of Faro it is of special importance because it turned out that the landing took place in crosswind conditions, where the sideslip angle becomes even more important. In program OUTFLOW an estimate of the sideslip angle is being used, based on the linear lateral dynamics of the aircraft (Ref. 4). This estimate applies for a number of assumptions, viz.:

- there is no lateral gust and wind component;
- there are no rudder inputs;
- the side-force derivative $Y_{\delta a} = 0$.

But you don't have data of the landing.

?? There was light turbulence during the last 70 s of flight. No gust and lateral wind component?

There were, nearly continuously by the copilot.

There were continuous roll control inputs by the copilot.

Is always required in cross-winds for aligning the airplane with the runway during the last seconds of flight.

These assumptions cannot be met, hence the sideslip estimation cannot be valid.

Ever verified your models with data of a flight after a real windshear encounter?

In view of the Faro-accident analysis it became clear that not all of the assumptions held, notably, that the condition that there are no rudder inputs is no longer valid, and that there is no lateral wind component.

So sideslip angle estimation not valid for crosswind landings? The pilot applied rudder inputs during the last 40 s of flight! It is of no use to continue with this analysis, sorry estimation.

In the DC-10 data there are two rudder inputs, viz. δ_{r_L} and δ_{r_U}, for Lower and Upper rudder respectively. Both reached quite large values during the approach. Hence the rudder inputs were included in the linearized lateral equation of motion, which resulted in a first-order filter for the sideslip angle estimate. This was called the improved estimator. However, because of the large rudder inputs and the fact that lateral acceleration has also been measured, it was felt better to use the lateral acceleration A_Y, or specific side force Y/m, to directly estimate the sideslip angle β. The specific side force is the result of an aerodynamic slip angle β, and rudder deflections δ_r, to first order as follows:

These values were very small, how accurate will resulting sideslip be?

Following pilot inputs.

$$A_Y = Y_\beta.\beta + Y_r.r + Y_{\delta_r}.\delta_r \qquad (1)$$

Missing here is another very important side force, the side force due to bank angle in the lateral body axis: W.sin phi.

from which one can estimate β:

$$\bar{\beta}(t_i) = [A_Y(t_i) - Y_r.r - Y_{\delta_r}.\delta_r(t_i)]/Y_\beta \qquad (2)$$

This is the "new" estimator. In order to obtain the new estimate, however, the side-force due to slip angle, Y_β, the side force due to yaw rate, Y_r, and the side force due to rudder deflection, $Y_{\delta r}$, have to be known. An estimate of these is provided in the next section.

In Eq. (1) δ_r is the average rudder deflection. From inspection of the data both the upper and lower rudder time responses were found to be identical, and hence only the lower rudder deflection, sampled once per second, has been used in the above equation, where $Y_{\delta r}$ is based on the total upper + lower rudder deflection.

2.2.2.1.1 Side force due to rudder control derivative $Y_{\delta r}$

The side force due to rudder control derivative is estimated using similar data for a DC-8, of which data was available (Ref. 5). For the DC-8, where there is no upper or lower rudder, the derivative $Y\delta_r$ is -0.0238 $(s.rad)^{-1}$ at

BT

an approach speed V_a of 74 m/s. Obviously the size of the rudder and aircraft play a role. When using a nondimensional expression, referenced to the tailfin area, one can write

$$Y_{\delta_r} = \frac{1}{m}\frac{\partial Y}{\partial \delta_r} = \frac{1/2\rho V^2 S_{tf}}{m} \cdot \frac{\partial C_Y}{\partial \delta_r} \qquad (3)$$

where S_{tf} = tailfin area = 28.3 m^2 for the DC-8. One can calculate now that for the particular condition of the DC-8 in the database (m=86100 kg; ρ=1.2256 kg/m^3)

$$\frac{\partial C_Y}{\partial \delta_r} = 1.594 \ \ rad^{-1}. \qquad (4)$$

This is converted to a "DC-10" value by incorporating a form factor, which depends on the ratio of rudder-to-tailfin area. For the DC-8 this ratio is 0.389, for the DC-10 it is 0.224. The side-projected area of the third engine pod of the DC-10 has been included in this estimate.
Then an estimate for the nondimensional side-force-to-rudder derivative for the DC-10 is:

$$\frac{\partial C_Y}{\partial \delta_R} = 1.594 \times \frac{0.224}{0.3889} = 0.918 \ \ rad^{-1} \qquad (5)$$

When inverting the process above by invoking Eq. (3), for a maximum landing mass (Series 30) of 182798 kg, ρ= 1.225 kg/m^3 and approach speed of 72 m/s (144 kts), the derivative for the DC-10 becomes (based on a total rudder area of 10.3 m^2)

$$Y_{\delta_r} = -0.0102 \ \ (s.rad)^{-1} \qquad (6)$$

This value is about half that of the DC-8, which, compared to the much higher mass of the DC-10, is reasonable.

When estimating the sideslip angle, it became apparent that rudder inputs only contributed very little to the total lateral acceleration. With a maximum rudder deflection recorded of -23 degrees (-0.4 rad), the maximum contribution to the lateral acceleration is then -0.0102 * -0.4 =.00408 m/s^2 = 0.04g. Maximum lateral acceleration recorded was ±0.1g.

Was this then allowed? Useful?

2.2.2.1.2 Side force due to sideslip angle β

One parameter in the equation for β is the side force derivative Y_β. For the DC-8 from the database this value is -8.26 m.(s^2.rad)$^{-1}$. Following a similar line of argument as for the control derivative, one can establish the following rule:

$$(Y_\beta)_{DC\text{-}10} = (Y_\beta)_{DC\text{-}8} \cdot \frac{(S_y)_{DC\text{-}10}}{(S_y)_{DC\text{-}8}} \cdot \frac{(V_a^2)_{DC\text{-}10}}{(V_a^2)_{DC\text{-}8}} \cdot \frac{m_{DC\text{-}8}}{m_{DC\text{-}10}}$$

$$\approx 1.026\,(Y_\beta)_{DC\text{-}8} \times \frac{(V_a^2)_{DC\text{-}10}}{(V_a^2)_{DC\text{-}8}} \times \frac{m_{DC\text{-}8}}{m_{DC\text{-}10}} \qquad (7)$$

Is this approved?

With an airspeed ratio which is about 1.0, and $(Y_\beta)_{DC\text{-}8}$ = -8.26 m.(s^2.rad)$^{-1}$, then one may estimate that $(Y_\beta)_{DC\text{-}10}$ = -3.87 m.(s^2.rad)$^{-1}$. In the above expressions S_y is the projected area in side view.

A comparison between the sideslip angle produced by the "new" estimator and the "improved" estimator is given in figure 15 for the flight at Faro. Clearly visible is the filtering behaviour of the improved estimator, whereas the new estimator includes the higher-frequency variations in the sideslip angle due to turbulence effects. A peak sideslip angle of about 20 degrees can be observed to occur at the end of the data. These turbulence effects will be taken care of by the windshear model identification process.

Where did you observe? The pilot applied near max. rudder, no turbulence effects! Chasing numbers?

2.2.2.1.3 Side force due to yaw rate r

The side force due to yaw rate is derived from the side force due to sideslip angle derivative Y_β, assuming that the vertical tail area contributes most to these derivatives. From Ref.5 one can obtain

$$Y_r = \frac{\rho S b U_0}{4m} C_{y_r} = -\frac{\rho S U_0 l_v}{2m} C_{Y_\beta} \qquad (8)$$

where Cy_β is based on the vertical tail area, and l_v is 25 m for the DC-10. With $(Cy_\beta)_{DC\text{-}10}$ obtained from

$$C_{Y_\beta} = \frac{2m}{\rho S V_a} Y_v = \frac{2m}{\rho S V_a^2} Y_\beta \qquad (9)$$

NLR lost contact with (1) flying in gusty winds, by a pilot who did not handle the controls as he was supposed to, and (2) with objective and real flight data as recorded on the DFDR.
Did you include effects of yaw damper, all feedbacks to the ATS, etc. etc, i.e. a dynamic environment?

Why is this analysis not in CR 94238 C anymore? Because it is not right, not applicable to this flight, is it?

follows simply:

$$(Y_r)_{DC-10} = \frac{l_v}{V_a} * (Y_\beta)_{DC-10}$$
$$= \frac{25}{72} * -3.87$$
$$= -1.34 \quad m.(s.rad)^{-1} \qquad (10)$$

With the low yaw rates involved in the Faro case, the contribution of the yaw rate term in computing the sideslip angle will be negligible.

2.2.2.2 Angle of attack calibration

Why are airspeed, density and temperature not included?

Originally the calibration used for the fuselage angle of attack, for a flap setting of 50 degrees, for the DC-10 was:

$$\alpha_f = 0.519\ \alpha_{vane} - 0.00566 \quad (rad) \qquad (11)$$

It turned out when this standard alpha-vane angle calibration was used, that the resulting vertical wind became unrealistically large, in a negative sense. Hence an alternative calibration was used, based on the assumption that the vertical wind velocity, when going through the core of a downburst, must be zero. The alternative calibration was

$$\alpha_f = 0.519\ \alpha_{vane} + 0.0499 \quad (rad) \qquad (12)$$

For pitch rate correction of the alpha-vane signal a distance between the alpha-vane and the center of gravity of 16.8 m was assumed to exist. The pitch rate signal was derived from the pitch angle by differencing the 10-second running mean pitch angle. This filtering was performed in order to avoid noise to enter the equation due to the relatively low resolution of the signal.

Elevator was far from max. deflected!

With this calibration the first windshear analysis was performed. It turned out that the windshear identification program had difficulty modeling the downburst vertical wind profile that existed, and relatively large residuals in the vertical wind remained. The reason was that there was a negative trend in the vertical wind towards the end, which was very hard to correct for. By visually inspecting the residuals, and by trial and error, it was found that the probable cause for this could be the effect of sideslip angle on the

Were there vertical winds? No. Look at the DFDR data, knowing the non-precision approach procedure, and the warnings in the AOM to discontinue PAPI guidance below 200 ft.

angle of attack, which is a real phenomenon. By correlating the vertical wind model error with sideslip angle, a statistically significant, corrective term in the alpha vane angle calibration could be found, which turned out to have a very beneficial effect on the overall windshear identification process. The main effect was to change the negative trend of the vertical wind towards the end of the data set. This made it possible to apply a correction to the alpha vane calibration, such that the vertical wind could be shifted downwards. This in turn made it possible for the windshear identification process to much better identify the downburst model in the beginning of the data run.

Are you really sure? No more than wishful thinking.

After having gone through such an iteration process twice, the final alpha vane angle calibration applied was as follows:

$$\alpha_f = 0.519\ \alpha_{vane} - 0.0888\ \beta + 1.50\ \alpha_{vane}\beta + 0.0312 \quad (rad) \qquad (13)$$

Do you really have faith in these calculations? Not really, is it? In flight-test we'd use a flight-test nose boom, because there is no other accurate way.

The reason that ILS and other landing systems exist shows that these calculations cannot be accurate enough. Too many uncertainties in variables and too many estimations.

2.2.3 Lateral and vertical flight profile

The resulting 3-dimensional flight path, obtained from the Kalman filter-smoother is given in this section. This consists of the lateral flight path (x,y) and the vertical profile (x,z).

Two axis systems can be used to portray the flight path. In the first one the position is given in a Cartesian axis system, with the x-axis pointing true north, the y-axis pointing true eastward, and the vertical z-axis pointing downwards. The height h=-z is positive upwards, in the normal sense. The origin of the axis system is located at the runway threshold.

In the second (righthanded) axis system, called the runway axis system, the x-axis is aligned with the runway, with the positive x-axis pointing from the runway threshold upwind in the take-off direction, the y-axis points to the right, and again the z-axis points into the ground, following the righthand rule. The origin of this axis system is also located at the runway threshold. The distance from the aircraft to the origin of this axis system, measured along the x-axis, is also called the downrange distance, and the distance to the right the crossrange distance (positive to the right of the runway centerline).

How did you calculate?

This figure cannot be right. Fig. 17 same.

How did it become clear?

a) lateral flight path (Figs. 16 and 17). The flight path in north-south and east-west distance is shown in figure 16. A larger-scale situation is depicted in figure 17. In these figures also the VOR/DME approach radial and the runway centerline are depicted. It becomes clear from this that the aircraft is north of the intended track, but is curving southward, and then proceeds to intercept the runway centerline. The final point has been estimated to be located 315 m downward of the runway threshold, on the centerline. This is based on the estimate that at the final sink rate of 1000 ft/min only 2-3 seconds of flight is left before impact with the runway. The distance flown during the flare has been disregarded. At a groundspeed of about 70 m/s the 2-3 seconds of flight equates to a distance of about 185 m. It was learned that touchdown markings were found on the runway about 500 m down the runway, placing the estimated final point of the data here at 315 m down the runway. A better definition of this final point can only be obtained using flight data from the flight data (crash) recorder. The larger-scale picture shows that the aircraft is curving slightly to the north above the runway, with the final segment indicating that the aircraft's track does not align with the runway.

Not in agreement with control inputs.

Did you not notice the pull-up for go-around?

Airspeed had decreased to 126 kt, 63 m/s with only cross-wind

on the left side (half outside of), but in the direction of

really that accurate? Can you believe those numbers? Where is your accuracy estimate?

b) vertical profile (Fig. 18). The altitude versus downrange distance profile during the approach is depicted in figure 18. The altitude vs downrange distance profile of the VOR/DME approach is also given. The aircraft seems to follow the required altitude reasonably well, but oscillations can be seen to develop after 07:30:40 GMT. Either the aircraft is leveling off at the minimum descent altitude (MDA) of 400 ft (122 m), before proceeding, or the pitch (phugoid) oscillations have grown to such an extent that the aircraft coincidently levels off at about 125 m. At 07:32:40 GMT the aircraft has arrived above the runway threshold (within the uncertainty of the final point as discussed before), at an altitude of 150 ft (45 m), and seems to have leveled off again when the power levers are closed. In view of the fact that the airspeed is not high at this point, this would not be necessary. With the aircraft in a high-drag configuration at this point (flaps 50 degrees), closing the power levers at this relatively high altitude has the potential of a hard landing. With the aircraft still crabbing, the combination of these factors has the potential of damaging the landing gear.

The copilot was interfering with the autopilot (in vert. spd mode) by pushing and pulling the controls inappropriately.

The AOM warns to not descend below PAPI lights below 200 ft to avoid the landing gear of the big DC-10 from touching down before the threshold.

No, just the transition from vert. spd mode to manual using CWS, at the prescribed altitude. The ROD set on the AP was obviously a little larger than required for the actual wind, making level flight for 10 s required to intercept the PAPI glideslope lights.

Considerable? Was the filter fed with pilot inputs as well? Are you not chasing numbers?

c) vertical speed (Fig. 19). The vertical speed, as estimated by the Kalman filter-smoother process, shows considerable oscillations after 07:31:20 GMT. At about 07:32:15 GMT the aircraft even starts climbing. Sink rate in the final portion of the flight is reduced to about 100 ft/min at about 07:32:40 GMT. This is the point where the throttles were closed. After this point the sink rate increases to about 1000 ft/min.

Climbing? Did you look at DFDR data? The pilot saw three red and one white PAPI lights, he was too low.

and the pilot pulled on the controls to avoid touchdown ahead of the threshold; the captain told him (CVR).

2.2.4 Wind profiles

The wind components were computed by the OUTFLOW-program by computing the difference between inertial and aerodynamic velocities. The inertial velocities were determined by the Kalman filter-smoother process. The aerodynamic velocities were determined using the calibrated airspeed, true airspeed, Mach number, static and/or total air temperature, and the alpha-vane angle. The calibration of the alpha-vane angle has been described before (section 2.2.2.2). The sideslip angle was estimated using the new estimator described in section 2.2.2.1.

What is the accuracy?

The resulting wind profiles are given in figures 20-26, and are discussed next. The last two figures, figure 25 and 26, contain results on wind profiles obtained from data measured on board a Martinair B767, which landed at Faro airport 5-6 minutes before the DC-10.

The beginning of light turbulence, copilot manipulated the elevator control against the autopilot.

a) vertical wind (Fig. 20). The time history shows a classic case of vortex passage, i.e. the aircraft must have passed through, or very close to, the core of a ring vortex which describes the phenomenon of a downburst. This is indicated by first a downdraft, and then an upward peak, followed again by a downward going trend in vertical wind. Maximum updraft measured is about 6 m/s, or 1180 ft/min. It is worthy to note that the greatest change in vertical wind, from the upward peak downwards to about zero, occurs at 07:31:40 GMT, which coincides with the moment of switch-over of autopilot mode, from autopilot to CWS. The rapid change in vertical wind, or negative gradient, will lead to a downward pitching motion of the aircraft, when gone unchecked. This can be explained by visualizing the wing to just have left the updraft region, but with the tail area still in the updraft, causing the nose to pitch down. The magnitude of this response depends on the magnitude

when the copilot pushed the pitch control against the vert. spd mode of the autopilot. Switch to CWS was at 07:31:56 your time.

It seems that the writer is biased by the requirement to write towards windshear effects, and did not objectively analyze all of the available the data.

of the gradient $\partial W_z/\partial x$, where W_z is the vertical wind, and x the (horizontal) distance.

Bad analysis

Then why does the heading to get to the airport not change? (the drift angle would change).

b) north and east wind components (Fig. 21). The typical characteristic of these wind profiles is the trend with time which exists, especially in the east-west wind component. There is a stiff southerly wind component of between 10 and 20 m/s (20-40 kts), with some large peaks at the end reaching even to 30 m/s (60 kts). At the initial point the wind is still coming from the east, i.e. there is a headwind, but this changes into a westerly wind component of 10 m/s (20 kts). The north-south wind component shows a reversal in trend at about 07:31:40 GMT. Overall there is quite some turbulence, on which more will be said in the next chapter.

What makes you say this?

In aviation called headwind

c) along-track and crosstrack wind components (Fig. 22). Because of the nearly east-west orientation of the runway (runway heading is 106 degrees magnetic, i.e. 100 degree true), the along-track and crosstrack wind components shown in figure 22 look very much like the north-south and east-west wind components discussed previously. The along-track wind changes during the approach from about 5 m/s (10 kts) headwind to 5 m/s (10 kts) tailwind. There is considerable crosswind, starting at about 15 m/s (30 kts) from the right, with momentary peaks (gusts) even of 35 m/s (70 kts).

How do you know?

d) total windspeed (Fig. 23). The total windspeed (vector sum in the horizontal plane) shows the reversal in trend observed before, with an increasing level of turbulence after the point where the reversal occurs, i.e. after about 07:31:40 GMT. Shown in the same figure is the windspeed as observed by the meteo for runway 11 on the airport as function of time. A mean wind and a maximum wind (gust factor) have been reported by the meteo for this runway, and are shown in figure 23. The wind at 07:32:40 GMT, as obtained from the windshear analysis, shows a windspeed above the runway reported maximum windspeed.

If so, then why didn't the airplane heading change during the last 80 s of flight?

e) wind direction (Fig. 24). The wind direction shows an almost continuing change with time, with the wind veering from about 160 degrees to 200 degrees during the approach. This is contrary to the boundary layer effect, where one would have expected the wind to back during the approach due to boundary

Boundary layer is on the wings, isn't it? You mean ground effect? (Below half wingspan height?)

layer friction. This indicates that some form of advection is taking place. The wind direction reported by the meteo shows the same identical trend with time, giving supporting evidence that some type of advection, or frontal passage, is taking place, and that the change in wind direction is a function of time, rather than distance from the airport.

f) north and east wind components from the B767 (Fig. 25). A Martinair B767 landed prior to the DC-10 at about 07:26 GMT, i.e. only about 6 minutes earlier. From this perspective it is very interesting to see what kind of wind profile this aircraft experienced, compared to the DC-10. The north-south and east-west wind components are shown in figure 25. It is worthy to note that here no trend with time is observed in the east-west wind component, and that furthermore there is a normal boundary-layer effect towards the end of the data. Average easterly wind is about 7 m/s (14 kts).

The north-south wind component also shows no trend with time, other than a ground effect near the end of the data stream. Average southerly winds are about 13 m/s (26 kts), and turbulence is evident in the time history. When comparing figure 25 with figure 21 the major difference is the time variation which characterizes the wind profile of the DC-10.

g) vertical wind from the B767 (Fig. 26). The time history shows a relatively uneventful profile, with the vertical wind generally around zero for the major part of the flight segment. However, there seems to be what amounts to an updraft region in the early part of the approach. This could well be the building up of the downburst which the DC-10 flew through about 5 minutes later.

The wind analysis presented above doesn't agree with DFDR data. Cannot be correct.

2.2.5 Turbulence profile

DFDR vert. g proves light turbulence, i.a.w. ICAO definitions.

As was evident in the data provided so far, there is quite some turbulence present in the wind. An impression of the amount of turbulence was obtained by smoothing the wind profiles and then taking the difference with the raw data. The remnant is defined as turbulence. It turned out that the spectra of the various wind components showed more or less random signals at average periods of 10s and shorter. Therefore the wind profiles were smoothed using a

10-second moving averaging window. For each sliding slot of 10s the rms (σ) was calculated. The results are shown for the total windspeed, wind direction and vertical wind component.
Generally the average turbulence σ is about 2 m/s, which scales very well with the average windspeed Vw of about 20 m/s. The ratio $K=\sigma/Vw$ is about 0.1, which is a standard value for normal turbulence generation in flight simulators for instance. For thunderstorm turbulence a value of 0.2 is normally used.

a) mean windspeed and variation (Fig. 27). The smoothed total windspeed indicates the same reversal in trend at about 07:31:40 GMT, where the windspeed reaches a minimum of about 14 m/s (27 kts); the turbulence σ reaches a local maximum at this point, and increases towards the end of the flight to a value of about 6 m/s (12 kts).

b) turbulence ratio K (Fig. 28). When calculating the ratio $K=\sigma/Vw$ using the *local* windspeed as function of height for instance, then, because of the decreasing windspeed and the increasing turbulence, the ratio K shows a relatively large peak value of about 0.25 at an altitude of about 220 m (660 ft). Also towards the ground the ratio K increases quite strongly, reaching a peak value of about 0.3. The line for K=0.1 and 0.2 is also indicated in the figure. It is evident from this figure that the turbulence level is heavy to severe.

c) mean wind direction and variation (Fig. 29). The mean wind direction shows of course the same trend with time as noticed before. A trend starts to occur at about 07:31:00 GMT, and this trend remains fairly constant. The variation in wind direction shows a bulge at 07:31:40 GMT, and also 40 seconds later. The first bulge coincides with the airplane exiting the downburst. Towards the end, however, the variation reduces (to about 1 degree rms), meaning the wind direction has become more or less smooth.

Then why no heading change to continue the flight to the runway?

Sure? Not pilot control inputs?

2.3 Windshear models identification

2.3.1 Available windshear models

The windshear model identification process has been performed using program GNI, and has been applied to the raw wind component profiles generated by program OUTFLOW. A description of program GNI is given in Ref. 6. For each application a number of windshear models can be included in the list of possible models to be identified.

The most interesting one is the downburst or microburst model. This is based on the ring-vortex model as developed by the British Defense Research Agency and defined by Schultz (Ref. 7). Whether the model is a downburst or microburst model is a question of definition. The only difference is the scale at which wind changes occur. The ring-vortex downburst model is defined by 6 parameters per model, i.e. the vortex strength Γ (m^2/s), the radius R (m) of the ring-vortex, the core diameter d (m), the height of the core z (m) and the position coordinates x and y (m). The model parameters are stationary. It may be possible to extend the model specification by including a velocity vector (2D) with which the model is moving, adding 2 more parameters, viz. Vx and Vy.

Normally, in conjunction with the downburst model(s), also a boundary-layer model can be employed. This model is specified by 6 parameters, viz. the exponent n, the velocity (m/s) and direction of the wind at the top layer of the boundary, the wind direction and speed (m/s) at the bottom layer, as well the boundary-layer thickness H (m).

Additionally a low-level jet can be included in the general study on windshear, but this was not appropriate here. An extra model had to be developed, however, and that was the time-varying wind. From the fact that wind direction, as experienced by the aircraft, changed with time at the same rate that the reported meteowind direction at the airport changed, it was deduced that the wind variation was primarily temporal (and not much dependent on position). Hence a time-varying model had to be employed. This added 8 more parameters, viz. the time at which it starts plus the wind

direction and speed at that moment, the time at which it stops varying, and the wind direction and speed at that moment, and the upper and lower heights of the layer in which this change takes place.

Another model available in the inventory is the frontal shear model. With this model wind variations in speed and direction can be described over a certain height interval. This model was also included in order to account for wind variations unaccounted for by the time-varying model. The phenomenon experienced at Faro may well lead to the requirement that the frontal-shear model may have to be extended to include sloping fronts, whereby the wind variations do not only occur over a certain height interval, but also within a certain distance horizontally.

2.3.2 The identification process

The windshear model parameter identification process is nonlinear. The process starts with an initial estimate of the type, position and value of the parameters of the windshear models, after which the algorithm will start to reduce the error between the model-generated wind profile and the one measured, by varying the windshear-model parameters. Because of the nonlinear nature of the estimation process, an initial estimate "twice" as far away from the true solution, will not automatically generate corrections that are also twice as large. They could even be totally different in sign and lead to divergence of the error. Manual inputs and insight in the process is required to stabilize the process.

As it turned out the windshear model identification process proved to be quite a laborious task, where convergence of the solution had to be checked carefully. Inspection of the residuals between model-predicted and measured wind components is an important step for determining the quality and, if necessary, the requirement for an update of the model structure for a better fit. A visual look at these residuals may indicate the presence of yet another vortex or not, since in the ideal case, i.e. when the residuals are the "noisy" remainder between model(s) and data, the trace with time should have a random appearance. Any significant lobe in a residual then indicates a non-random signal still present, which can possibly be accounted for.

Apart from that also the physical implementations of the solution had to be checked. Because of the nonlinear nature of the identification process the program may have converged to a local minimum rather than a global minimum, and more than one solution is possible.

The basic characteristic of the program is that it minimizes the sum of squares of the errors between the measured and model-predicted wind components. Normally each wind component is weighed equally in this sum, but differing weights can be applied to each specific wind component. For example, if one has reasons to believe that the vertical wind component is very accurate, compared to the other components, one may place a heavier weighting in the error sum on the vertical wind component than on the other ones. A good choice for these weighting factors is to take them inversely proportional to the uncertainties with which the wind components have been determined, if this information is known.

3 RESULTS

The results provided are three-fold, viz. in terms of the windshear models detected/identified and the associated wind profiles (section 3.1), the remnant between the windshear-derived and actual winds, i.e. the windshear turbulence (section 3.2), and as an additional result the calculated windshear hazard indices will be provided in section 3.3. These indices were calculated by operating both on the raw wind profiles and on the windshear model-generated wind profiles, and are an indication of the severity of the windshear experienced.

3.1 Windshear

3.1.1 General

When applying the GNI-program, not all the parameters were left free to be determined. In some cases doing so resulted in numerical difficulties associated with convergence. There simply were too many parameters to

estimate from the data. Therefore some parameters were kept fixed at some (estimated) value, that had been determined by some other menas.
The type of windshear model and the number included in the identification process were the downburst (3), the time-varying shear model (1) and the frontal-shear model (1), for a total of 32 parameters. Eleven were kept fixed, leaving 21 to be determined by the program. In the solution presented an equal weighting factor was employed to all wind components.

The GNI-program also yields the covariance matrix, which provides information on the error variance of each free parameter, and the correlation matrix, which indicates the correlation between all free parameters involved. The correlations can be used, if necessary, to determine interdependence of parameters, and can provide further insight as to why certain parameters vary, when others are varied. In the data given below it has been indicated whenever a parameter has been kept fixed.

For the solution presented the overall residual variance, or model mismatch, was 4.0 m^2/s^2, i.e. the overall rms is 2.0 m/s. This "windshear model turbulence" rms is again about 0.1 times the average windspeed of 20 m/s (40 kts), and provides an indication that a lower value than this (i.e. a better fit) cannot very likely be achieved.

3.1.2 Identified windshear models and discussion

After several trials three windshear models were used in the identification process, and proved to give a stable solution. These are a time-varying windshear model, three downbursts/microbursts, and a frontal-shear model. The positional coordinates are given in the same (righthanded) Cartesian axis system as described in section 2.2.1, with the origin located on the runway threshold, and with the x-coordinate in the true north direction, the y-coordinate in the true east direction, and the z-coordinate downwards (i.e. altitude h=-z).

a) time-varying windshear. Concerning the overall time variation of the wind, the time-varying model identified contained the following parameters:

- wind direction at initial time at the lower level of 150 degrees (fixed) and 208 degrees at final time;
- wind direction at initial time at the upper level of 170 degrees (fixed);
- layer thickness of 333 m;
- lower height where layer starts is 0 m (fixed).
- velocity at initial time is 21 m/s at the lower level, and 0 m/s (fixed) at the upper level.

The major driving factor in this model identification was the time-varying wind direction observed earlier in the meteo wind records, which started changing at about 07:31:30 GMT.

b) downburst. The first downburst identified is defined by the following set of parameters:

- core diameter d = 700 m (fixed);
- radius R = 2646 m;
- vortex strength Γ = 12008 m^2/s;
- position x = 2801 m;
- position y = -6069 m;
- height of vortex z =-381 m.

The strength of the vortex of this downburst is about 0.3 times that of the one which is known as the Fort Worth Dallas crash (Γ=40,000 m^2/s), indicating some relevant severity of this system. The major driving factor in the identification of this model was the vertical wind component, especially the initial peak at 07:31:40 GMT observed earlier. The horizontal wind components did not contribute much because the aircraft flew first over, and then underneath the core, so that the horizontal outflow from the model near the ground, which is sensitive to the strength of the vortex, did not affect the horizontal wind variations experienced at this altitude by the aircraft.

c) microburst no. 1. The second ring-vortex system is more of a microburst in terms of size and/or strength, with the following parameters:

- core diameter d = 113 m;
- radius R = 1948 m;
- vortex strength Γ = 1776 m^2/s;
- position x = -921 m;

- position y = -2949 m;
- height of vortex z =-181 m.

The strength of this vortex is about 0.15 that of the downburst, and can be classified as small. The major driving factor in its identification is the headwind change that takes place, at about 07:32:20 GMT. The peak in the headwind is the result of a combination of this microburst with the one described next.

d) microburst no. 2. The third ring-vortex system is also a microburst, with the following parameters:

- core diameter d = 10 m (fixed);
- radius R = 494 m;
- vortex strength Γ = 1382 m^2/s;
- position x = -162 m;
- position y = -530 m;
- height of vortex z =-120 m.

This ring-vortex is about as strong as the other one, to which it is very close. It could be established that the major driving factor in this identification is not so much the vertical wind, which is relatively small in value, but is the headwind change that occurred shortly before the runway, at about 07:32:40 GMT.

e) frontal shear. Fourthly a frontal shear model was identified, with the following parameters estimated or fixed:

- layer thickness of 600 m (fixed);
- wind direction at lower level χ_L = 178 degrees (fixed);
- wind direction at upper level χ_U =178 degrees;
- velocity at lower level = 0. m/s (fixed);
- velocity at upper level = 27 m/s;
- lower height of lower level at 0 m (fixed).

Some of the fixed values of this model (as well as of the time-varying model) were estimated from the meteo data on windspeed and direction. The driving factor in this identification was the initial windspeed trend and wind direction change before 07:31:40 GMT, at which point there is a reversal in windspeed trend.

3.1.3 Situational sketch

For a situational sketch of the location of the various windshears, a bird's eye view is presented in figure 30 and a side view in figure 31. The difference in size between the three downbursts (or one downburst and two microbursts) becomes apparent. The aircraft passes over and underneath the first vortex (a downburst), which lies at a height of 381 m, at an altitude of 473 m and 221 m respectively.

The second vortex, i.e. the ring-vortex of the first microburst, lies at a height of 181 m. At the first intersection of the flight path with the ring-vortex the aircraft is at an altitude of 208 m, and hence passes about 26 m overhead the vortex core; at the second intersection between the flight path and this ring-vortex the aircraft is at an altitude of 105 m, i.e. it passes about 76 m underneath the core of the vortex.

The third vortex lies at an altitude of 120 m. The first intersection point between the flight path and the third ring-vortex is at an altitude of about 71 m, and the second one is at 38 m, hence the aircraft passes underneath this vortex. This is also shown in figure 31.

3.1.4 Matched wind profiles

The wind components generated by the windshear models combined are given in figures 32-34 for the three wind components. The wind components apply to the flight path as flown by the aircraft. The measured wind components are also included in these figures. A discussion follows.

a) east-west wind component (Fig. 32). The windshear-model derived east-west wind component follows the measured wind profile quite well. The effect of the first vortex system, a downburst, is noticeable in the start of the time history, where the windspeed increases from about zero to 2 m/s. This is generated by the aircraft passing just over the vortex core. Furthermore it curves the time history somewhat, and causes a "bulge" at about 07:31:40 GMT. The effect of the second and third vortex system combined (i.e. the first and

second microburst), is to cause a peak in the east-wind of about -7.5 m/s (-15 kts) at about 07:32:20 GMT.

The effect of the third vortex system, a microburst, albeit a much smaller one in vortex strength than the first microburst, can clearly be seen in the east wind (i.e. headwind) change that takes place from about 07:32:30 GMT to 07:32:40 GMT. There first a small drop in east wind to -2.5 m/s (-5 kts), followed by an increase to about -12 m/s (-23 kts) occurs, with a drop back to about -9 m/s (-17 kts), for a total wind change of about 23-5=18 kts in about 8 seconds. Since the east wind is almost identical to headwind because of the orientation of the runway, the effect of this small microburst is a headwind-to-tailwind change of about 18 kts per 8 seconds, i.e. a "shear" value of about 2.2 kts/s. In the final 5-10 seconds of the data the headwind increases again to about -9 m/s, i.e. a 17 kts tailwind.

b) north-south wind component (Fig. 33). This component shows the change in slope at about 07:31:10 GMT. The effect of the first downburst is to cause the time history to become constant, from 07:31:00 GMT to 07:31:40 GMT. The first linear segment is from the frontal-shear model. The second part of the time history shows the downward "bulge", which is a combination of the time-varying shear and the downburst outflow. The effect of the microbursts show up in the small peak and irregularity at about 07:32:30 GMT. The final value at the end of the time history is about -18 m/s (-35 kts), which is a very strong mean crosswind.

c) vertical wind component (Fig. 34). The effect of the three vortices can be clearly discerned. The first one, the downburst, shows the pronounced downward/upward peak, of a size of about ±3 m/s (± 590 ft/min). The second and third vortices combined cause an upward peak in the vertical wind, to a value of about 1-2 m/s. Note that the vertical wind always will reach a zero value when on the ground. This is the theoretical boundary condition, that there can be no vertical wind component when at ground level.

3.2 Windshear-model turbulence

3.2.1 General

The difference between the windshear model-generated wind profile and the measured wind profile, i.e. the remnant or residual, is defined as the "windshear-model turbulence" ν. In fact also here there are three components, viz. ν_x, ν_y and ν_z. The GNI-program operates such that by definition the sum of these windshear-model turbulence components is zero. An auto-correlation check on this remnant also indicated that the autocorrelation function was essentially zero for all 3 components, meaning that the windshear-model turbulence data sequence is a white noise sequence, i.e. an uncorrelated random sequence.

The "windshear-model turbulence" ν as defined here differs formally from the turbulence determined earlier in section 2.2.5. There the turbulence was defined as the difference between the measured and the 10 s mean (smoothed) wind component. The windshear-model turbulence displayed in this section is the difference between the measured and the *windshear model-predicted* wind component, where now the windshear model prediction acts as a sort of filter. Hopefully both definitions will yield the same result, in which case having these windshear models available will allow one to study the structure of the windshear-model turbulence.

The overall rms of ν is 2.0 m/s, which is 0.1 times the average windspeed of about 20 m/s. For generation of turbulence, e.g. in flight simulators, normally a standard rule is used, which relates turbulence intensity σ to mean windspeed, of the following form

$$\begin{Bmatrix} \sigma_u \\ \sigma_v \\ \sigma_w \end{Bmatrix} = \begin{bmatrix} K_u \\ K_v \\ K_w \end{bmatrix} . V_w \qquad (14)$$

A "standard" value for $K_{u,v,w}$ is 0.1, but in thunderstorm situations sometimes a value of 0.2 is used. Furthermore the turbulence is modeled as a coloured noise process, i.e. a low-pass filter acts on the random zero-mean white

noise sequence with intensity σ with a cut-off frequency, related to scale length, dependent on altitude above the ground. The lower the altitude, the "whiter" the turbulence signal becomes. This kind of modeling detail will not be attempted on this data, because that would be beyond the scope of this work, but it will be an area of further research to be addressed in the WINDSTREAM-project in the near future.

The windshear-model turbulence was computed as function of time, which can be replotted as function of either distance (e.g. distance from the runway threshold) or altitude. For convenience, and since turbulence is quite often scaled versus height, the windshear-model turbulence in this case will be plotted against height.

The windshear-model turbulence rms components $\sigma_{x,y}$ and σ_z were calculated by squaring the signals $v_{x,y}$ and v_z, taking the 10-second running moving average, and taking the square root of this signal again. The windshear-model turbulence signal $v_{x,y}$ was derived from the difference between the measured and windshear model-generated horizontal wind vector component, i.e.

$$v_{x,y} = V_w - V_{w_{mod}} \tag{15}$$

3.2.2 Mean wind and windshear-model turbulence profile

In this section a discussion is given about the mean wind profile, as well as the profile of windshear-model turbulence intensity versus height.

a) Mean wind vs height profile (Fig. 35). In this figure the mean horizontal and vertical wind profile is given versus height, together with the measured wind components. It shows a constant minimum in windspeed at about 250 m altitude, which coincides with the change in vertical wind component. Also there seems to be more turbulence, i.e. larger deviations, about the mean horizontal wind profile at this point, and also near the ground, where some large variations can be observed.

b) windshear-model turbulence vs height (Fig. 36). Besides the mean horizontal wind profile, generated by GNI, also the windshear-model

turbulence intensities $\sigma_{x,y}$ and σ_z are plotted against height in figure 36. It shows that the vertical windshear-model turbulence rms σ_z remains fairly constant throughout the altitude range, apart from a "bulge" at about 250 m altitude. Also the horizontal windshear-model turbulence $\sigma_{x,y}$ shows a bulge at the same altitude, and also has another peak near the ground.

c) ratio between windshear-model turbulence and windspeed (Fig. 37). An interesting outcome is to plot the ratio K between windshear-model turbulence rms σ and windspeed Vw. This is done in figure 37 for the horizontal and vertical windshear-model turbulence intensities $\sigma_{x,y}$ and σ_z respectively. Two "standard" values of K=0.1 (normal turbulence) and K=0.2 (thunderstorm turbulence) are also drawn in this figure.

Because of the previously noted decrease in windspeed Vw at about 250 m, together with an increase in turbulence intensity σ, the ratio σ/Vw becomes even more pronounced. For the horizontal windshear-model turbulence $\sigma_{x,y}$ the ratio $K_{x,y}$ exceeds 0.2 at this height, and close to the ground it even reaches a value of 0.3. The vertical windshear-model turbulence ratio $K_z=\sigma_z$/Vw shows more or less the same trend, but peaks at no more than about a value of 0.1. It appears therefore that there are more variations in the horizontal wind component than in the vertical wind component. Because of the ratio between turbulence intensity and windspeed occasionally far exceeding the value of 0.2, one could classify the windshear-model turbulence experienced during this landing approach as heavy or severe.

3.3 Windshear severity

3.3.1 General

Classifying windshear, or windshear-turbulence for that matter, into categories of light, moderate, heavy, etc. is very difficult, also because of subjective criteria that affect the evaluation. A quite common windshear hazard criterion, used almost exclusively in the USA, is the so-called F-factor. This factor is nothing else but a measure of the change in thrust (ΔT)-to-weight (W) ratio an aircraft needs to compensate for airspeed loss or gain due to windshear. When this value exceeds a certain level the extra

thrust-to-weight ratio $\Delta T/W$ is beyond the performance limit of the aircraft, hence there is insufficient extra thrust available to compensate for airspeed loss or gain, and the airspeed of the aircraft will change (disregarding engine thrust response lags, etc.). When this situation lasts for too long a time, the aircraft may lose or gain a critical amount of airspeed. In Technical Standard Order TSO-C117 (Ref. 8) this critical value is set at 20 kts airspeed loss or gain. This document has recently been drafted by the FAA in order to provide a specification document for manufacturers which build on-board windshear alert systems of the reactive type. Application of this type of windshear hazard, however, is hampered by the problem of turbulence entering in the equation. Several filtering constants have therefore been provided for, where filtering consists of time-averaging the F-factor signal over a certain time interval. Depending on the lengths of these time intervals hazard limits are defined. Especially for the shorter filter time intervals these limits still need further definition, in order to solve the question of nuisance alerts due to turbulence.

One of the practical drawbacks of filtering is the time delay associated with it. This means that a critical warning will be delayed by a certain amount, which will not benefit the aircrew.

A typical formula for determining the F-factor is:

$$F = \frac{1}{g}\frac{dW_x}{dt} + \frac{W_z}{TAS} \qquad (16)$$

where W_x is the local headwind component, and W_z the vertical wind component. A decrease in headwind, i.e. dW_x/dt is negative, also has a negative interpretation, i.e. a loss in performance ($F<0$). A critical level of about ± 0.1 is normally used, meaning that the residual extra margin for acceleration-deceleration available is about 0.1g, i.e. $\Delta T/W \approx 0.1$. For most transport aircraft this is the case.

3.3.2 Windshear hazard at Faro airport

The windshear hazard experienced at Faro airport, in terms of the F-factor, is depicted in figures 38-41. It should be reminded that dW_x/dt in the

equation for F (Eq. (14)) is the total derivative, computed from the partial time derivative $\partial W_x/\partial t$ and pitch and yaw rates q and r as follows:

$$dW_x/dt = \partial W_x/\partial t + q.W_z - r.W_y \qquad (17)$$

Both the pitch rate and the yaw rate were derived from differentiating the 10-second running mean pitch and heading angles, in order to avoid getting quantization noise due to low resolution in the pitch and heading angle.

a) raw F-factor (Fig. 38). The F-factor, based on the unfiltered local headwind component, and shown in figure 38, shows a "noisy" pattern. Several times the critical value of ±0.1 is exceeded, notably near the end of the approach. A negative peak is followed by a "positive" peak. The limits of ±0.1 are limits where an airborne system may have given a warning, pending further analysis of turbulence nuisance alert avoidance. By inspecting the "raw" along-track wind component (Fig. 22) it is clear that the major contribution to F comes from the headwind, and not from the vertical wind component.

For practical purposes (i.e. to avoid nuisance alerts), reactive windshear warning systems employ two mechanism. One is the de-activation of the alarm function when the aircraft is below a certain radio height. In operational systems the alert function is inhibited, i.e. all values of the raw F-factor are invalidated, for (radio-)altitudes below 20 m. This inhibition has also been adopted in the data given here.

The second mechanism is filtering, or averaging, that is employed in order to reduce peaks in the signal, and hence to alleviate alerts due to turbulence. The question still to be answered is what type of filtering to use. Various filter time constants can be taken, and TSO-C117 (Ref.8) indicates a relationship between the value of the filter time interval t_x and alert level. For the purpose of demonstrating the effect of filtering, three filter time intervals, of t_x=3, 6 and 10 seconds are applied.

b) 3-second filtered F-factor (Fig. 39). A filter averaging time interval t_x of 3 seconds was chosen to filter the raw F-factor. Associated hazard limits are ±0.1 where an alert may be given (a "must" alert level was far outside

the range of data). The 3 s filtered F-factor is shown in figure 39. It is evident that the limits of ±0.1 are also exceeded several times. There is a negative peak of-0.2 at 07:32:20 GMT and of -0.3 at about 07:32:36 GMT. Both correspond with the location of the microbursts. The last peak corresponds with the headwind-to-tailwind change due to the second (last) microburst about 1 km before the runway. The airspeed at this point (Fig. 4) can be seen to have dropped from 150 kts to 140 kts (CAS), and then to increase again to 145 kts due to the throttle action and engine response. There is no danger involved in this kind of airspeed fluctuation, hence an unambiguous relationship between windshear hazard or F-factor and airspeed margin for this type of filtering does not exist. This is one of the major subjects of further research in the framework of the WINDSTREAM-project.

c) 6-second filtered F-factor (Fig. 40). The 6-second filtered F-factor is given in figure 40. Here a windshear alert system must give an alert for a value of beyond ±0,175, as indicated in the figure. It can be seen that this "must" alert level was never exceeded, but the "may" alert level was exceeded twice. These moments occur at 07:32:20 GMT and at 07:32:40 GMT, which, because of the 6 seconds filtering, would have given a warning that would have come about 6 seconds late, had a windshear warning system been installed. Both occurrences can be attributed to the headwind-to-tailwind changes associated with the small microbursts mentioned before.

d) 10-second filtered F-factor (Fig. 41). The final filter time used is 10 seconds. The resulting filtered F-factor is shown in figure 41. In this case the alert level of ±0.1 has now become a "must alert" level (Ref. 8). This level is exceeded only once, viz. at about 07:32:45 GMT. This moment coincides again with the last microburst identified at this location. The other peak, at about 07:32:20 GMT, from the first microburst, just does not reach the critical level. Hence it appears that the (possible) windshear alert due to the last microburst occurs quite consistently.

e) windshear-model generated windshear hazard (Fig. 42). An interesting comparison in terms of windshear hazard is the F-factor as produced by the wind profile, generated by the windshear models themselves. This gives an indication of the windshear severity detected by the windshear identification

process. Since all random fluctuations due to turbulence have already been left out, no filtering of the F-factor has been applied here. The resulting windshear hazard is shown in figure 42. It is evident that the greatest variations occur at the end, where the fluctuations in F can be shown to be entirely attributable to changes in the horizontal windspeed. Also the moment where it occurs coincides with the peaks found in the other F-factors (figures 39-41). The double peak corresponds with the interaction of the first and second microburst, and the wind change of this second microburst, found to be situated near the runway threshold. The final F-Factor reaches about zero (when the airplane is reaching the runway threshold).

4 CONCLUSIONS AND RECOMMENDATIONS

Then why did you conduct this analysis? Is unreliable, isn't it?

Conclusions and recommendations are predicated upon the data set delivered to NLR, which was not complete. Flight data for the segment of between 44 ft height and the ground were not included. Also control forces were not available, there were no signals available for NLR indicating the status of the autopilot/autothrottle system, and the angle of attack calibration had to be altered in order to provide realistic vertical wind components. Furthermore the effect of the sideslip angle on the angle of attack vane had to be incorporated. Because of its nonlinear estimation process the windshear identification process itself does not yield unambiguous results. Nonetheless, however, the following conclusions can be inferred.

only light, i.a.w. ICAO scale.

1. The weather was quite turbulent. Since the flight was conducted in a right-quartering crosswind, hence with turbulence, gusts, etc. from the right, this turbulence could increase the pilot workload in handling the aircraft under these conditions.

?? Auto pilot and CWS mode...

2. The aircraft successfully negotiated a downburst early in the approach, from which it emerged at about 700 ft without any detrimental effect, other than a possible onset of a phugoid (see later). Immediately afterwards, and at about 1 km before the runway threshold the aircraft passed through two more microbursts, which can be classified as small. The last microburst caused headwind-tailwind changes of a magnitude

The copilot pushed and pulled the controls...

No, flight path corrections by the copilot, as part of the non-precision approach, and preventing to touchdown early, i.a.w. AOM procedure.

that would have triggered a windshear alert system, had such a system been on board. The potential airspeed loss due to the microburst was successfully negotiated, however, by a rapid power lever increase. Resulting airspeed loss was therefore kept to about 10 kts.

3. The windshear experienced was occasionally beyond the performance limits of the aircraft. The hazard index (F) indicated that such a situation occurred close to the ground, at an altitude of about 50 m. This was accompanied by a rapid power lever increase. There certainly were no "downdrafts" or downward-going wind components which could press the aircraft into the ground. Maximum airspeed changes that were recorded were within acceptable limits during the portion of flight considered in the analysis. Because of the rapidly varying winds it is sometimes hard to differentiate between windshear and turbulence.

4. The overall windshift that was noted to exist during the landing approach caused the aircraft to land at a crosswind which was close to, or might even have exceeded the landing crosswind limit. Calculated crosswind component above the runway threshold was about 40 kts from the right, but this was exceeded several times during the approach. Maximum calculated crosswind component (peak) was about 70 kts, which occurred at about 10 seconds before reaching the runway. Also due to the windshift the aircraft crossed the runway threshold with a tailwind component of about 10 kts, while about 10 seconds earlier the tailwind component was even 22 kts.

5. There are indications that the aircraft made a traverse landing. The vertical acceleration shows the onset of a high rate of descent in the final seconds of data available. This can be attributable to the fact that the power levers were closed at an altitude of about 150 ft. Why the power levers were closed at this altitude is not clear. If not checked this could lead to at least a very firm landing, certainly with the flaps set at 50 degrees. In combination with the crab angle still existing at the end of the available data set, this could lead to a potentially dangerous situation, where the landing gear might be damaged. More flight data is needed, however, to substantiate this.

Are you really sure? Is wind change used to trigger a windshear alarm? You didn't look at pilot control inputs, didn't you? Not very scientific.

Because of the ATS response to an elevator up command by the pilot.

The ATS increased thrust because pilot pulled on the control, and pitched up. Not due to microburst.

Control inputs are windshear, acc. to NLR!?

Looked at formal required approach and threshold speeds? And to the gust filter in the ATS?

There were no rapidly varying winds, refer to DFDR data

How was this noted?

Are you sure? Have you done an approach heading analysis? Why was the heading to get to the runway a constant 125° (DFDR data)? How accurate were your calculations?

Why do you conclude this without having seen the pitch angle increase during the last s of flight?

DFDR data was available until 7.5 s after touchdown.

6. The response of the power levers in the last 10 seconds of data available is very unusual. It looks like the power levers were retarded to idle, although the autothrottle (AT) system was alleged to be functioning. With an airspeed at 07:32:40 GMT of about 145 kts, which is only 5 knots above Vref, closing the power levers at this point, at a height of about 150 ft, is an unlikely course of action for the autothrottle system, unless some failure has occurred, or the autothrottle system has been manually overridden.

Because the copilot did not use CWS as it should be used. He continuously applied pitch control forces.

7. After the change-over in autopilot mode, from AP to CWS (Control Wheel Steering), the approach became unstable. Recorded pitch oscillations of about 6 degrees amplitude occurred, which can be classified as large. The rather sudden start of oscillations in pitch angle at the moment of switch-over could be attributable to the vertical updraft existing at this moment. Why such a departure was allowed to develop is not clear.

In view of some uncertainties the following recommendations are made:

NLR drew conclusions with a limited data set, very very unprofes-sional.

1. It is recommended to acquire the complete set of flight data, using the recorded data from the flight data (crash) recorder in addition to the data from the ACMS, and to analyze the remainder of the airborne portion of the flight, i.e. the segment from about 44 ft radio-altitude to touchdown. and verify the segment before that.

2. It is recommended to further analyze the flight data, especially to correlate control wheel forces and flight parameters, in order to investigate the possibility of PIO (Pilot-Induced Oscillations).

3. It is recommended to further study the functioning of the autothrottle system, by correlating the AT input and output parameters, software, control laws, etc., in order to simulate the AT-behaviour to these signals.

4. It is recommended to obtain transcripted data from the cockpit voice recorder, and to synchronize the crew communication with the flight data as portrayed in this document, in order to better understand the

occurrence of certain phenomena. This should allow several questions to be answered in this report.

5. A flight simulator exercise should be carried out, e.g. to establish the following:
   - to check the effect of closing the power levers at 150 ft altitude on vertical speed at touchdown;
   - to validate the effect of pitch response due to vertical wind (shear) using the derived windshear models;
   - to check on the autopilot mode response, and the possibility of system failure.

   The flight simulation exercise should be performed in a windshear and turbulence environment as identified in this report. Especially the effect of wind gradients on pitching and rolling motion of the aircraft should be included in the aerodynamic model as well as the turbulence model used.

5 ACKNOWLEDGEMENT

I would like to thank Karin Schaap, of the department IN of NLR, for her immediate and willing contribution in this project by processing the ACMS data, and getting the program updated to handle the DC-10. Also I would like to thank Henri Kannemans for his much appreciated contribution by updating and working with program GNI, and providing valuable insight and expertise in analyzing and interpreting the windshear results.

6 REFERENCES

1. Haverdings, H., "WINDSTREAM: WINDShear Technology REsearch Advances Masterplan", NLR Memorandum VV-89-001, 1 May 1989.
2. Haverdings, H., "WINDSTREAM - WINDShear Technology REsearch Advances Masterplan. Status and outlook for 1992 and beyond", NLR Contract Report CR 92073 C (Restricted), 27 February 1992.

3. Haverdings, H., "Preliminary specification of program OUTFLOW: Organisation and Usage of Time histories of Flight data containing Low level Observations of Windshear", NLR Memorandum VV-90-010, 17 September 1990.

4. Haverdings, H., "Statistical analysis of windshear during approach and landing, obtained from AIDS-derived data, Final report, NLR TR 85011 L, 16 January 1985.

5. McRuer, D.; Askenas, I.; Graham, D., "Aircraft dynamics and automatic control",. Systems Technology, Inc., August 1985.

6. Kannemans, H., "Description of program GNI: Gauss-Newton Iteration -for wind shear applications-", NLR Contract Report CR 90396 C (Restricted), 12 October 1990.

7. Schultz, T.A., "Multiple vortex-ring model of the DFW microburst", NASA Ames Research Center In: Journal of Aircraft, Vol. 27, No. 2, February 1990.

8. FAA, "Airborne windshear warning and escape guidance systems for transport airplanes", Technical Standard Order TSO-C117, 27 July 1990.

Control forces by pilots not included? Good enough for accident reconstruction? Difference with AIDS?

Table 1 Parameters registered by the AGMS

parameter	sign conv.	par. No.	Sampling rate (1/s)
Flight controls			
aileron inb. left	+: up	6	1/4
aileron outb. right	+: up	326	1
elevator inb. left	+: nose up	7	1
elevator outb. right	+: nose up	327	1
flap position		19	1
pitch trim		5	1/2
upper rudder deflection	+: right	8	1
lower rudder deflection	+: right	328	1
spoiler lefthand	+: up	32	1
spoiler righthand	+: up	33	1
Aerodynamic data			
alpha vane angle	+: nose up	425	1
CAS		236	1
Mach		239	1
TAS		238	1/2
Inertial data			
Latitude	+: North	170	1/4
Longitude	+: East	172	1/4
Pitch angle	+: nose up	3	2
Bank angle	+: right	4	1
Ground speed		174	1
Drift angle	+: left	357	1
Ground track angle		176	1
longitudinal acceleration	+: forward	108	4
lateral acceleration	+: left	9	4
vertical acceleration	+: up	1	8

parameter	sign conv.	par. No.	Sampling rate (1/s)
Miscellaneous			
Weight		315	1/4
pressure altimeter		232	1
radio altitude		26	1
TAT		241	1/2
SAT		240	1/4
GMT		25	1
Flight Mode			
Navigation data			
Glideslope	+: above	30	1
Localizer	+: right	28	1
magnetic heading		2	1
Engines			
N1#1		58	4
N1#2		59	4
N1#3		60	4
N2#1		61	4
N2#2		62	4
N2#3		63	4
Throttle#1		55	1
Throttle#2		56	1
Throttle#3		57	1

Did ACMS not record VOR radial data?

81

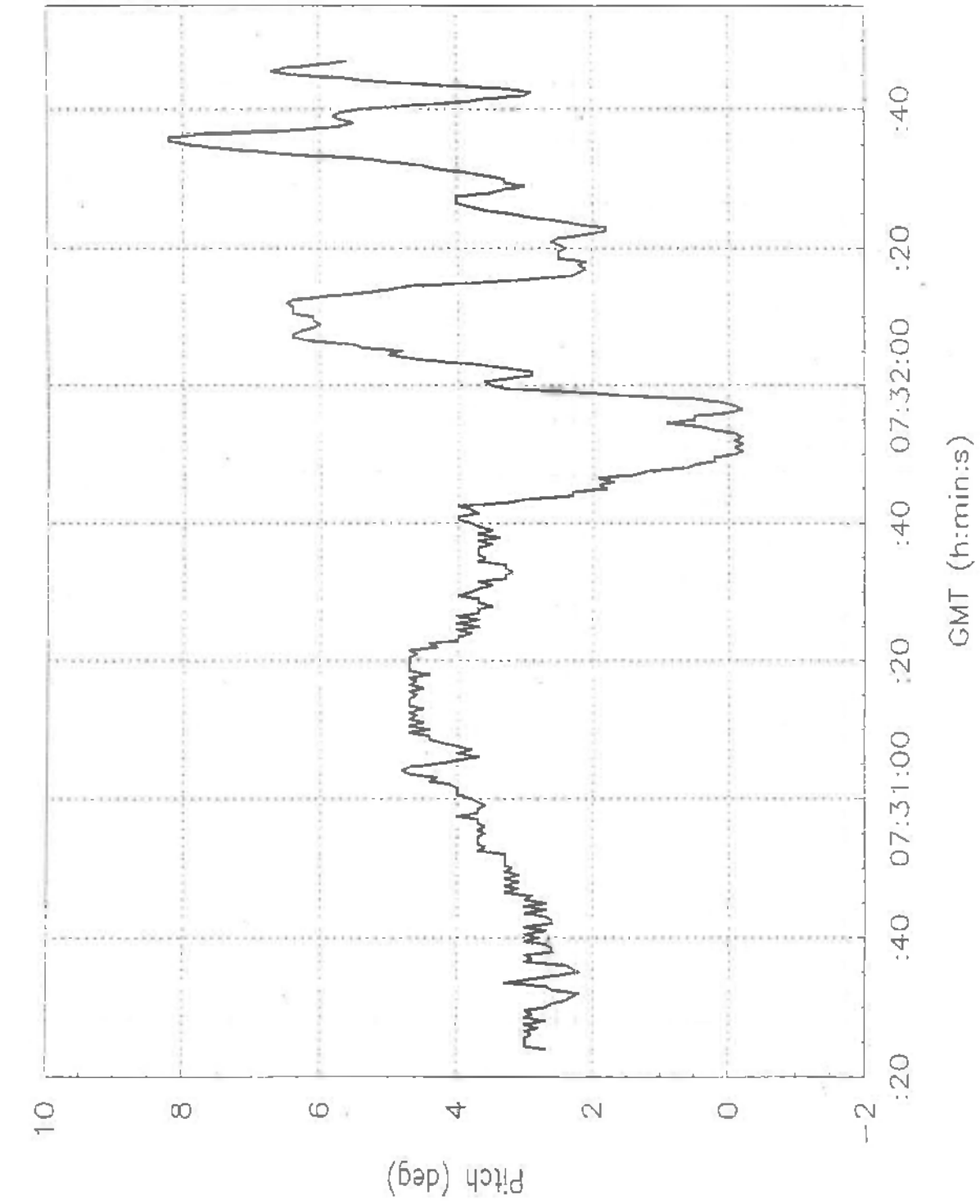

Fig. 1 Pitch angle time history

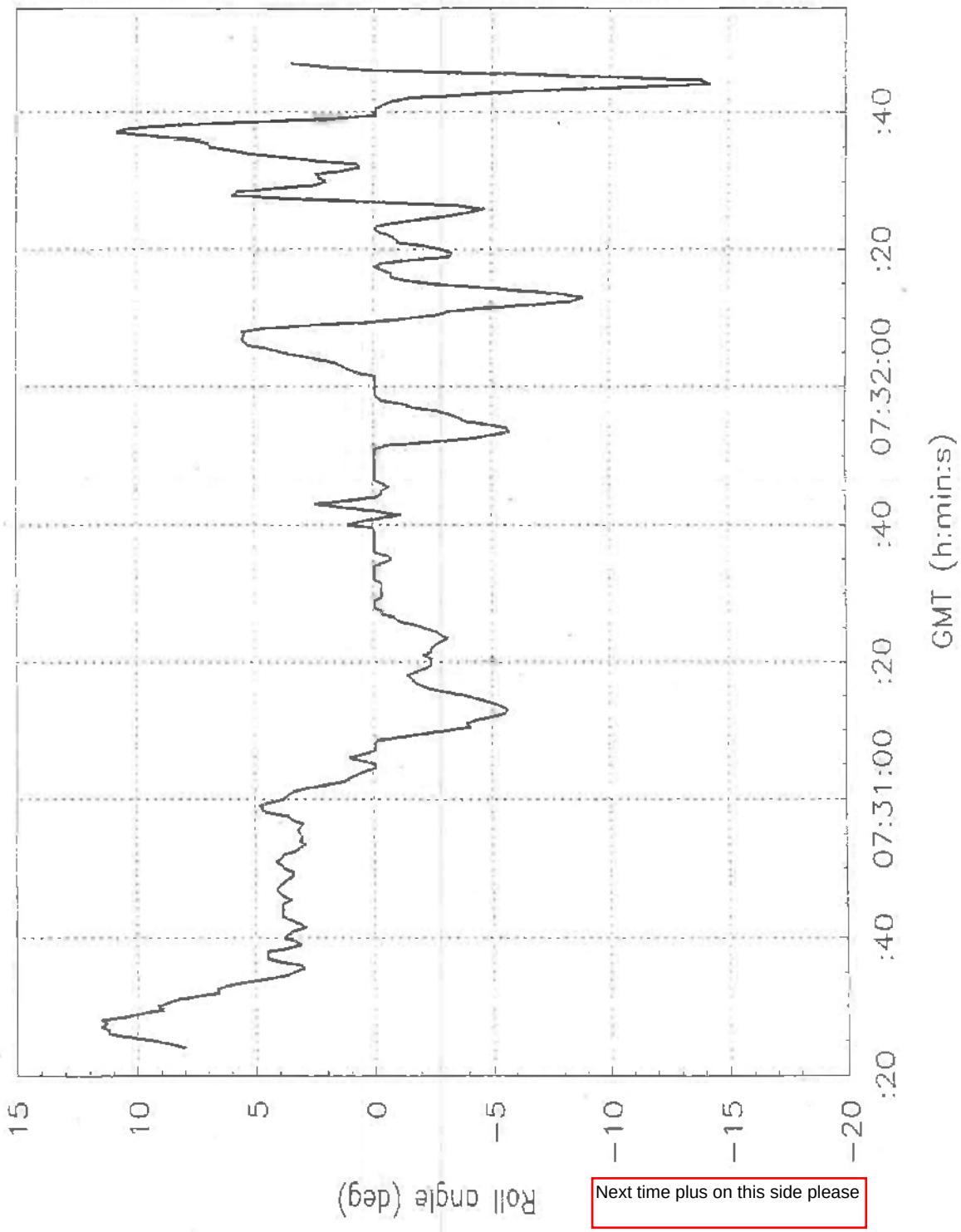

Fig. 2 Bank angle time history

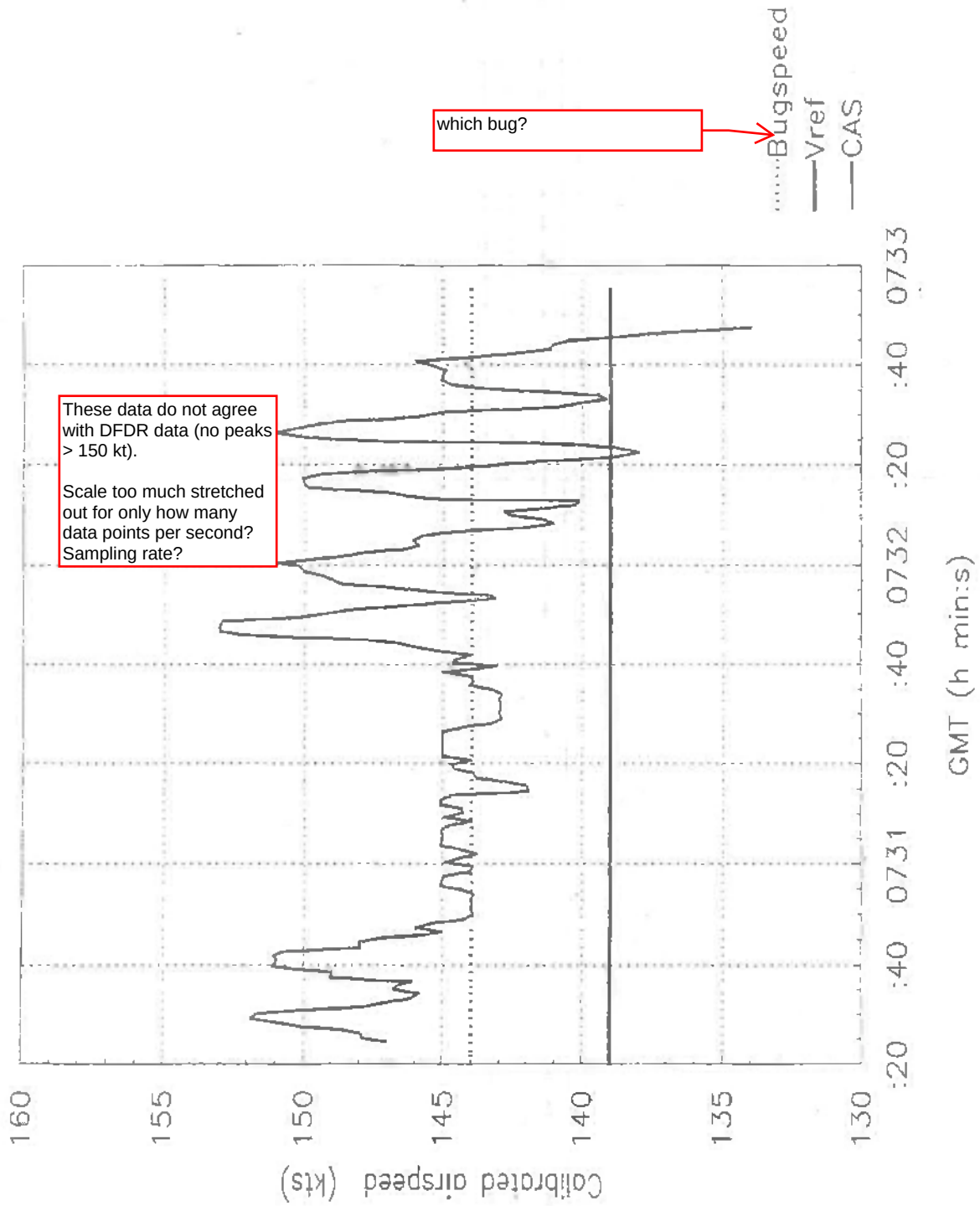

Fig. 3 Calibrated airspeed time history

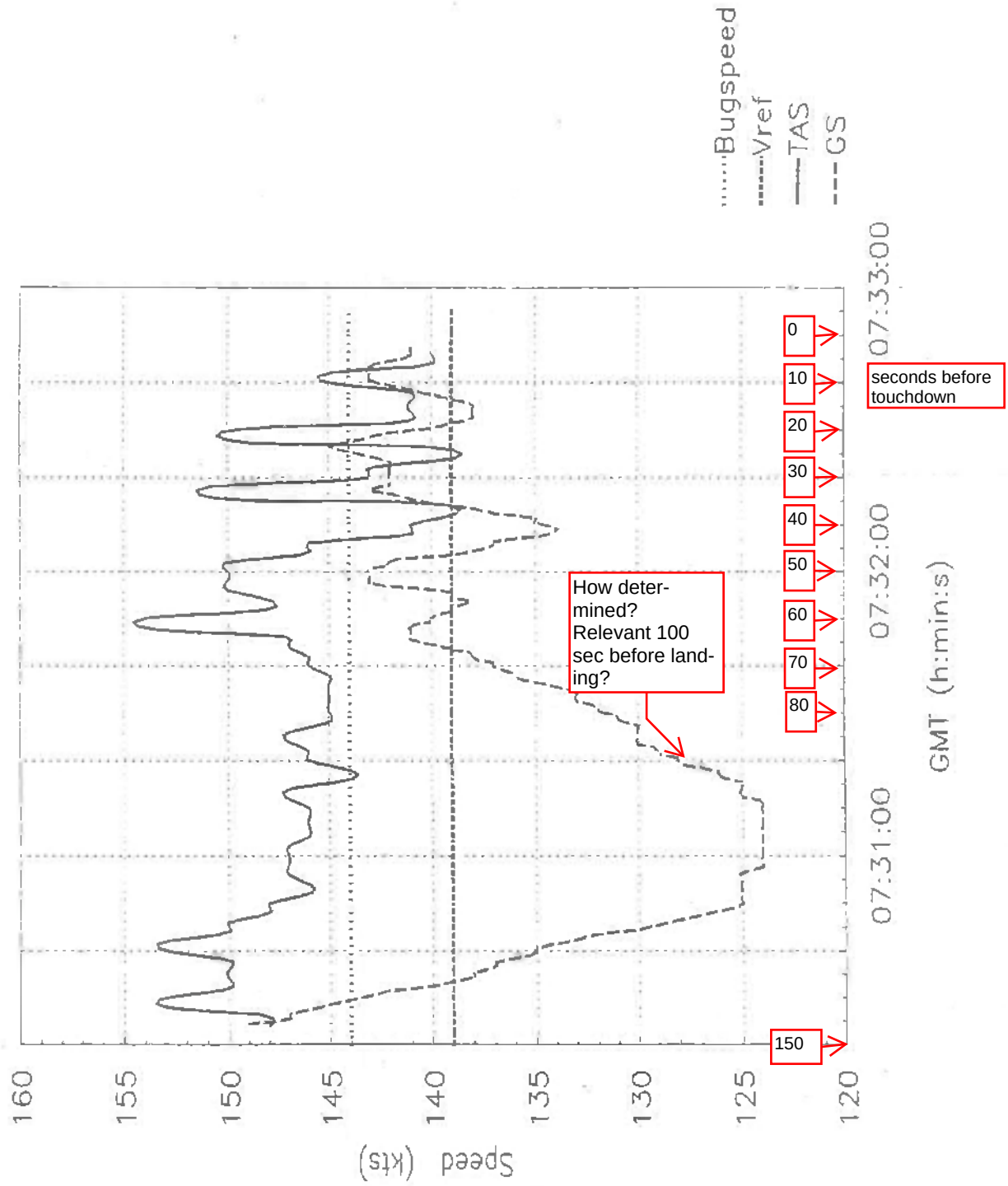

Fig. 4 Groundspeed and True Airspeed time history

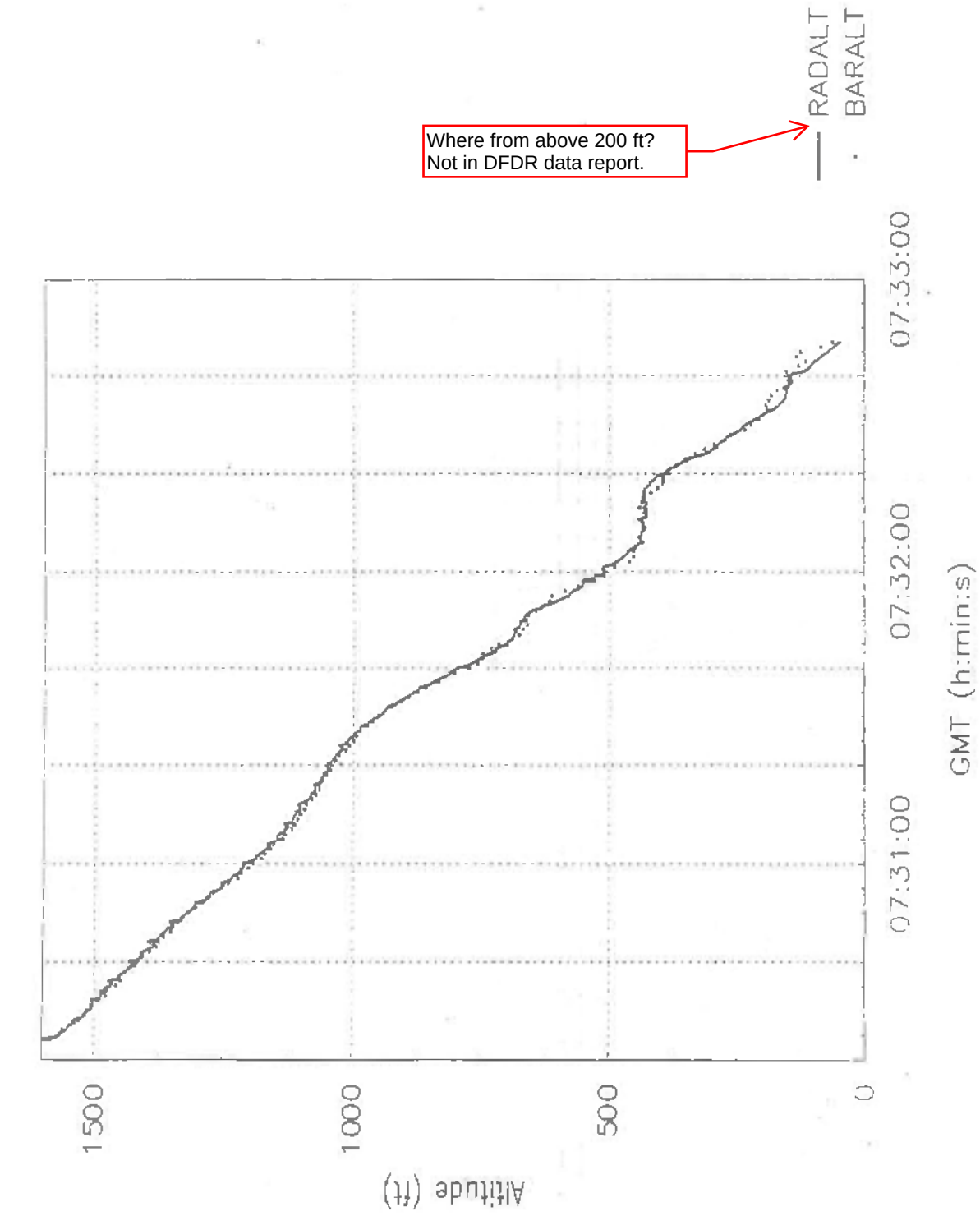

Fig. 5 Barometric and Radio altitude time history

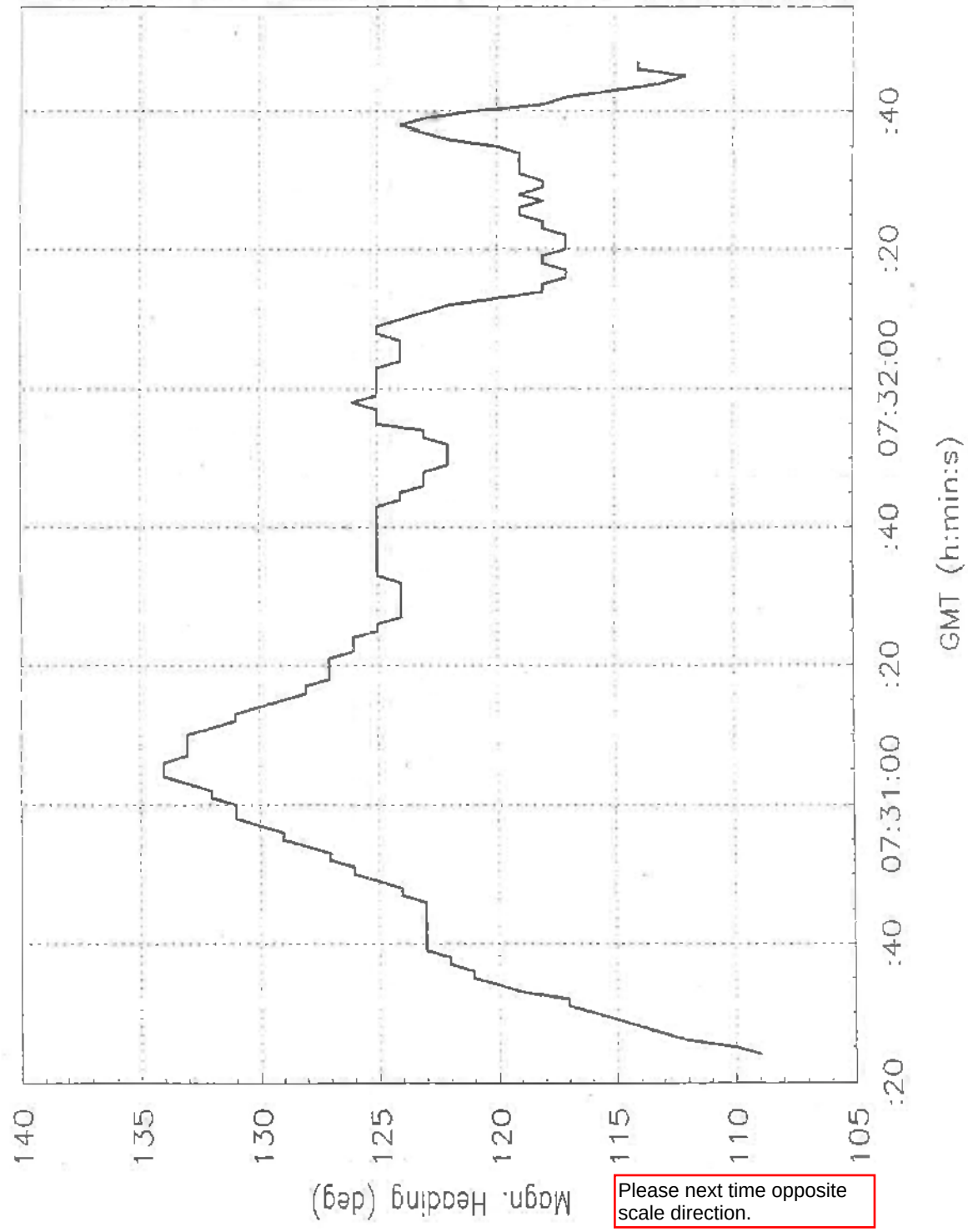

Fig. 6 Magnetic heading time history

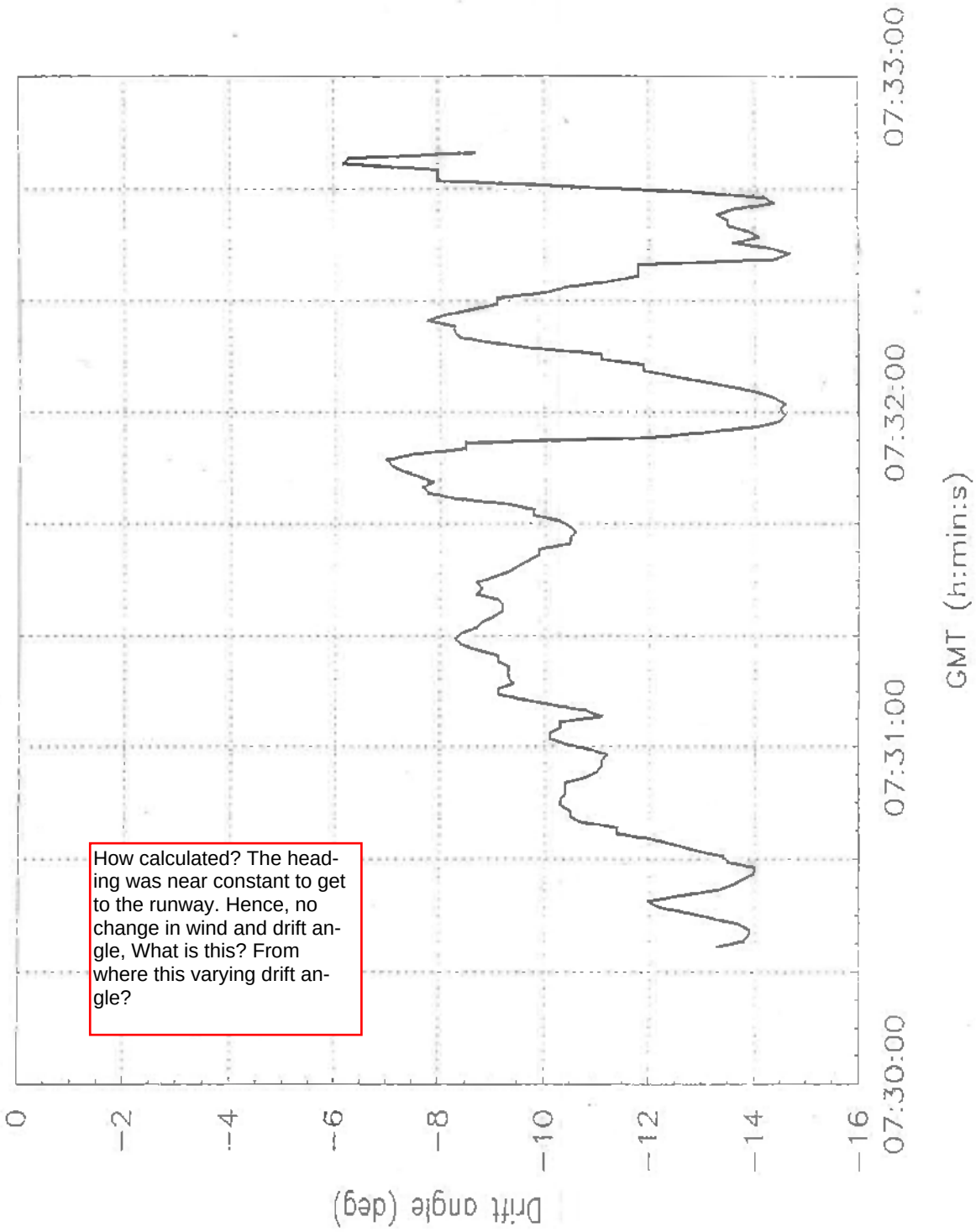

Fig. 7 Drift angle time history

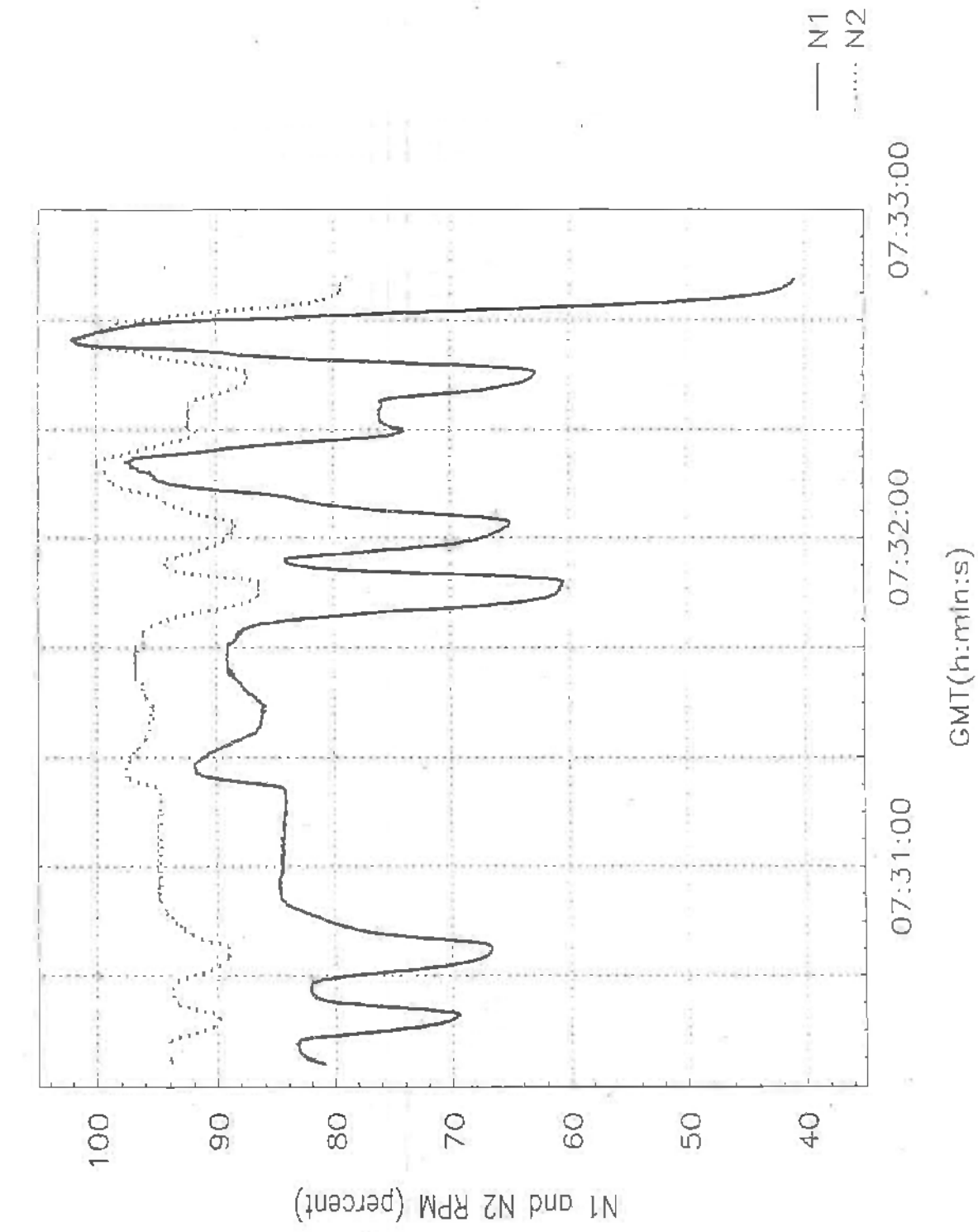

Fig. 8 Engine N1 and N2 rpm time history

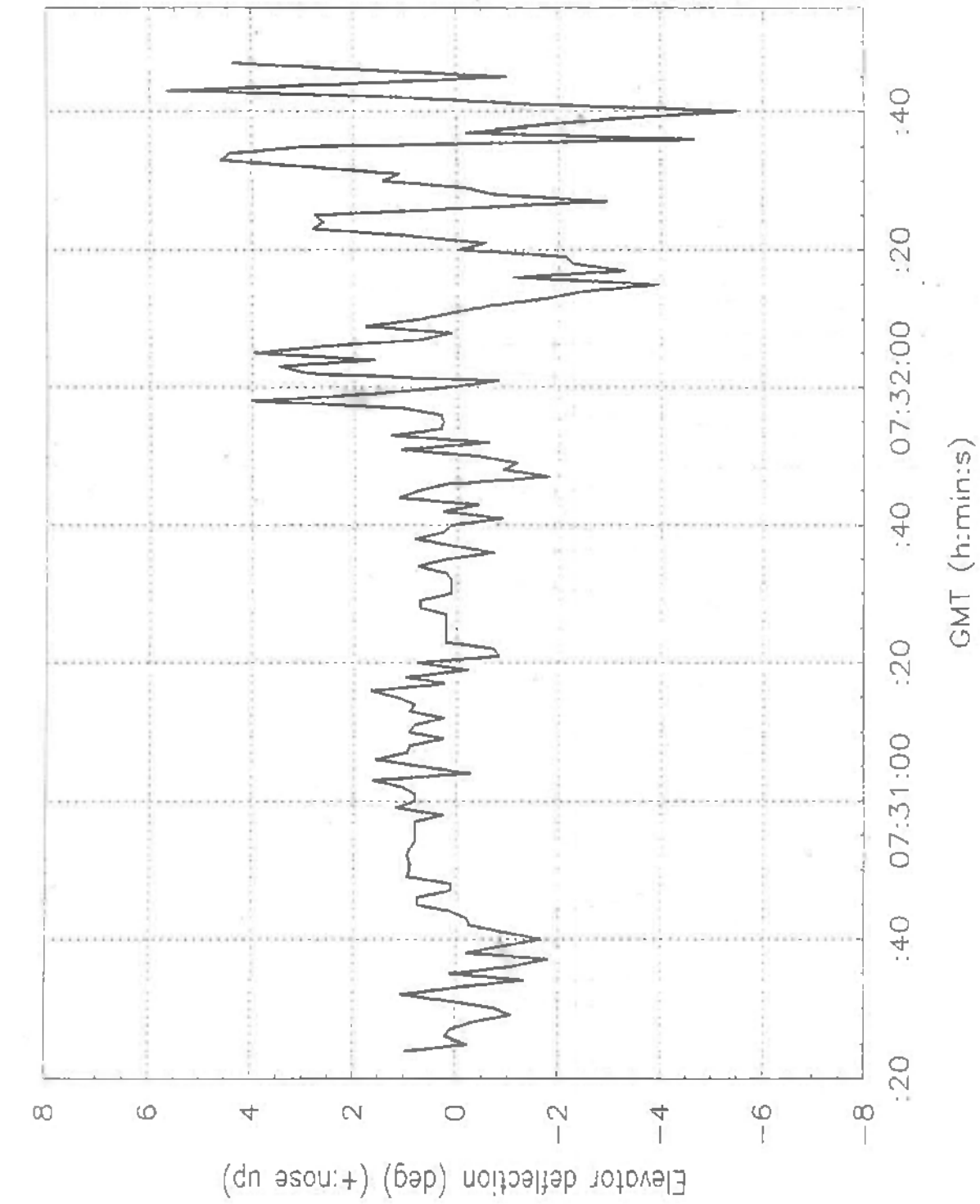

Fig. 9 Elevator time history

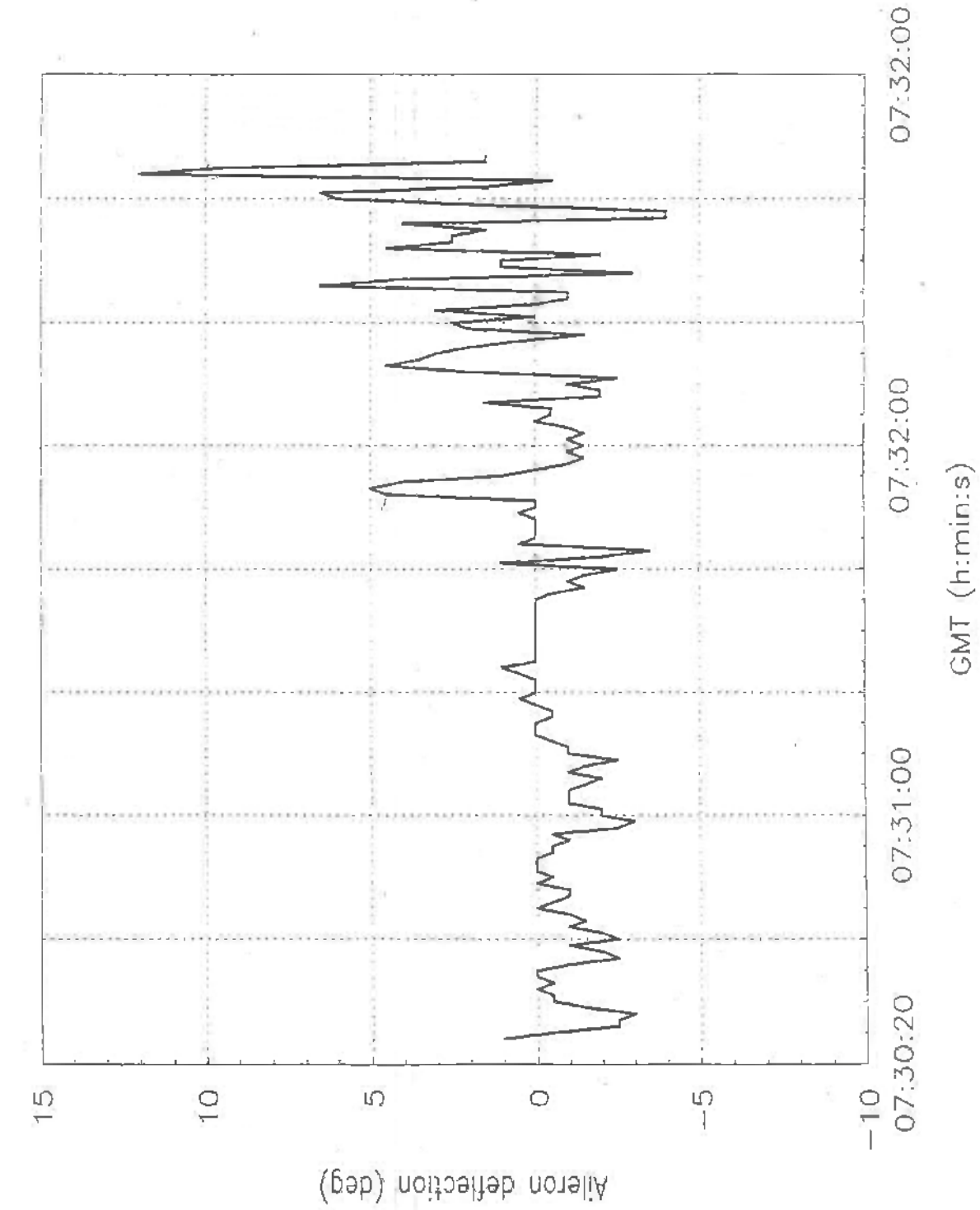

Fig. 10 Aileron deflection time history

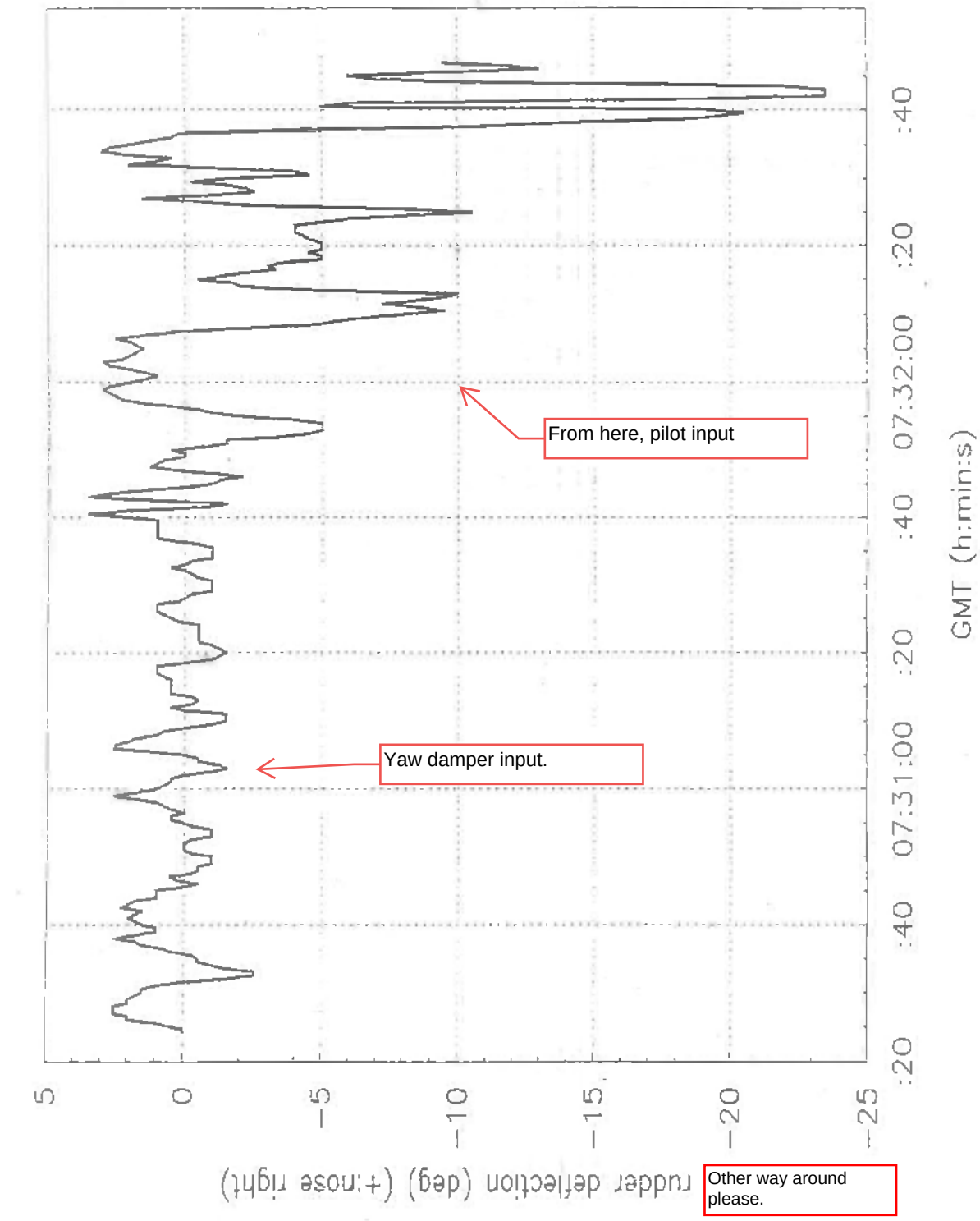

Fig. 11 Rudder deflection time history

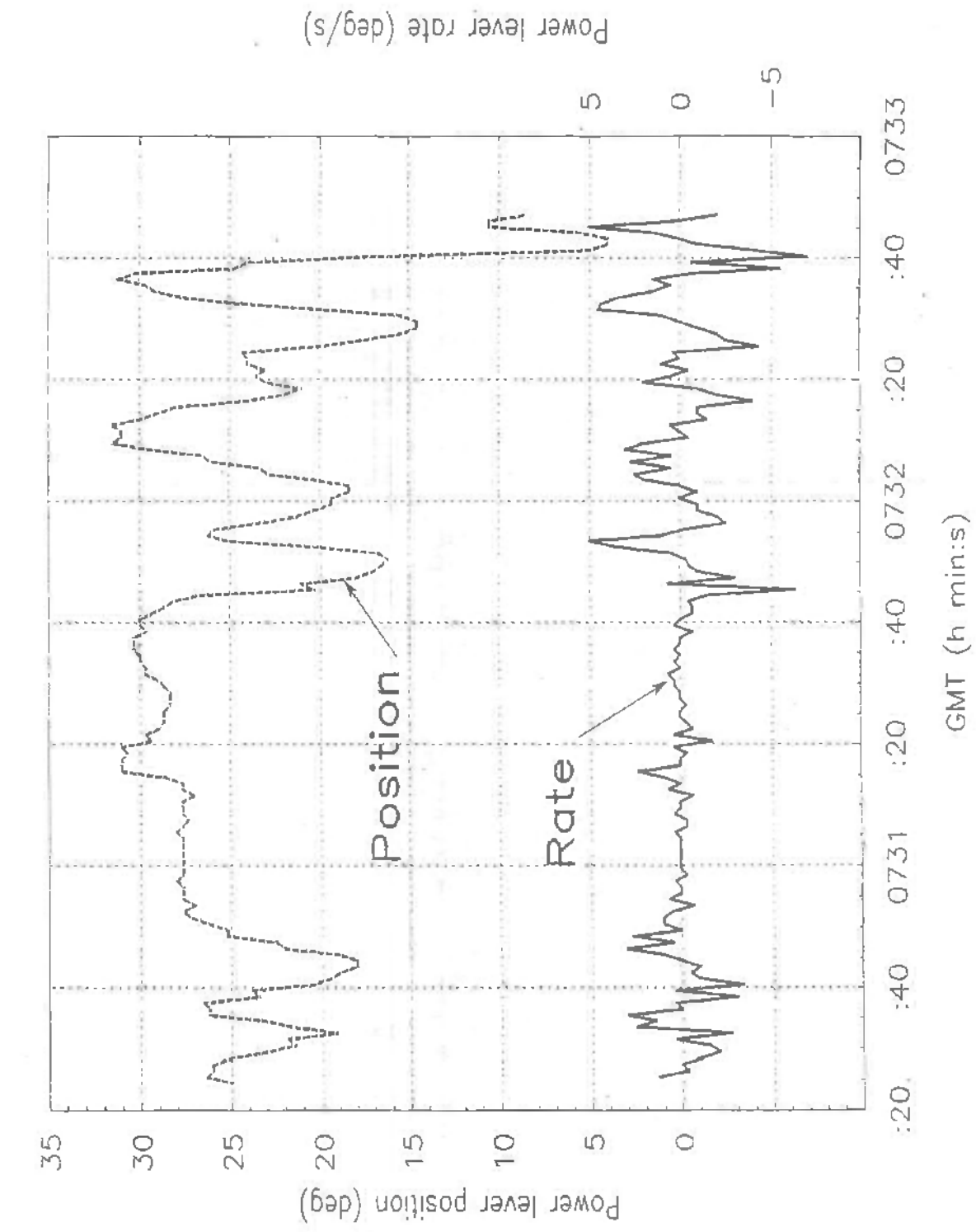

Fig. 12 Power levers time history

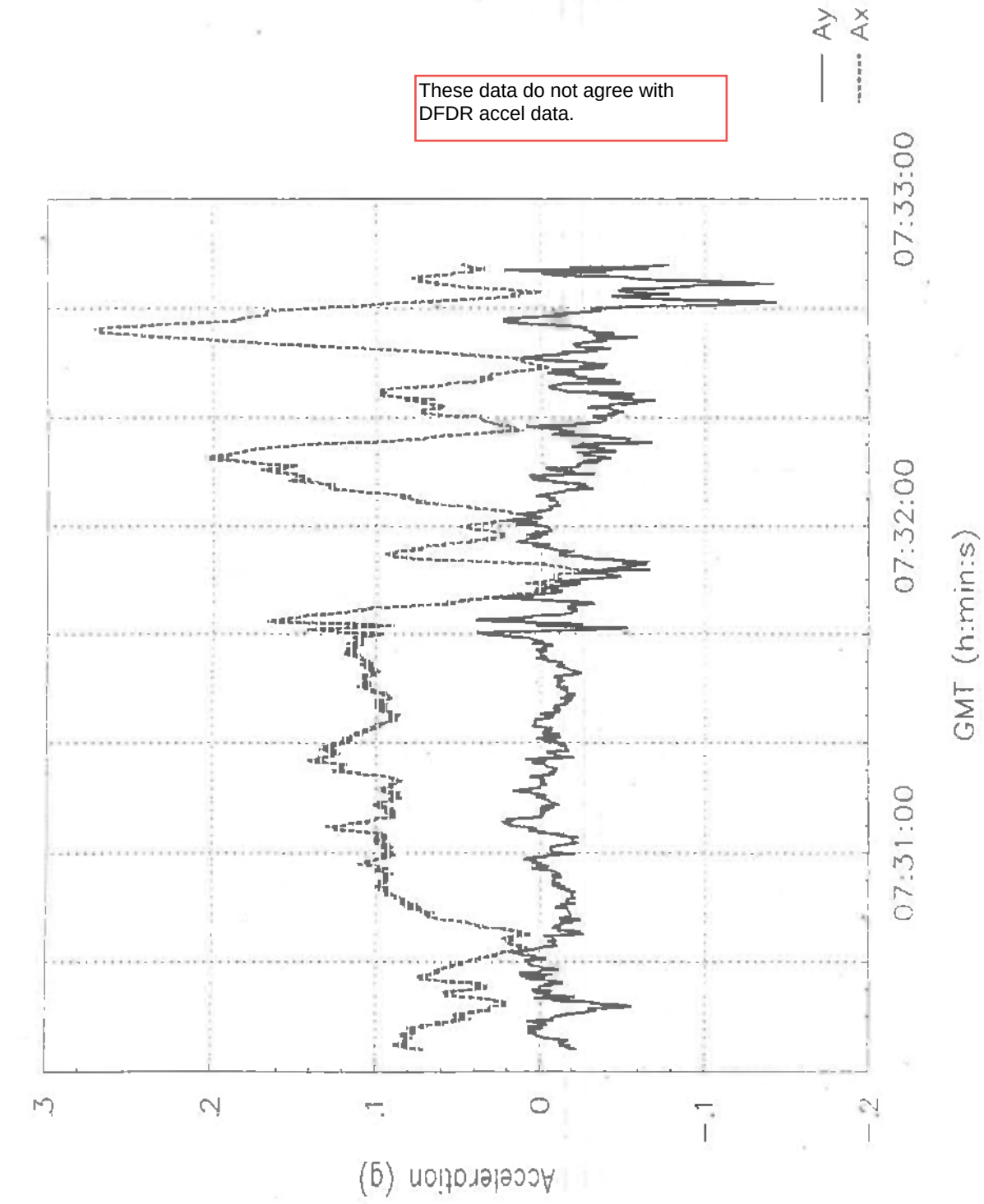

Fig. 13 Longitudinal and lateral acceleration time history

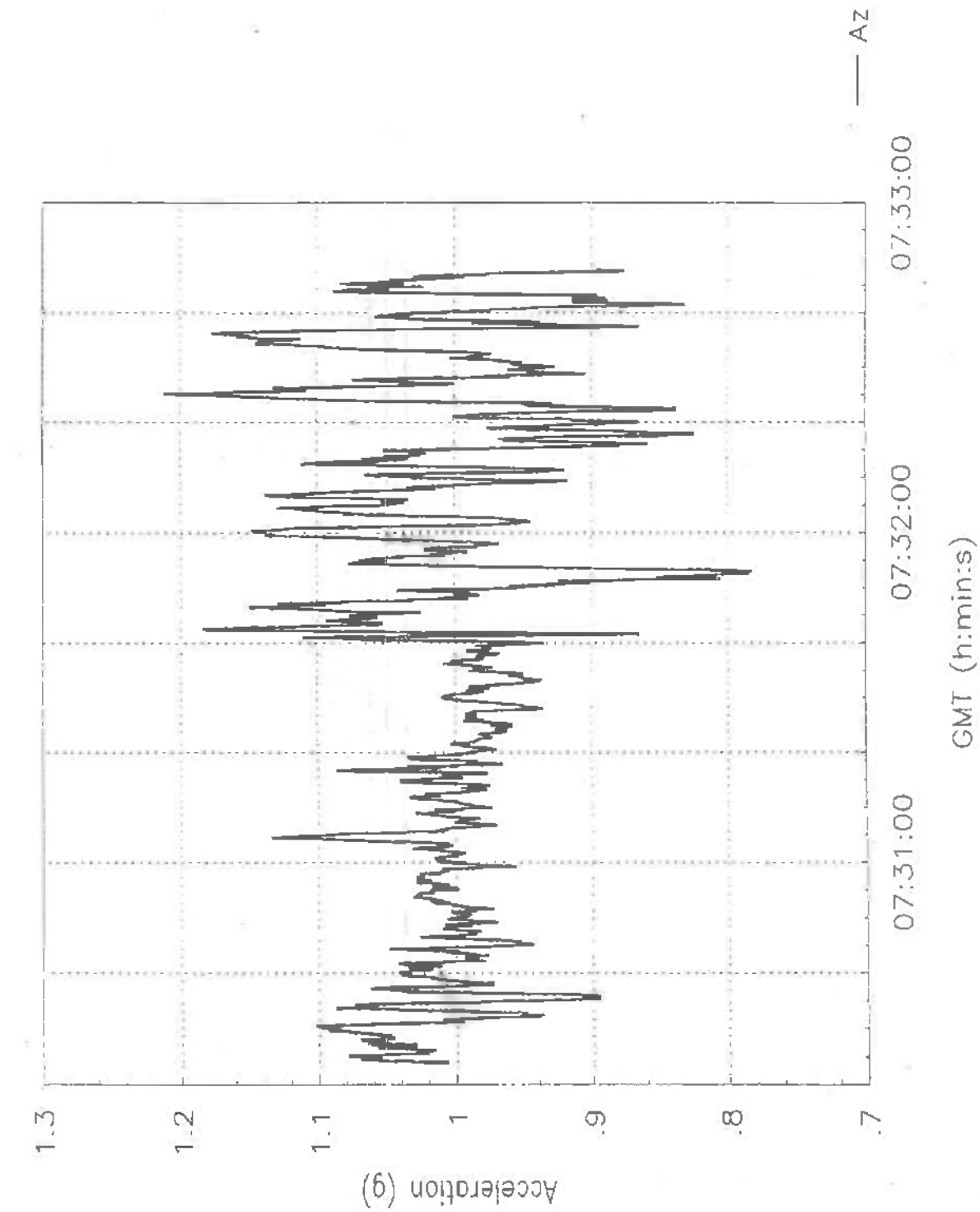

Fig. 14 Vertical acceleration time history

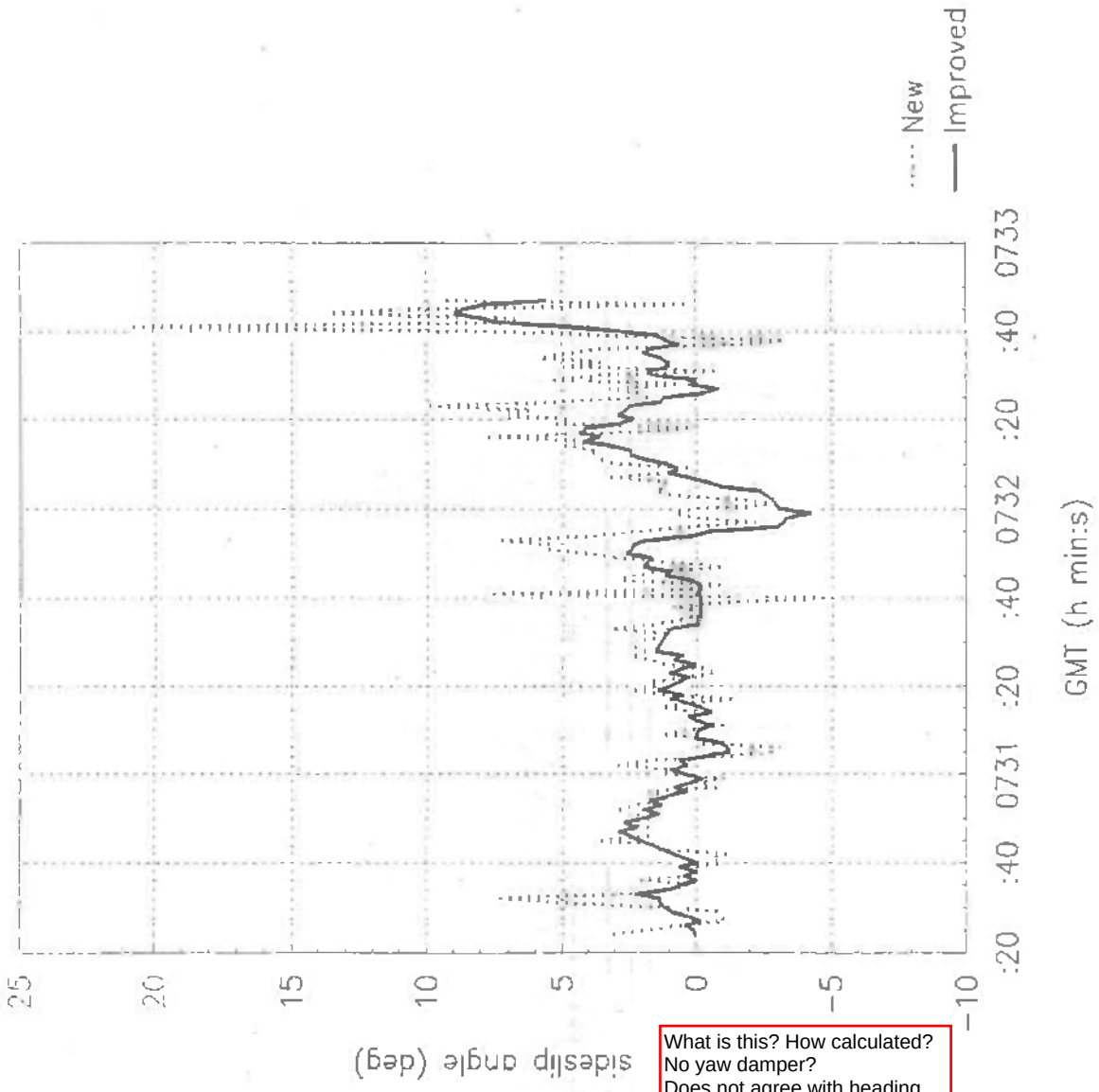

What is this? How calculated?
No yaw damper?
Does not agree with heading Fig. 6.

Fig. 15 Comparison of sideslip angle estimators

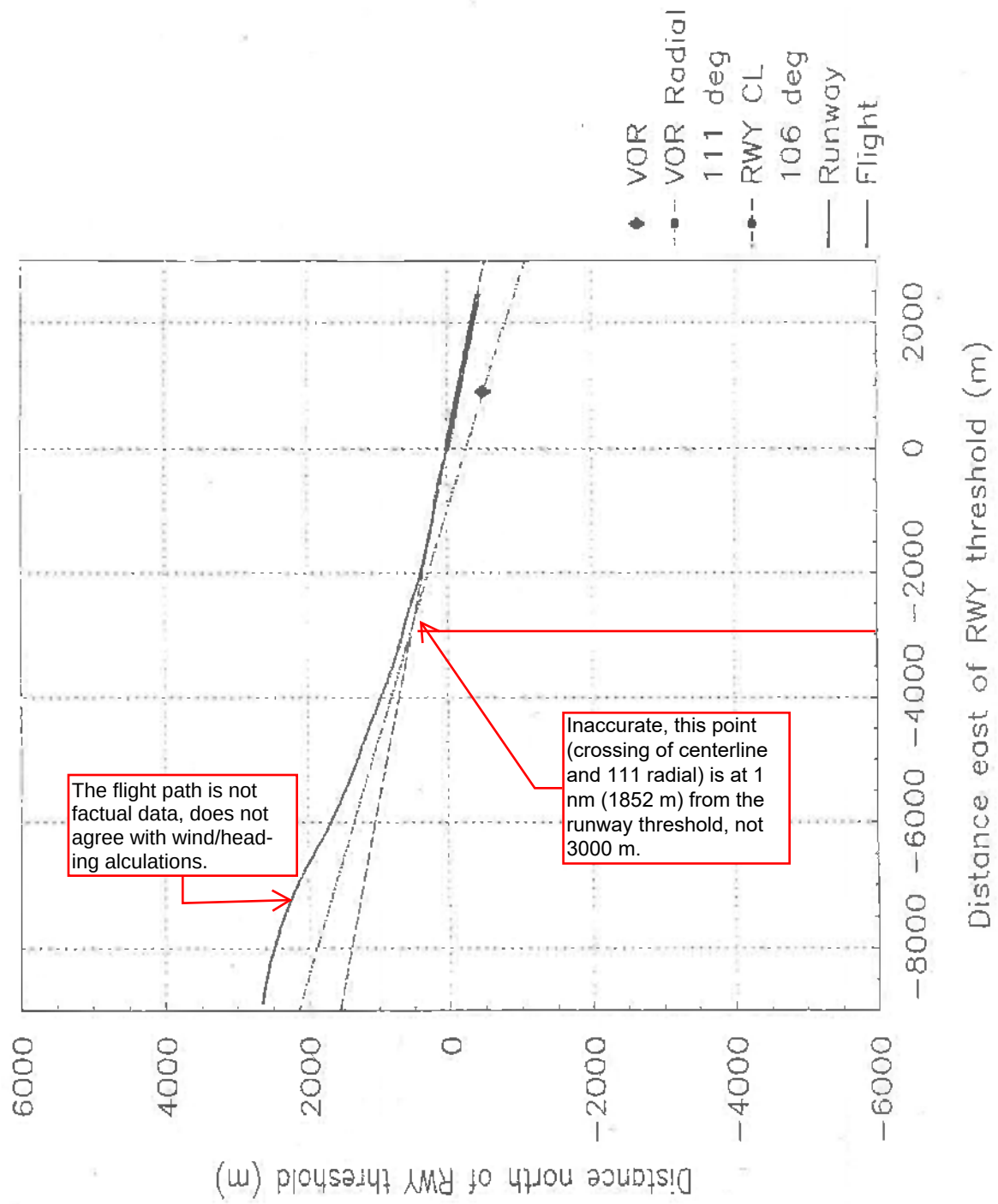

Fig. 16 Lateral flight path - small scale

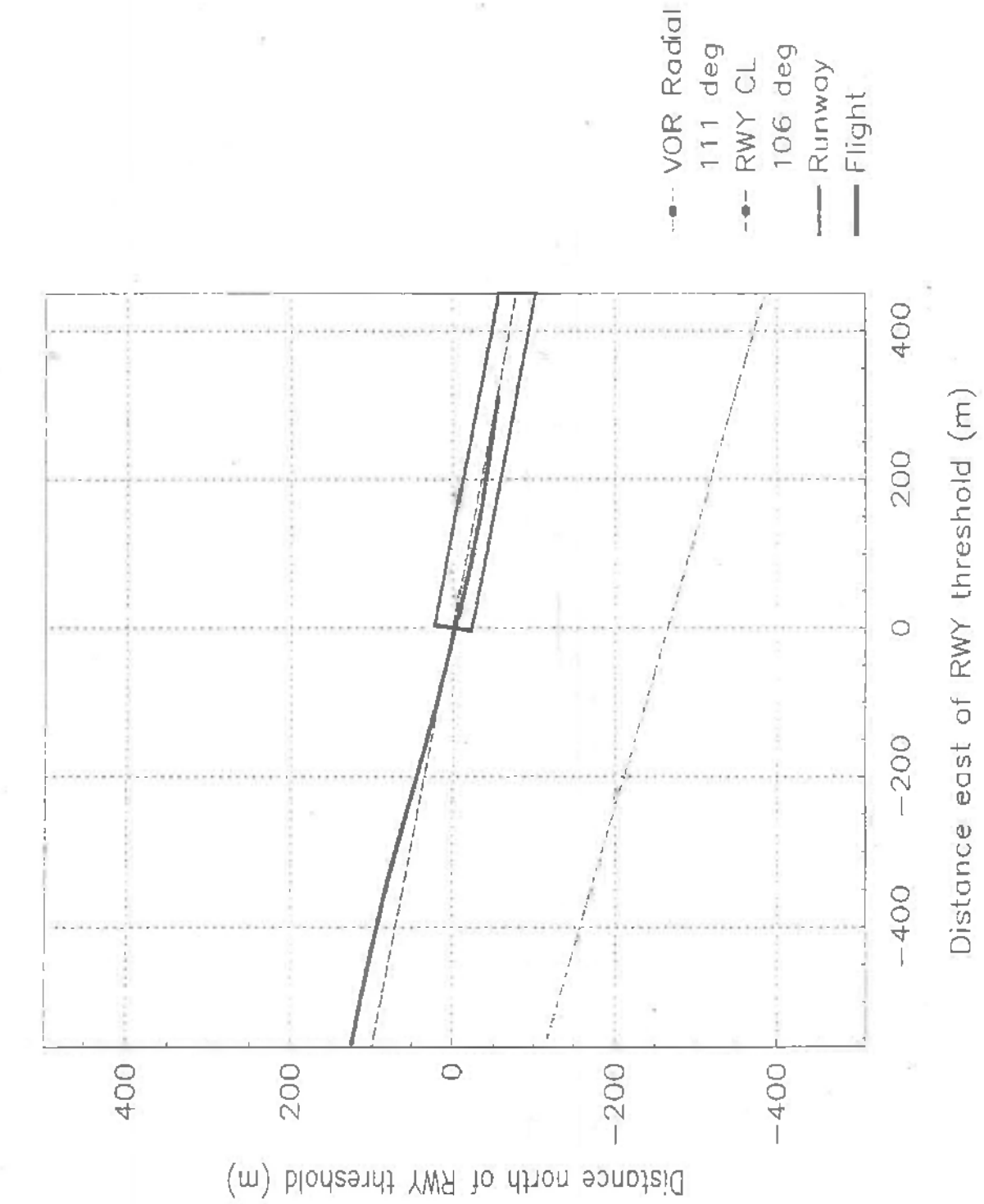

Fig. 17 Lateral flight path - large scale

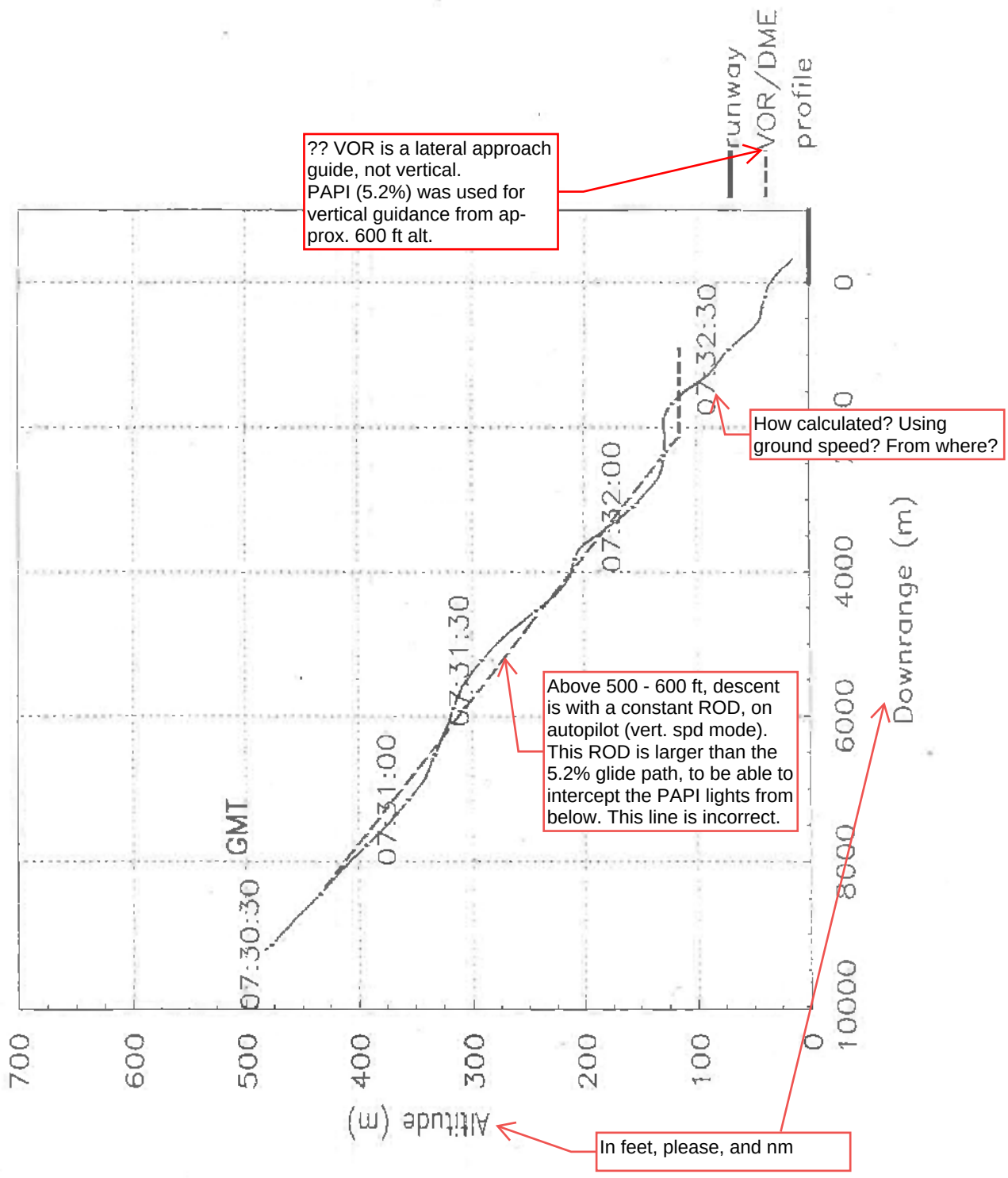

Fig. 18 Vertical profile

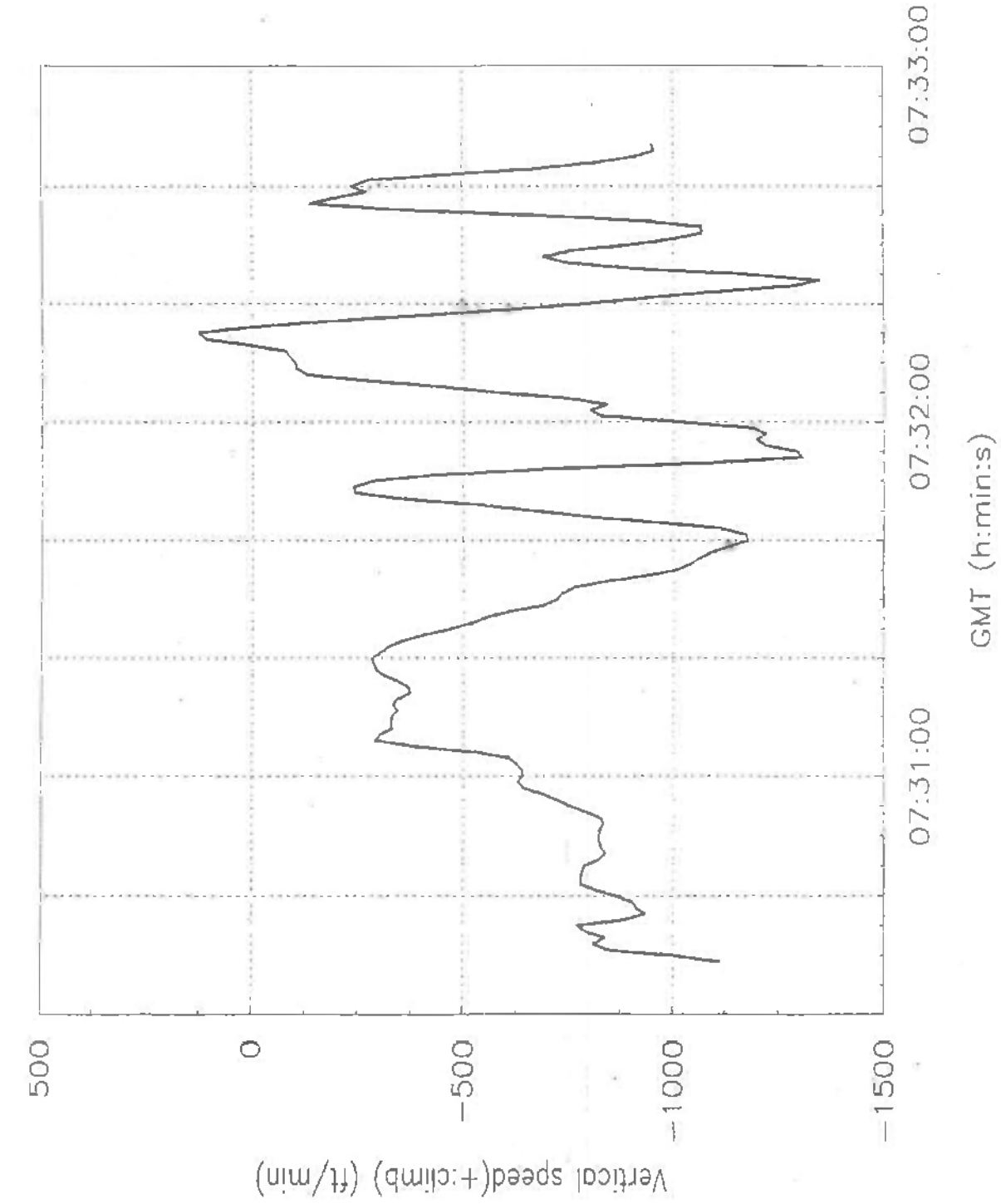

Fig. 19 Vertical speed time history

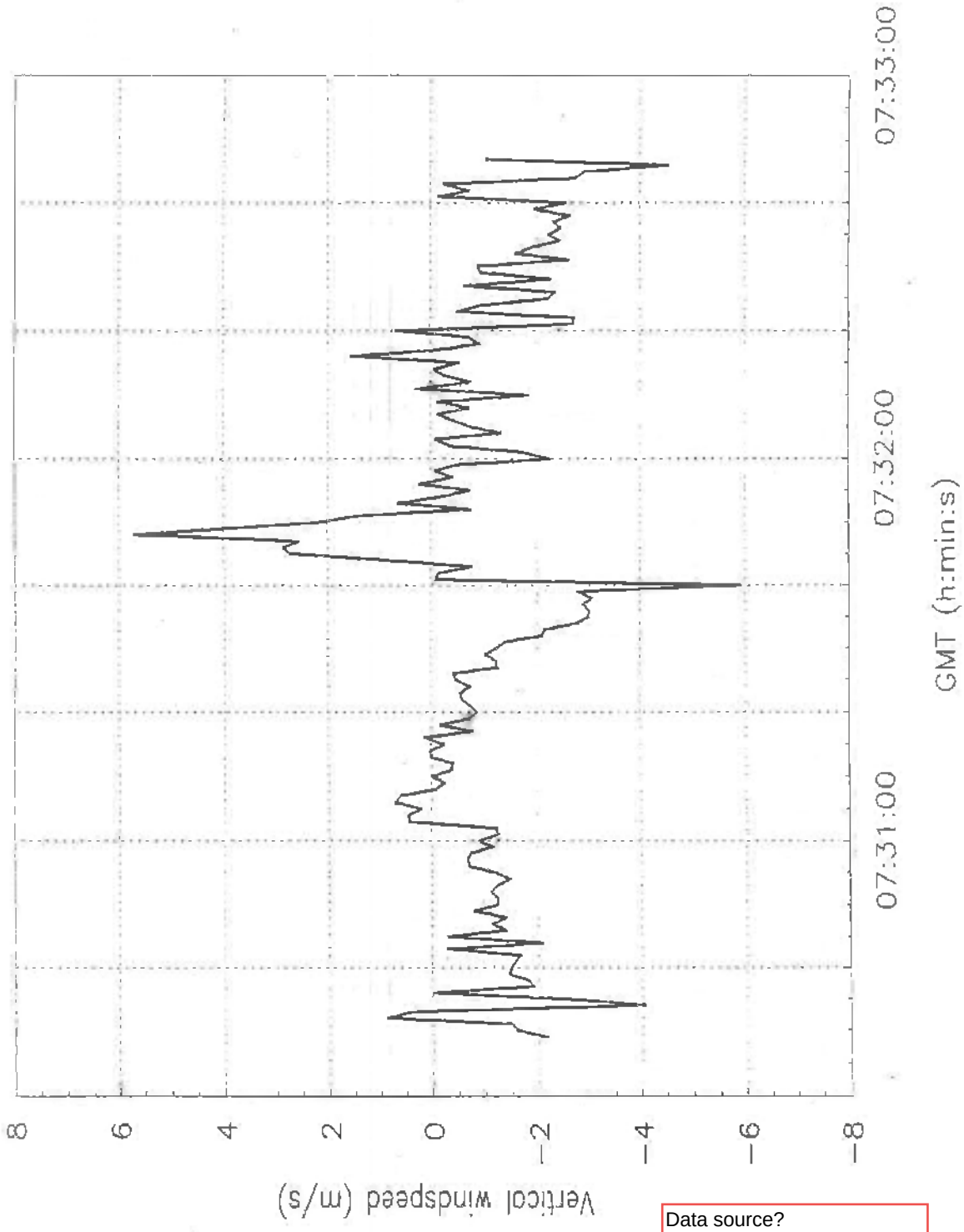

Data source?
Where is the proper legend?

Fig. 20 Vertical wind component time history

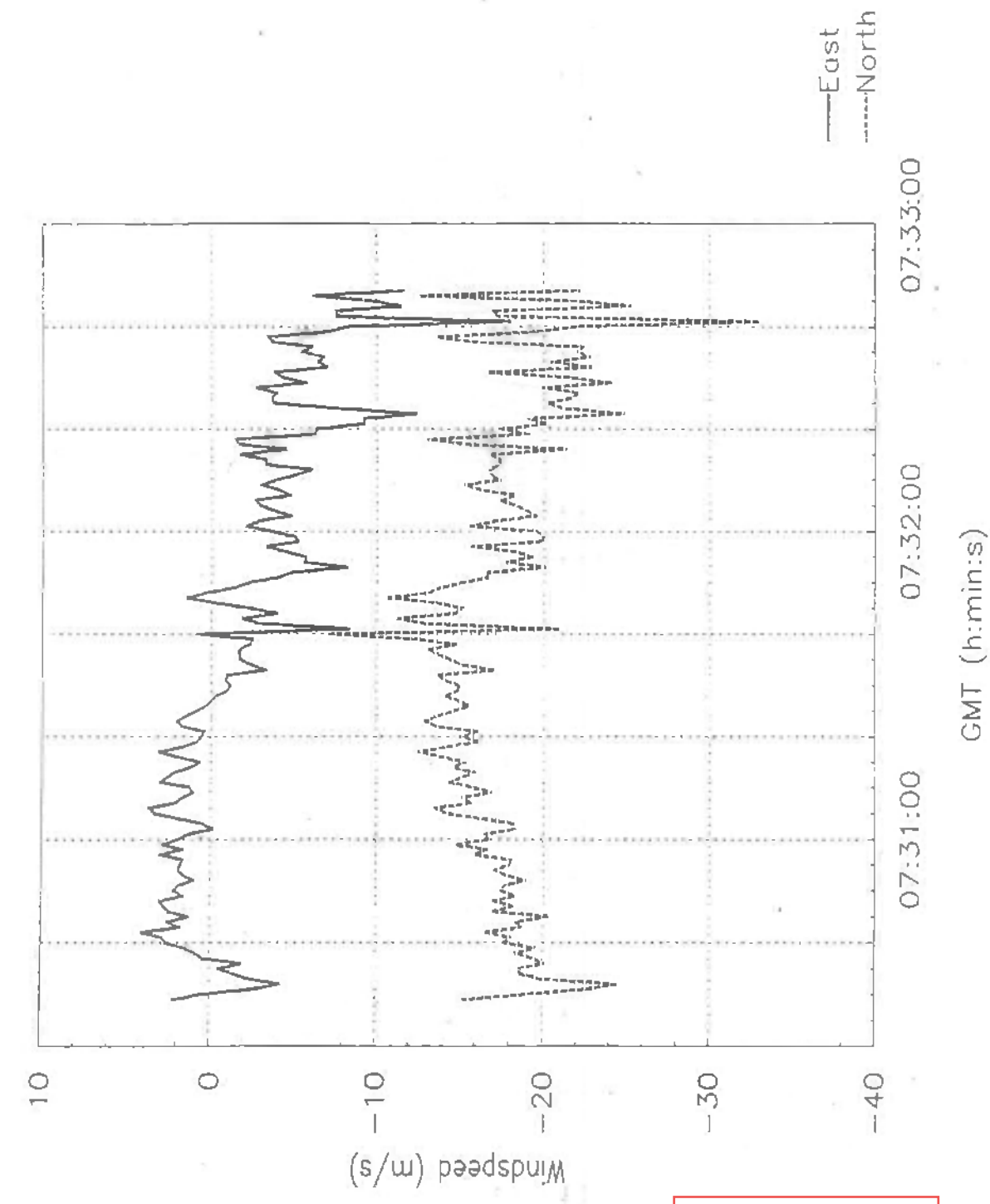

Data source?

Fig. 21 North and East wind component time histories

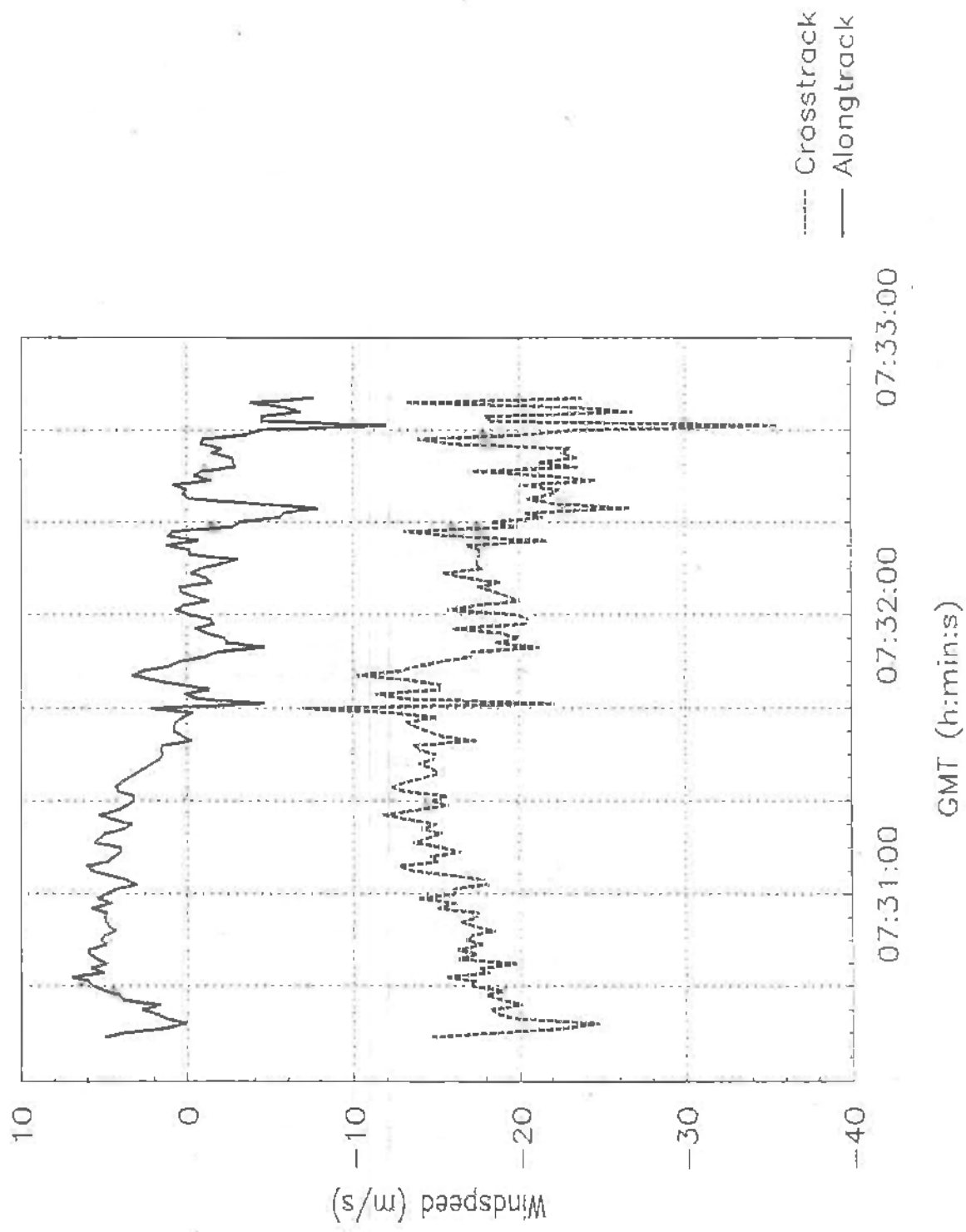

Fig. 22 Along-track and crosstrack wind component time histories

Data source?

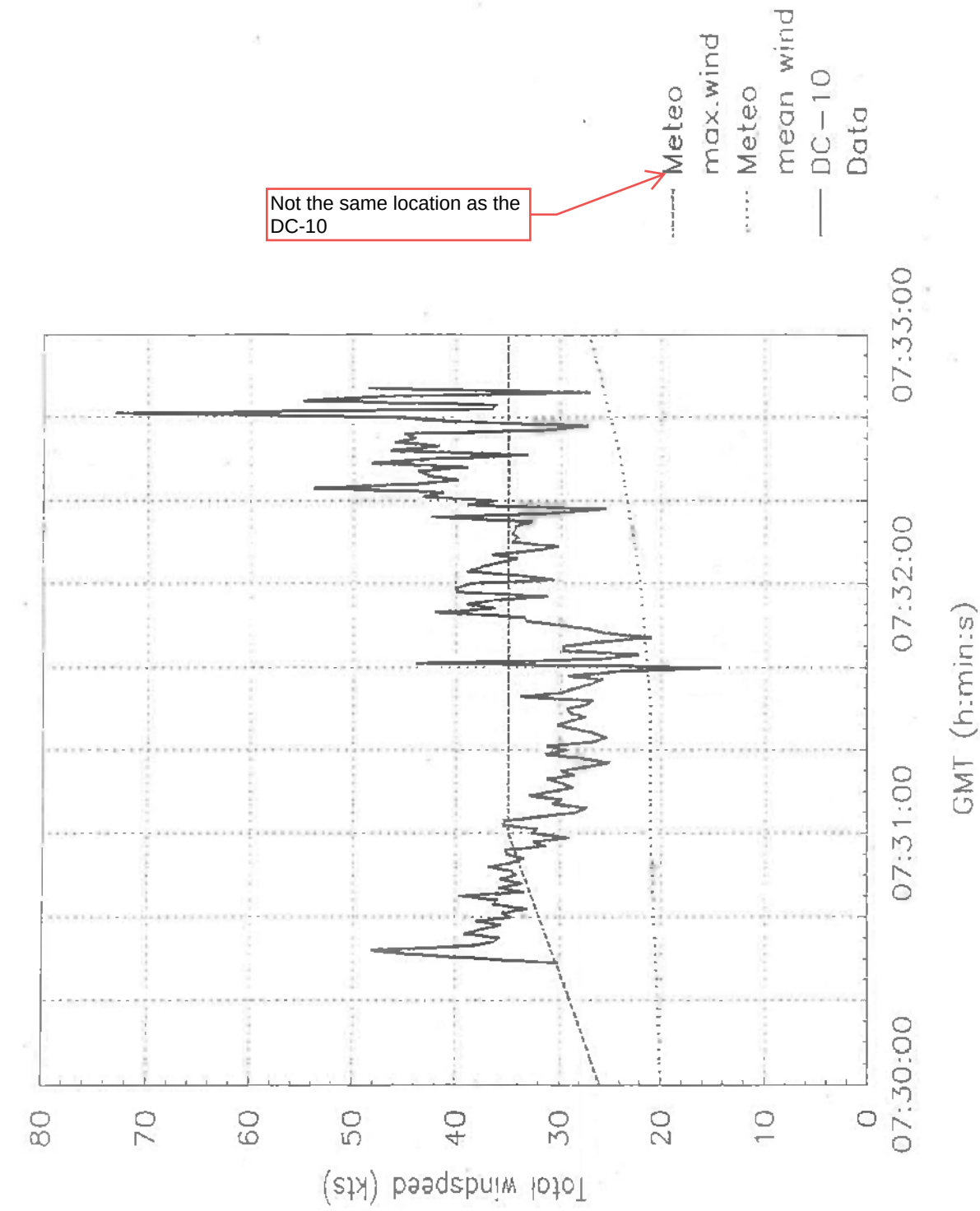

Fig. 23 Windspeed from DC-10 data and meteo time histories

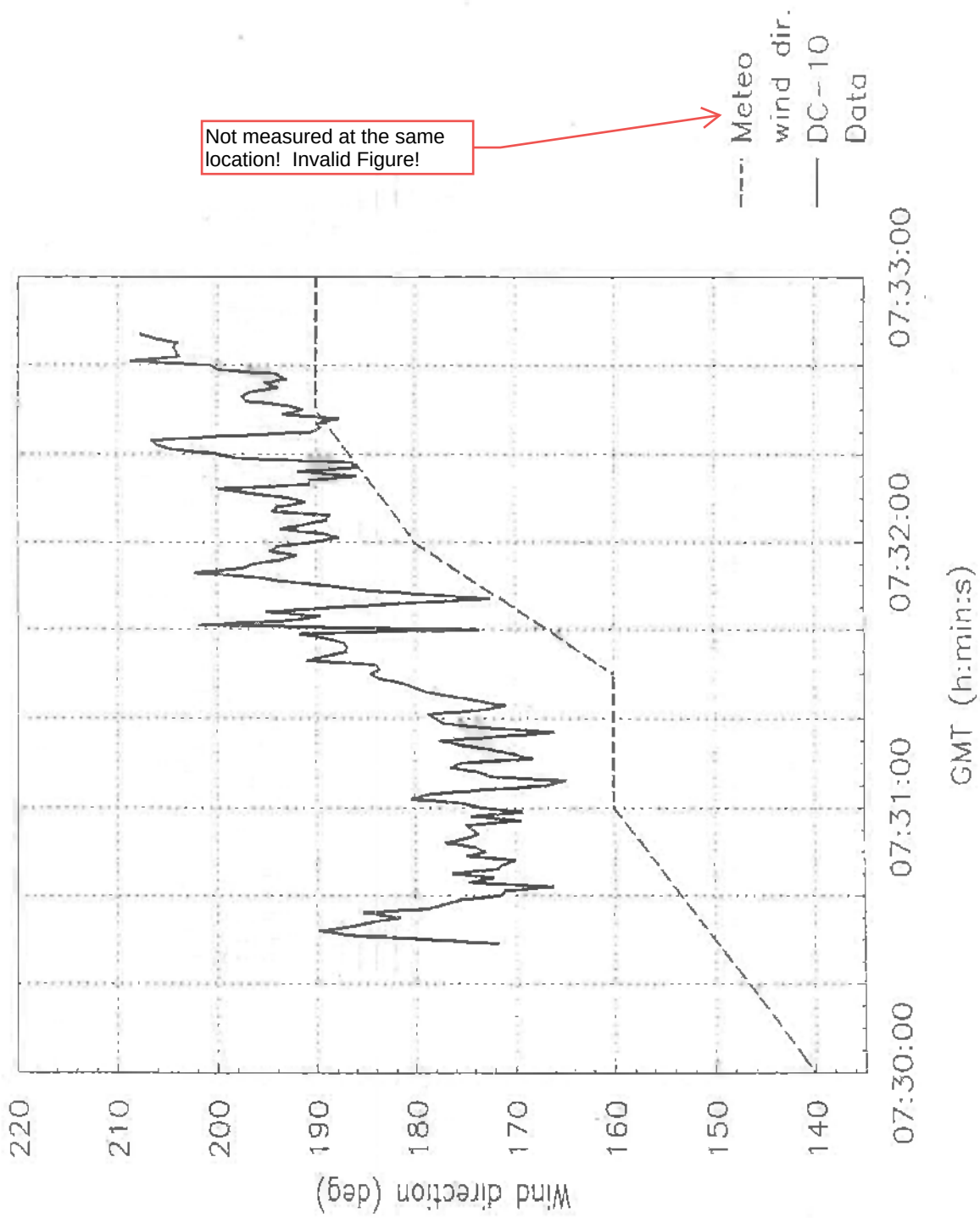

Fig. 24 Wind direction from DC-10 data and meteo as function of time

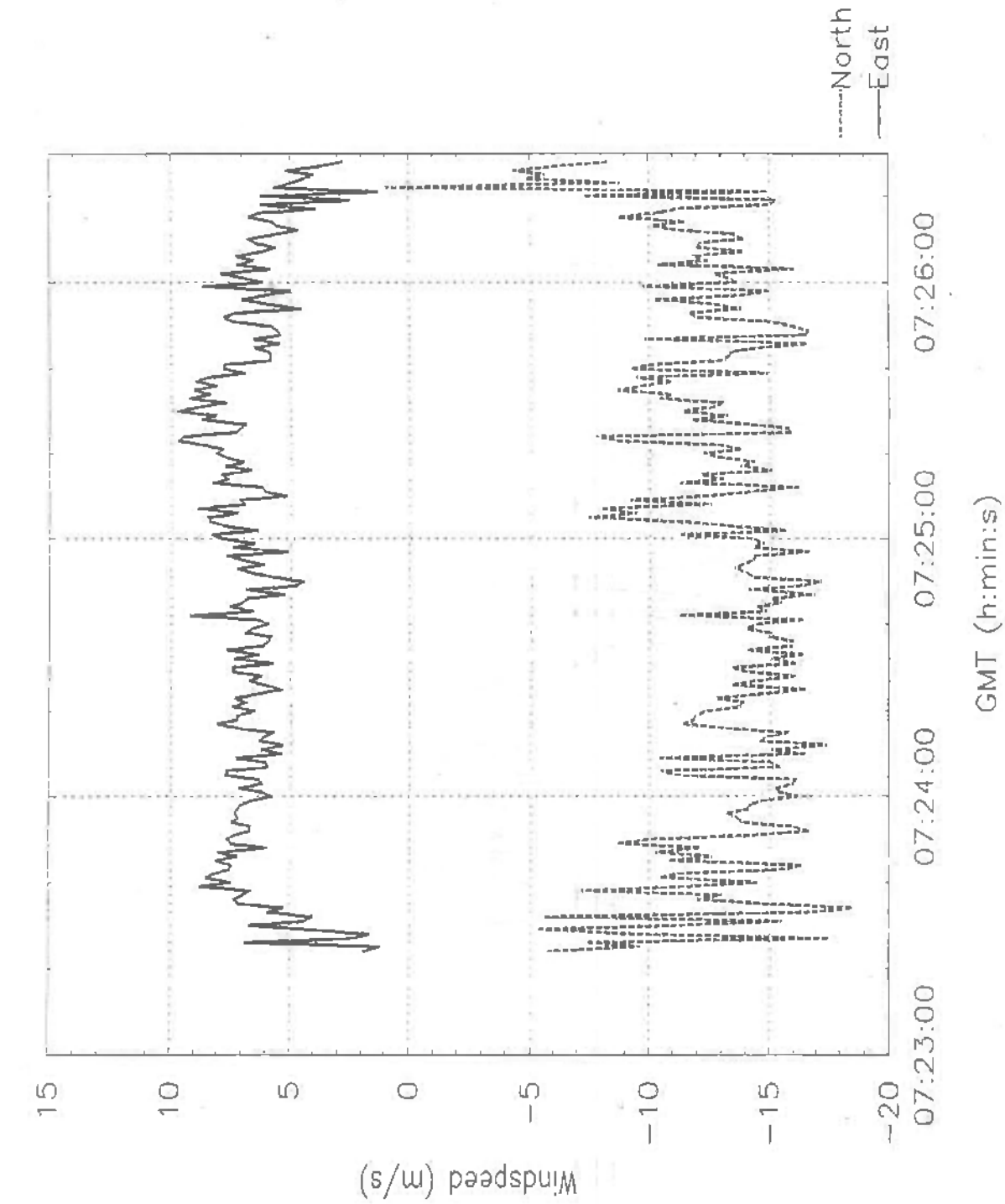

Fig. 25 North and East wind components during B767 landing at Faro

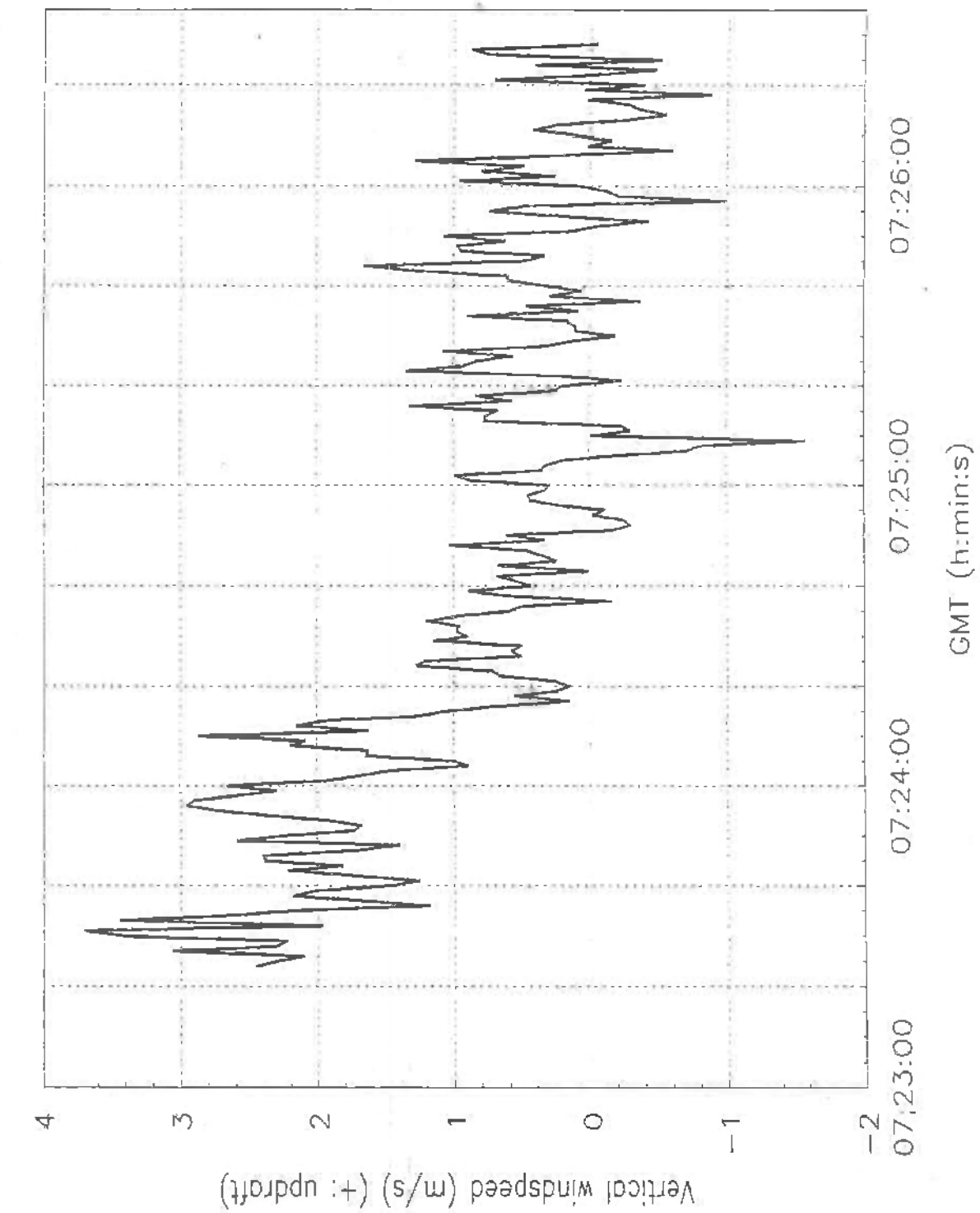

Fig. 26 Vertical wind component during B767 landing at Faro

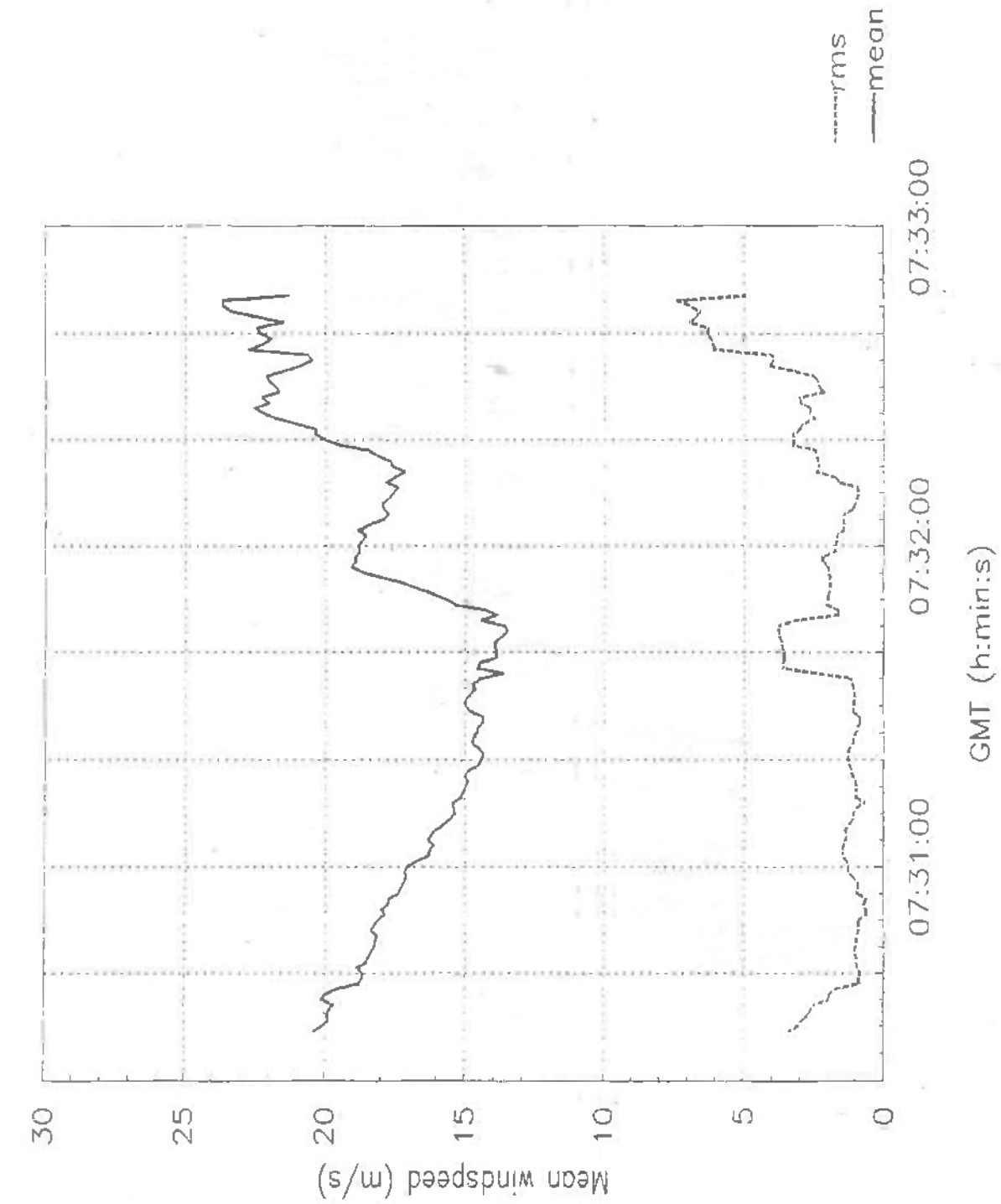

Fig. 27 Mean windspeed and variation

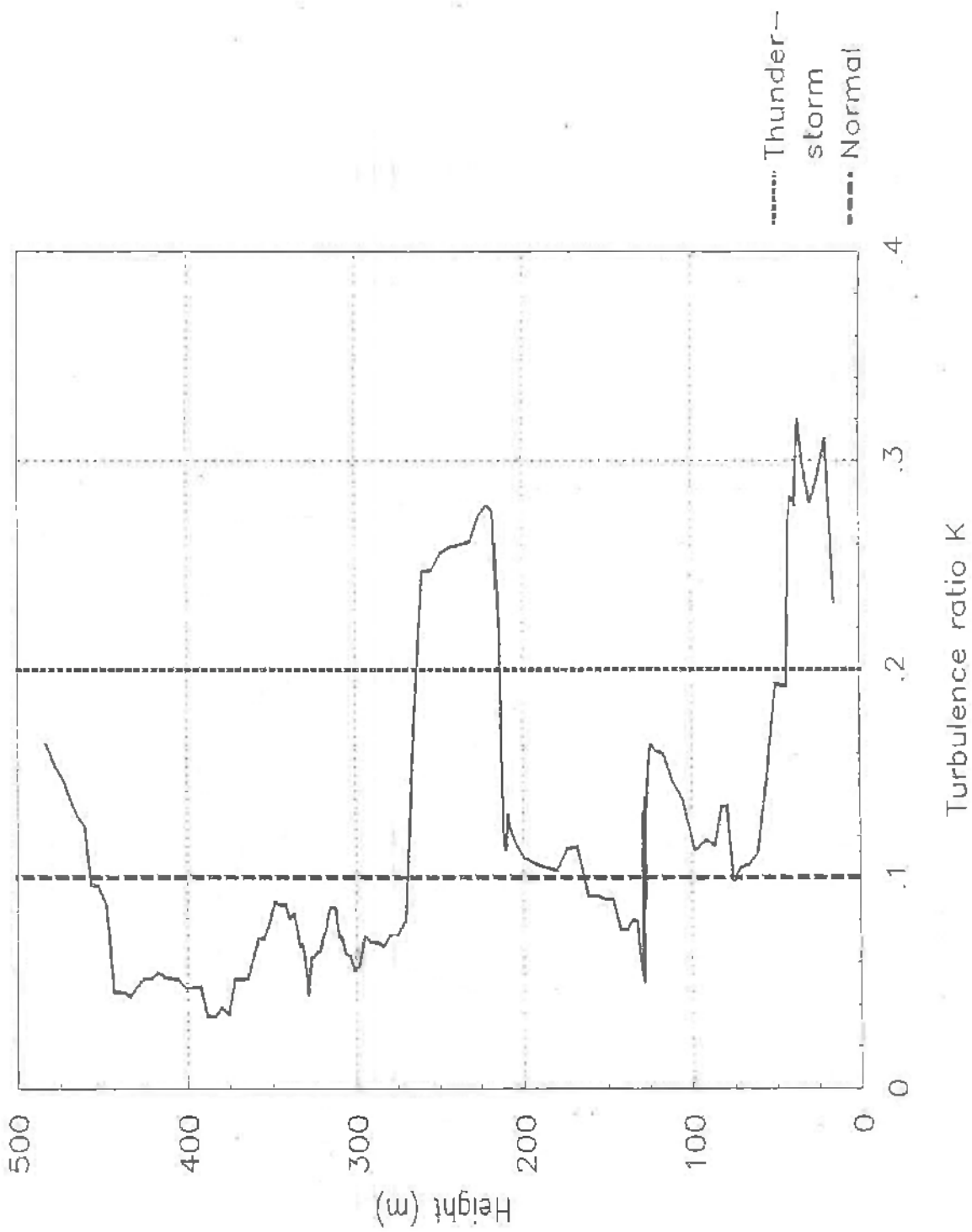

Fig. 28 Turbulence-to-windspeed ratio K

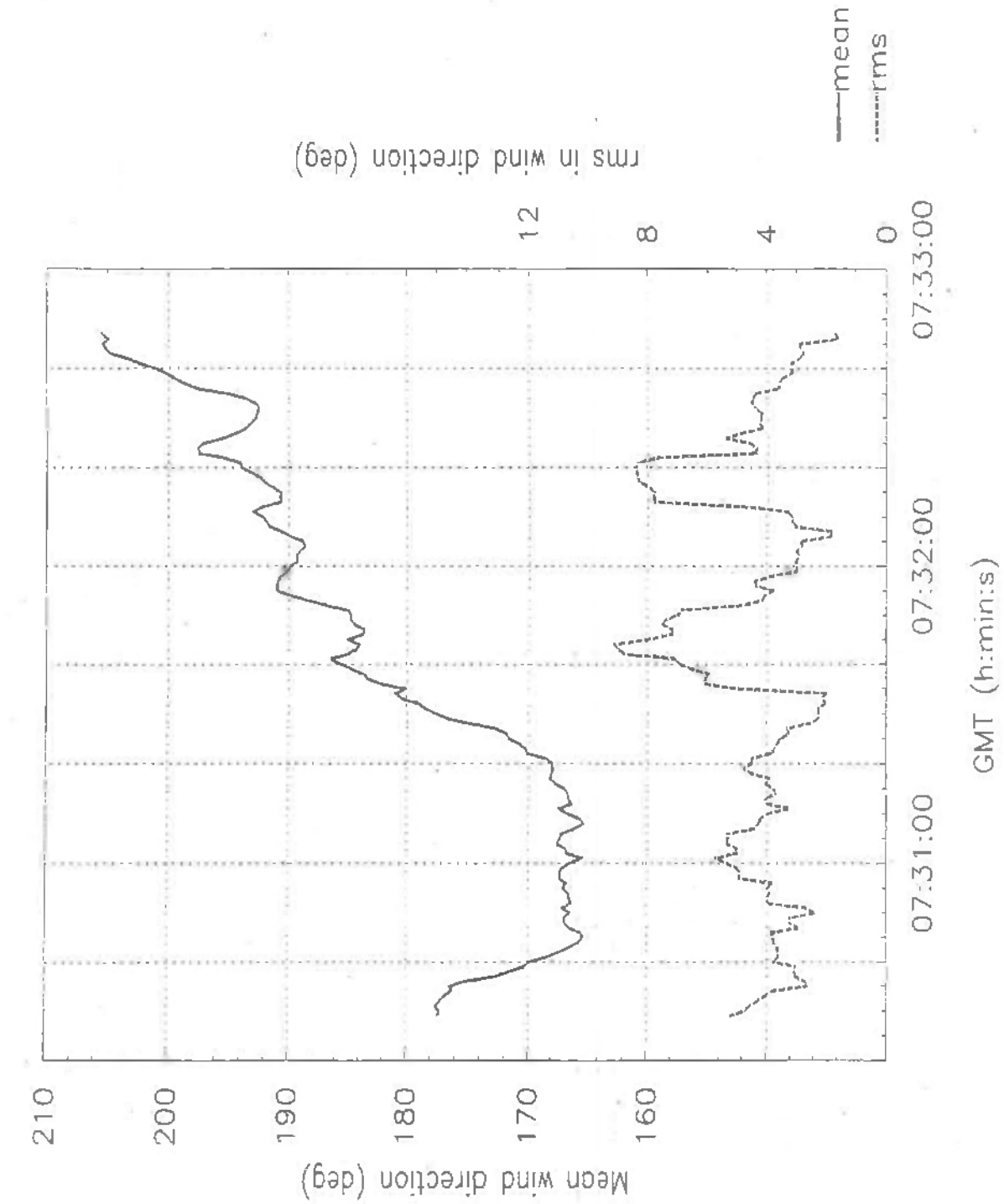

Fig. 29 Mean wind direction and variation

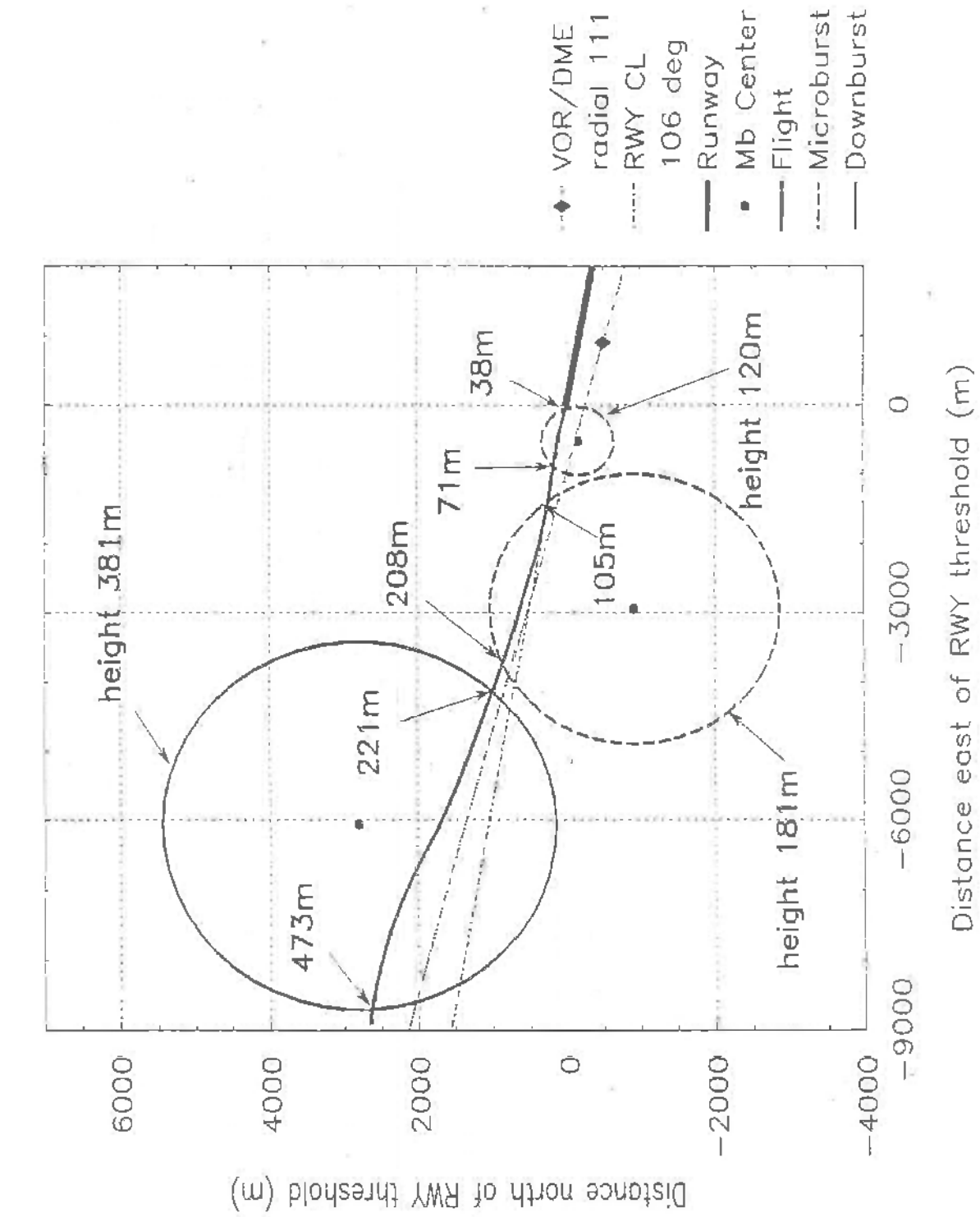

Fig. 30 Situational sketch of downburst models and flight path

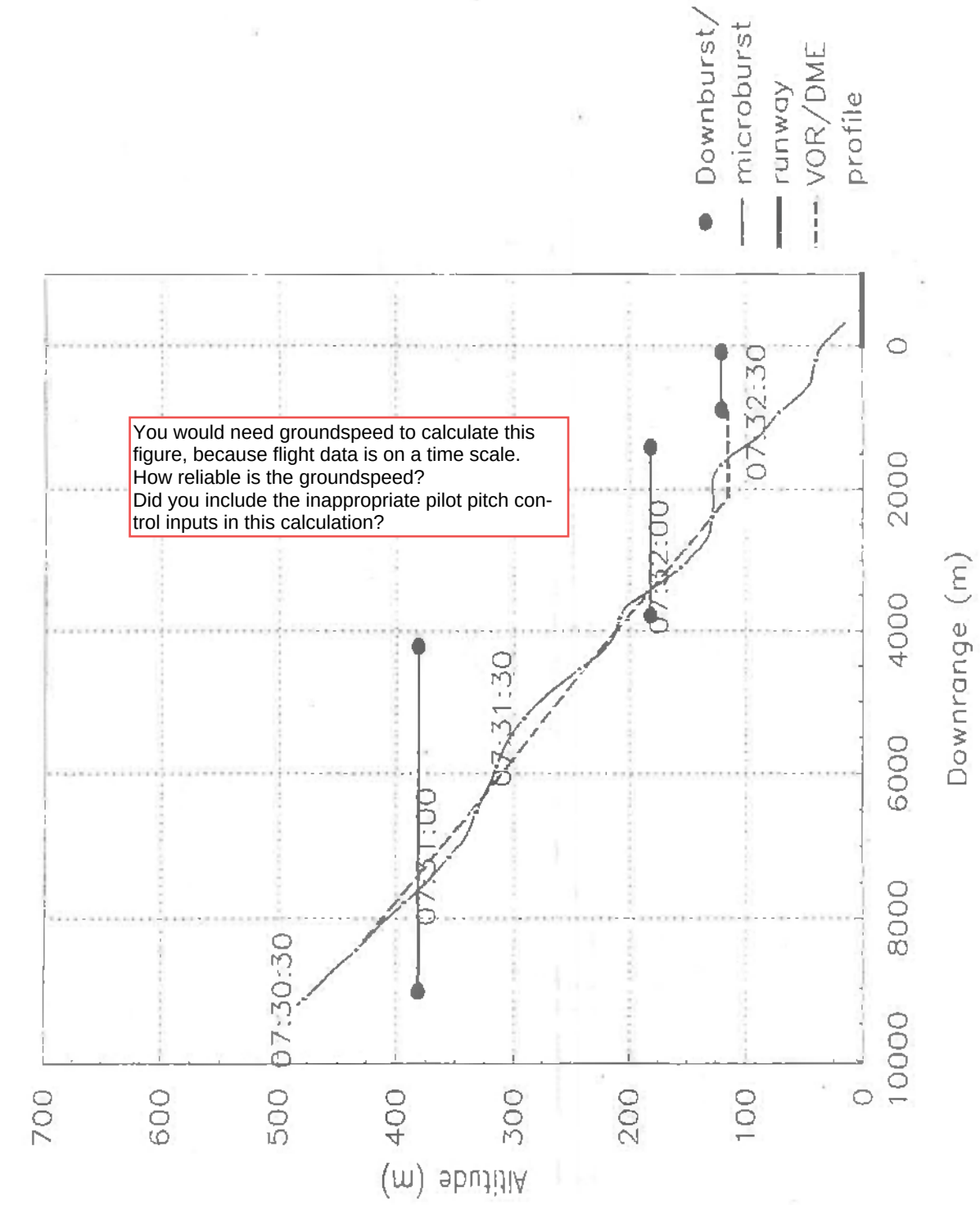

Fig. 31 Situational sketch of windshear and flight path

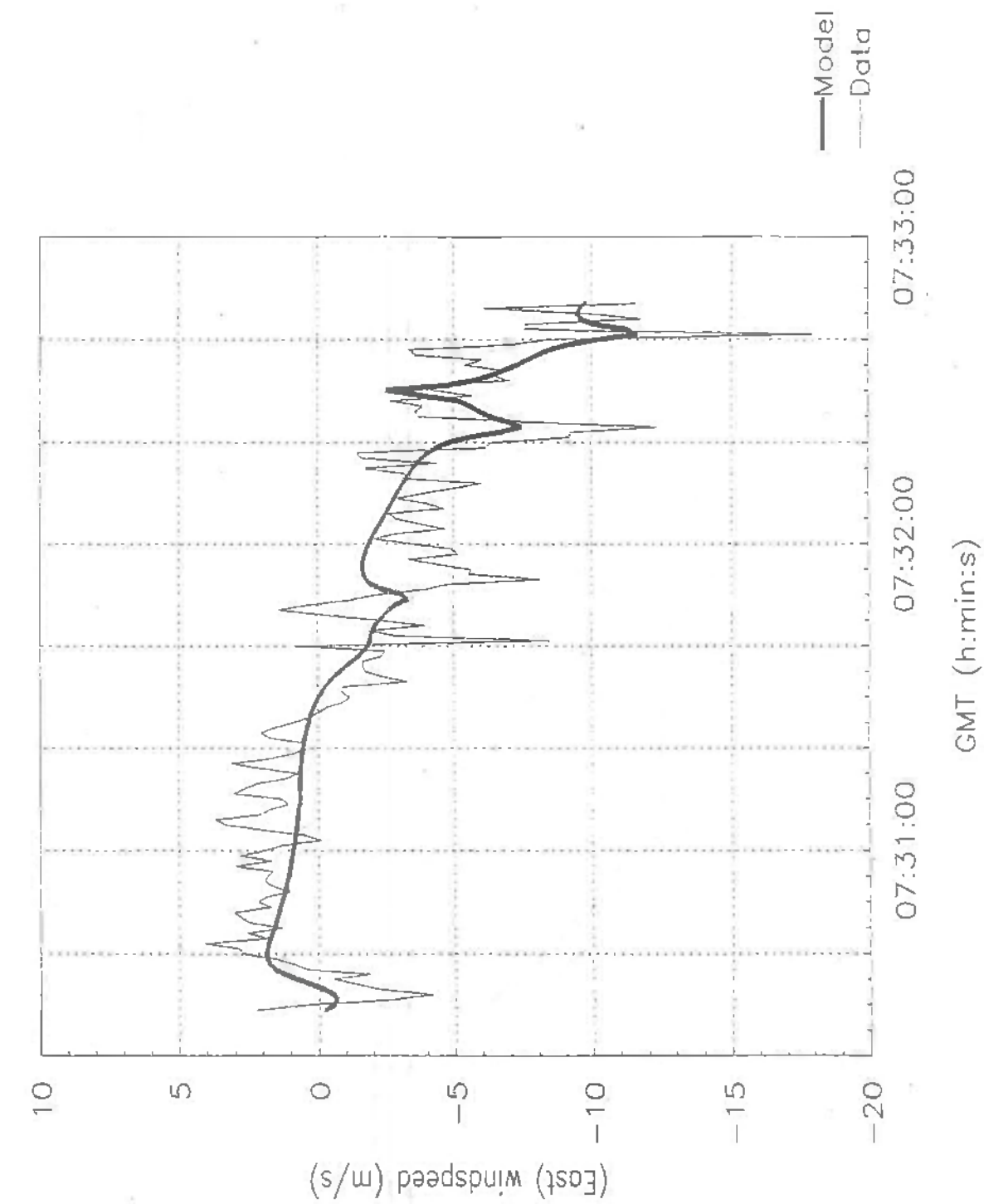

Fig. 32 East wind component - data and model match

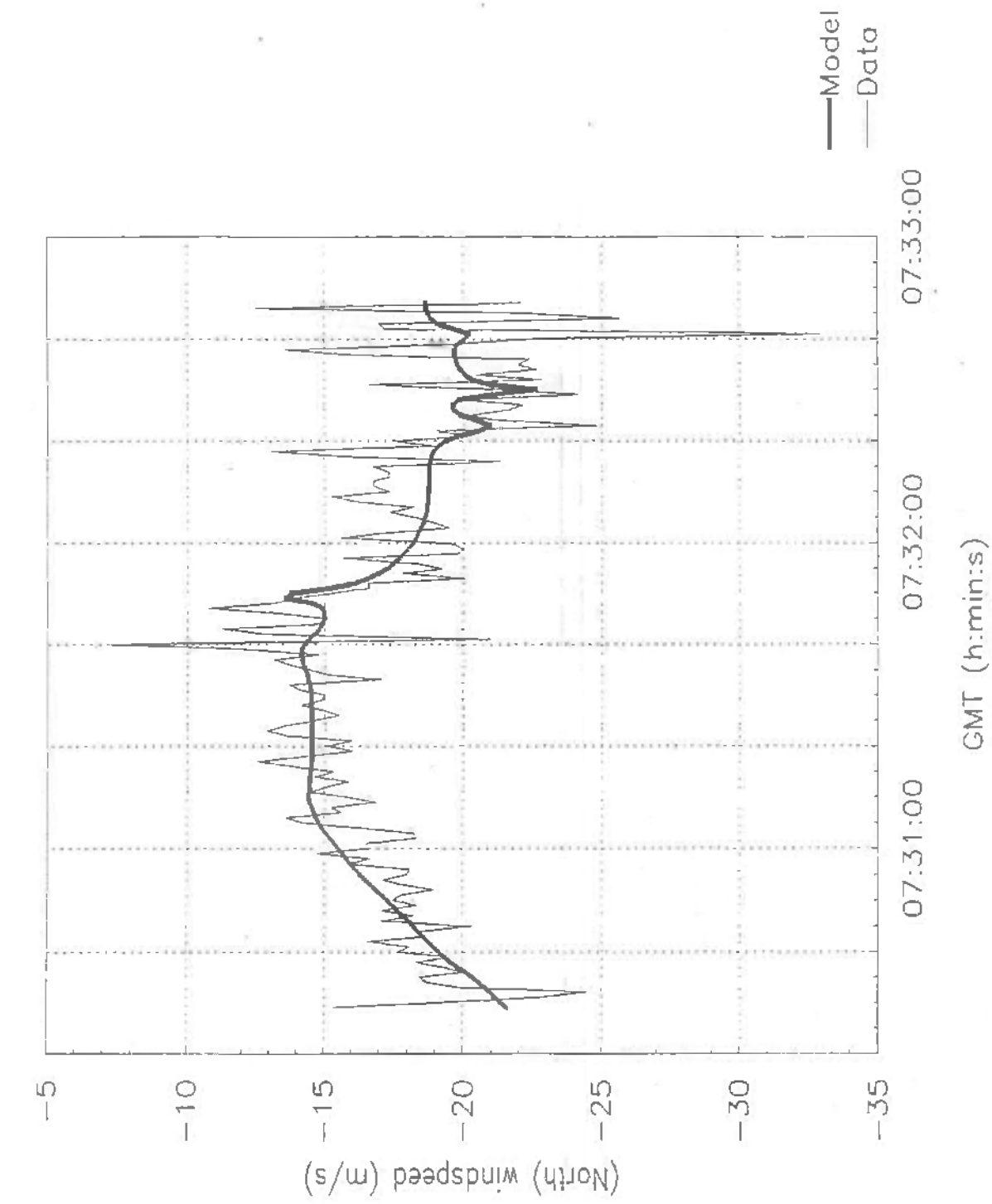

Fig. 33 North wind component - data and model match

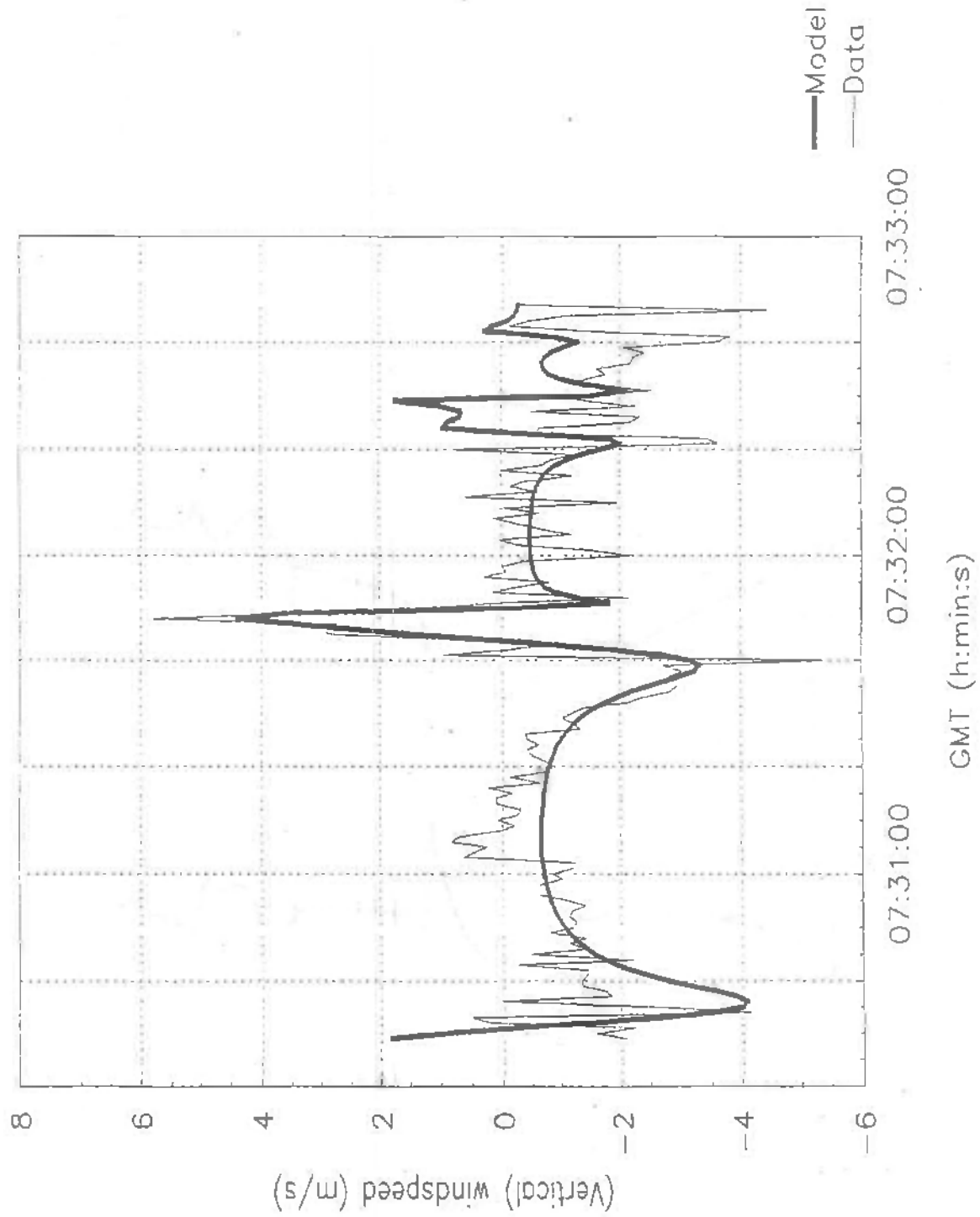

Fig. 34 Vertical wind component - data and model match

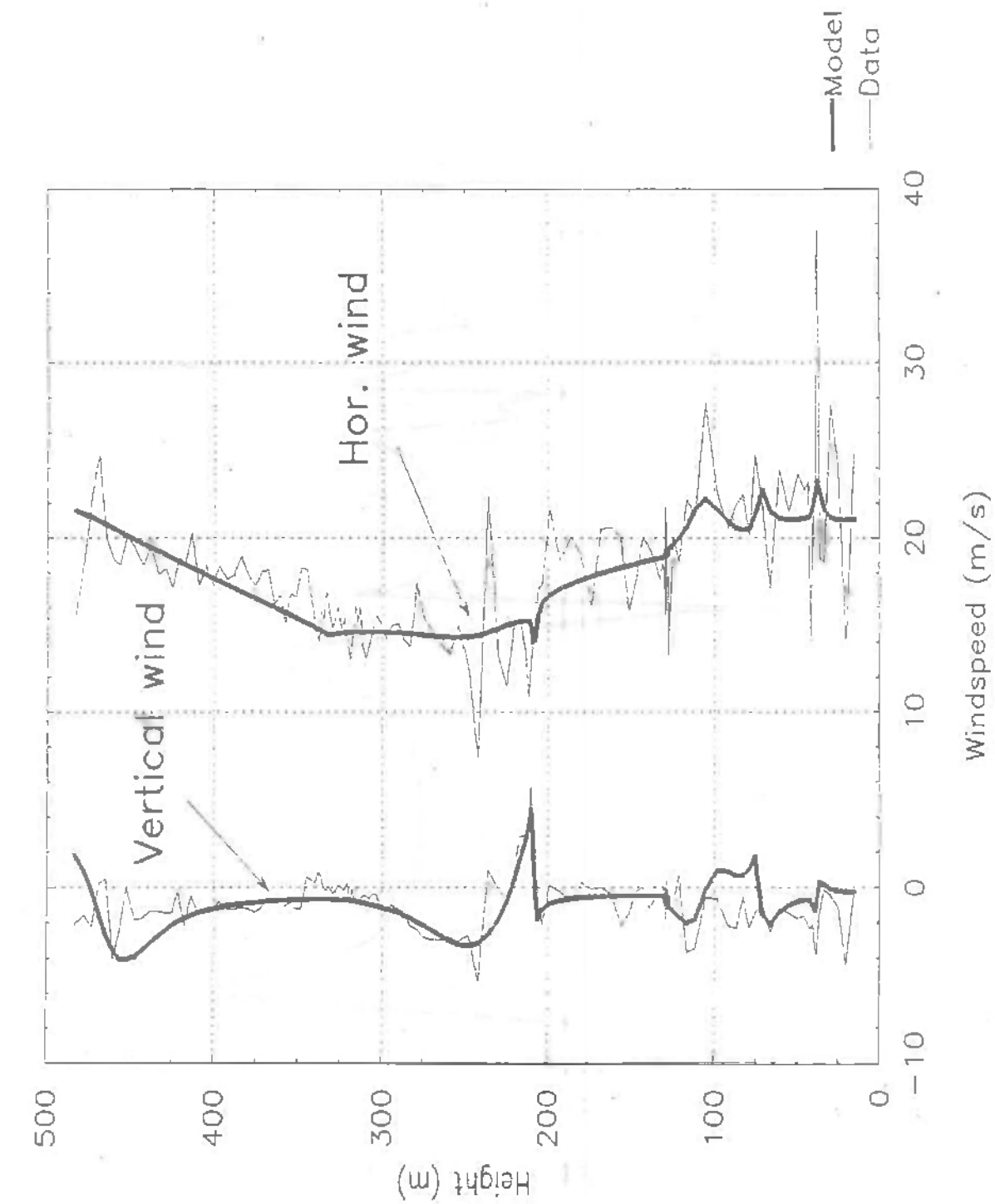

Fig. 35 Mean wind versus height profile

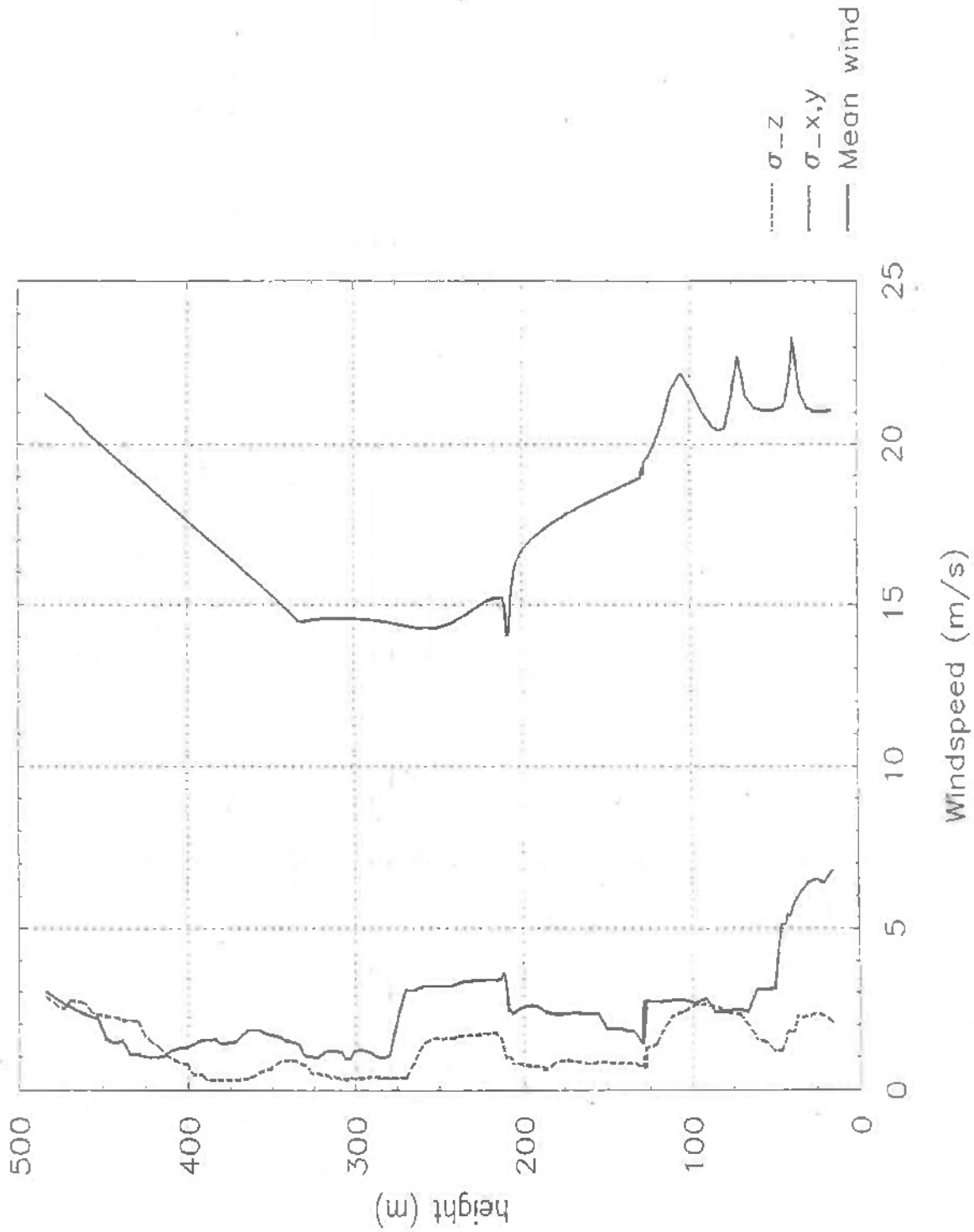

Fig. 36 Windshear turbulence vs height

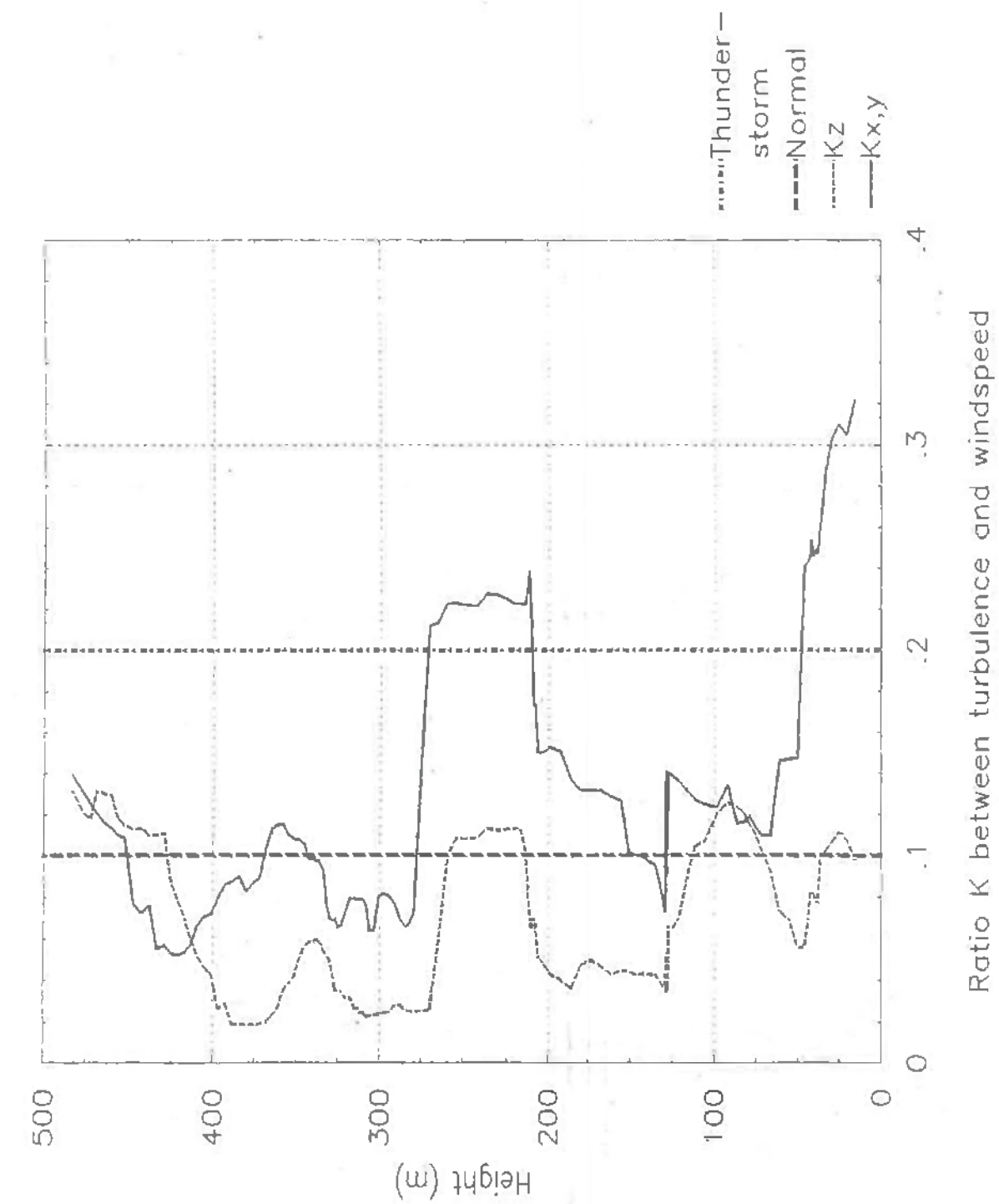

Fig. 37 Ratio between windshear turbulence and windspeed

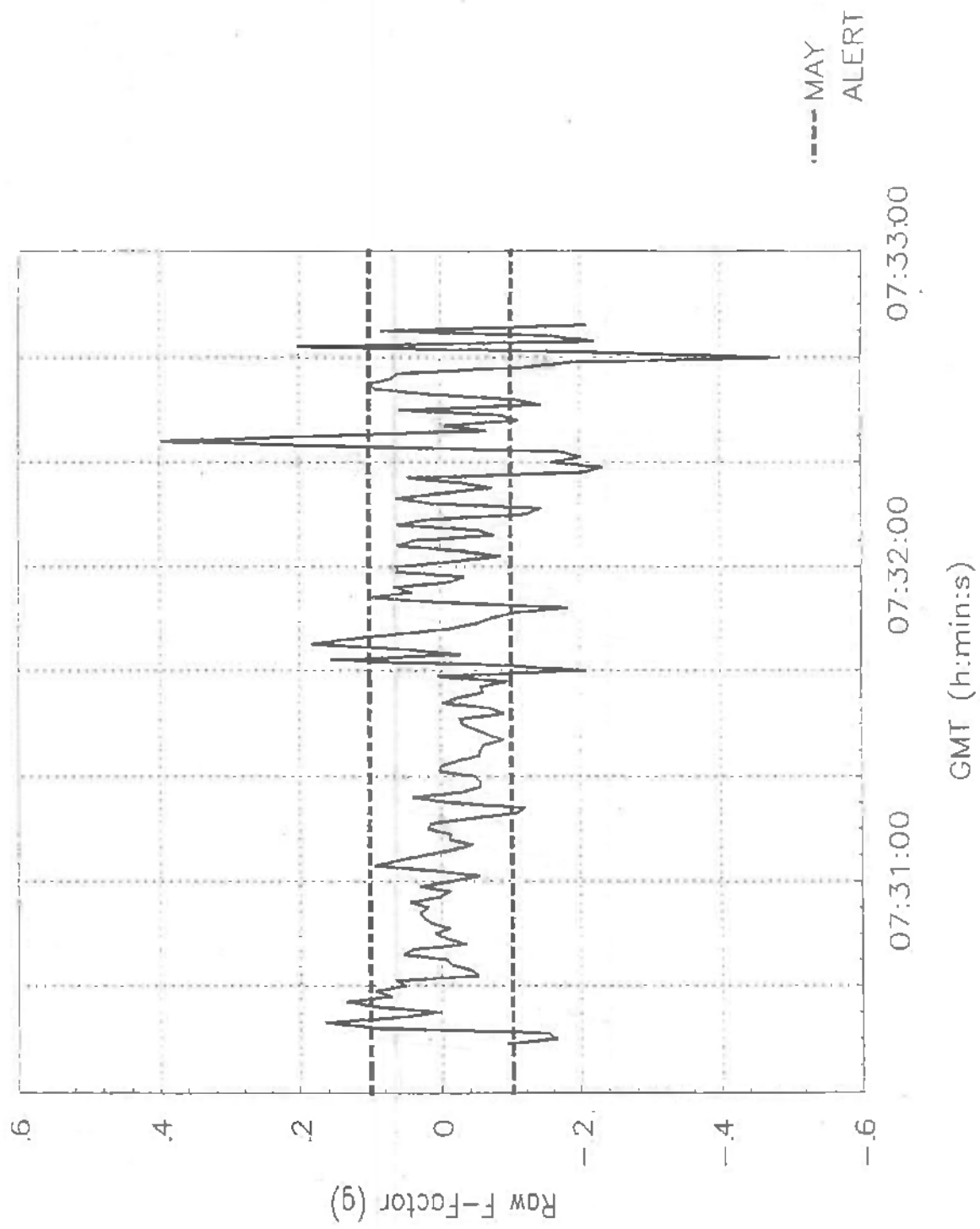

Fig. 38 Raw F-factor (windshear hazard index) as function of time

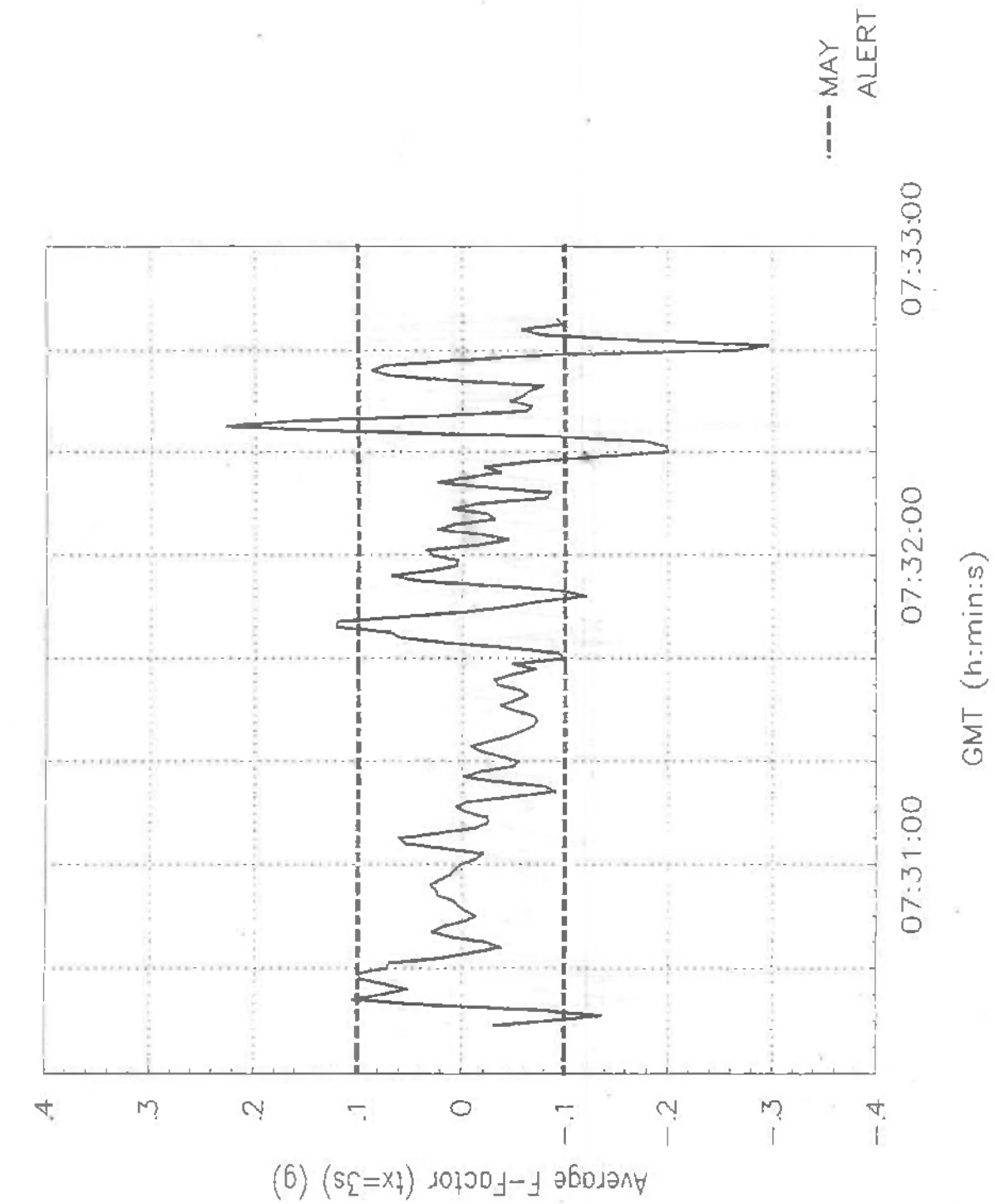

Fig. 39 Three-seconds filtered F-factor as function of time

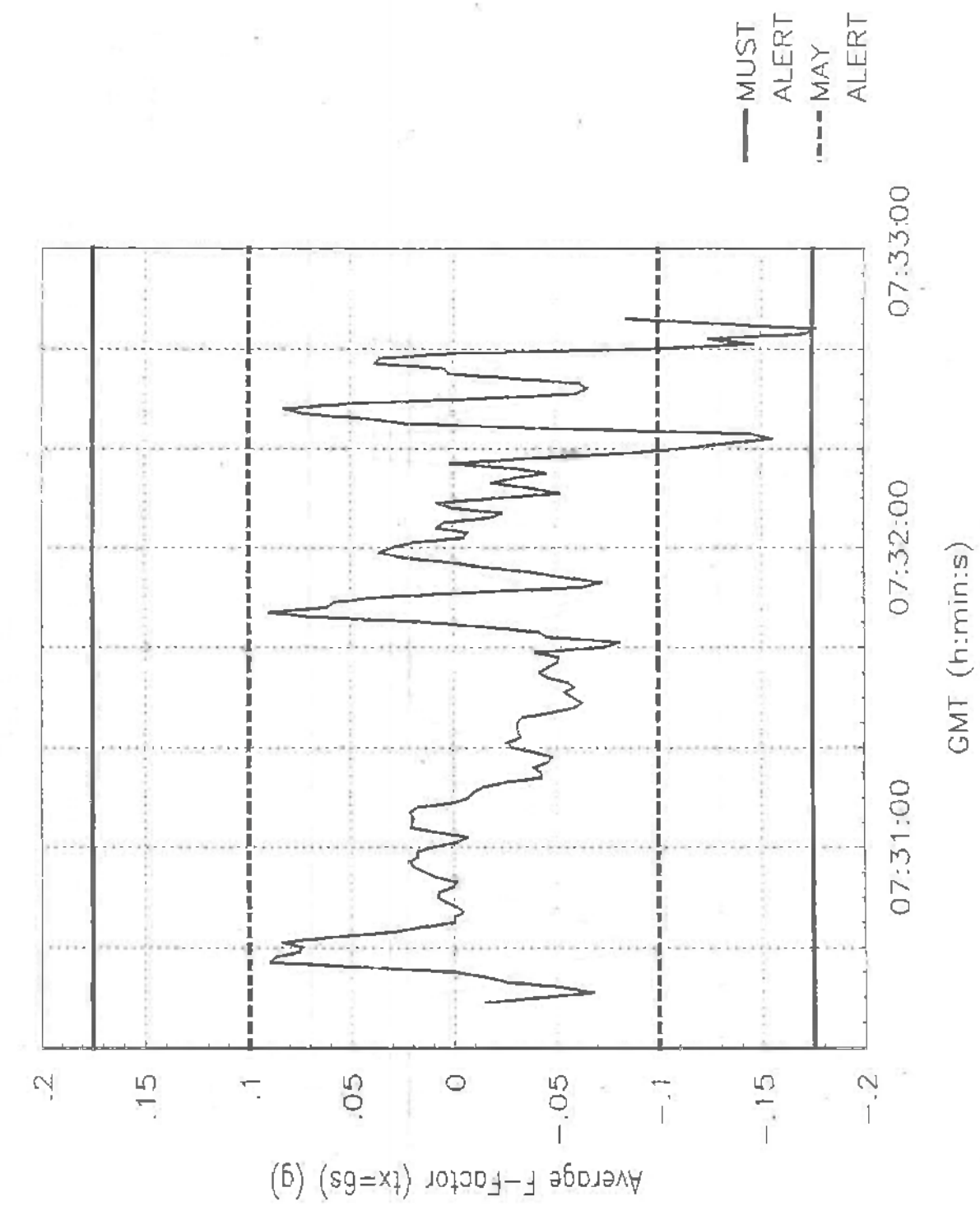

Fig. 40 Six-seconds filtered F-factor as function of time

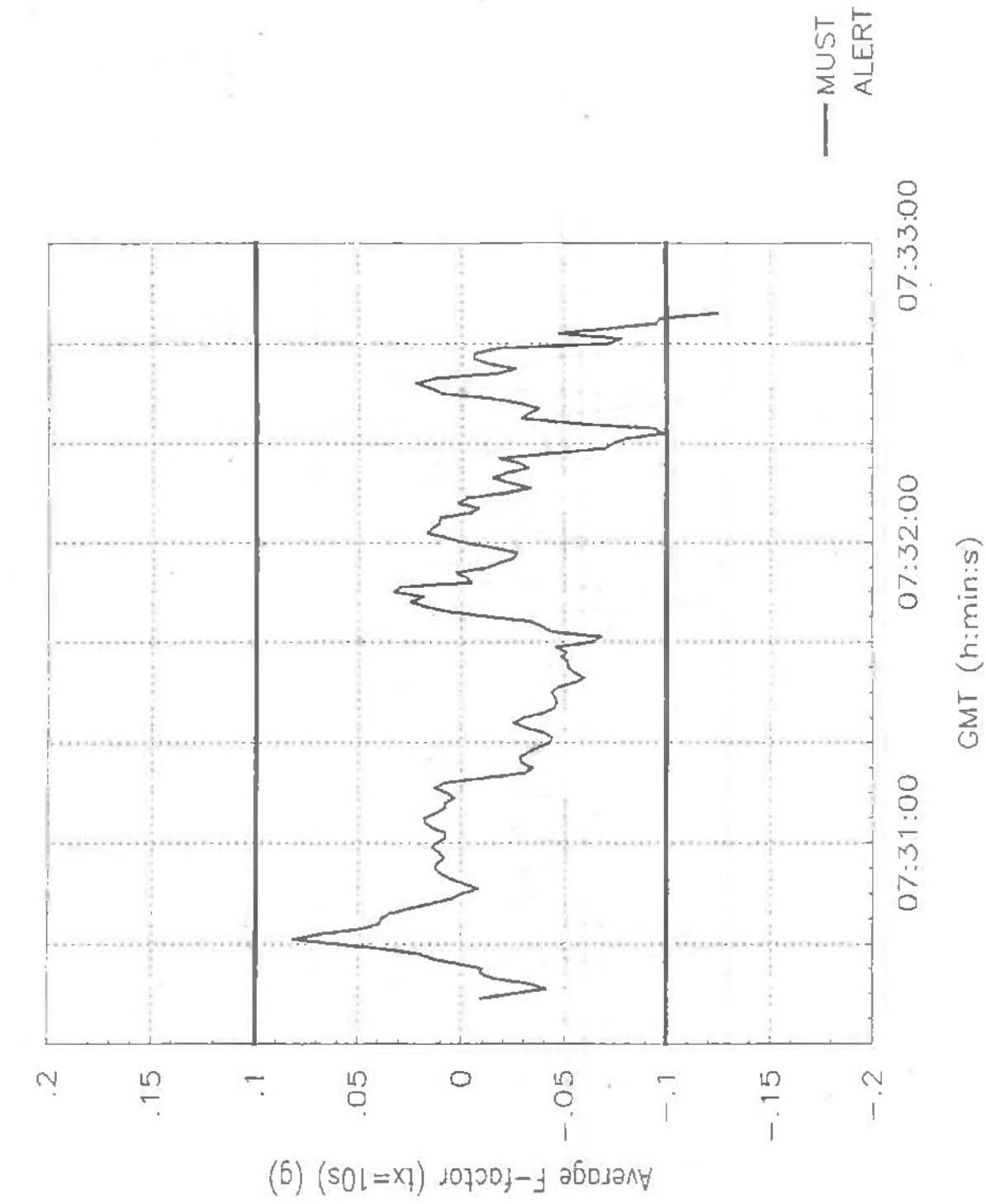

Fig. 41 Ten-seconds filtered F-factor as function of time

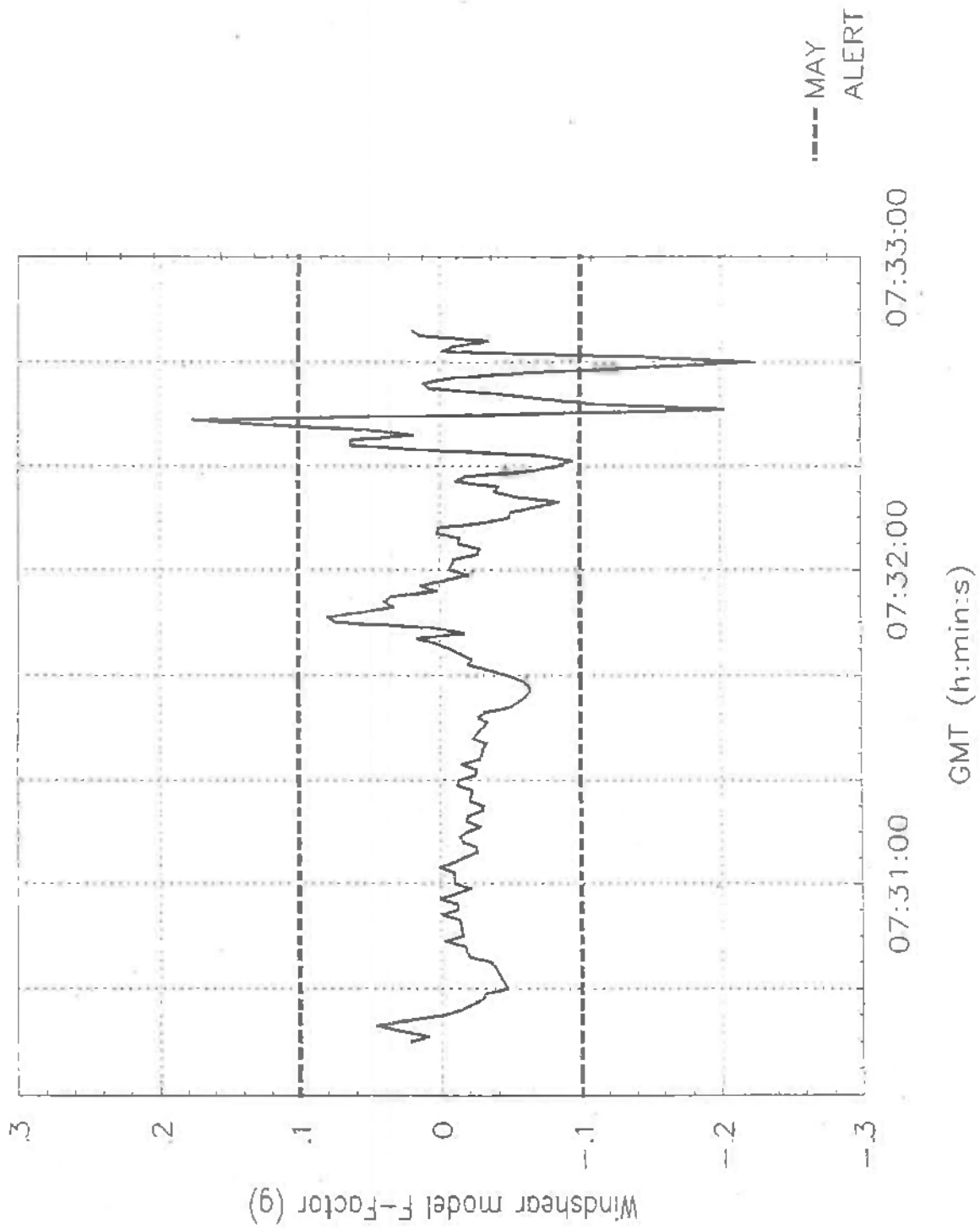

Fig. 42 Windshear model-generated F-factor as function of time